

REPORT DOCUMENTATION PAGE

Form Approved OMB No. 0704-0188

Public reporting burden for this collection of information is estimated to average 1 hour per response, including the time for reviewing instructions, searching existing data sources, gathering and maintaining the data needed, and completing and reviewing the collection of information. Send comments regarding this burden estimate or any other aspect of this collection of information, including suggestions for reducing this burden to Washington Headquarters Services, Directorate for Information Operations and Reports, 1215 Jefferson Davis Highway, Suite 1204, Arlington, VA 22202-4302, and to the Office of Management and Budget, Paperwork Reduction Project (0704-0188), Washington, DC 20503.

1. AGENCY USE ONLY (Leave blank)		2. REPORT DATE 5 May 1997	3. REPORT TYPE AND DATES COVERED Final Report
4. TITLE AND SUBTITLE Photometry Observations of space objects on Russian Northern Caucases Station			5. FUNDING NUMBERS F6170896W0289
6. AUTHOR(S) Dr. Viktor Shargorodsky			
7. PERFORMING ORGANIZATION NAME(S) AND ADDRESS(ES) Scientific Research Institute of Precision Device Engineering (SRIPDE) ulitsa Aviamotornaya 53 Moscow 111250 Russia			8. PERFORMING ORGANIZATION REPORT NUMBER N/A
9. SPONSORING/MONITORING AGENCY NAME(S) AND ADDRESS(ES) EOARD PSC 802 BOX 14 FPO 09499-0200			10. SPONSORING/MONITORING AGENCY REPORT NUMBER SPC 96-4084
11. SUPPLEMENTARY NOTES			
12a. DISTRIBUTION/AVAILABILITY STATEMENT Approved for public release; distribution is unlimited.		12b. DISTRIBUTION CODE A	
13. ABSTRACT (Maximum 200 words) This report results from a contract tasking Scientific Research Institute of Precision Device Engineering (SRIPDE) as follows: The contractor will investigate photometry observations of space objects on Russian Northern Caucases Station Kosmoten. The contractor will conduct photometric observations from kosmoten of ten satellites in geosynchronous orbit, an data resulting from photometric observations to detect non-orbital motion of satellites and provide results of analysis to include description of measurement methods and evaluation of accuracy, including effects on measurement quali atmospheric instability.			
<i>DETQ QUALITY DOCUMENTATION</i>			
14. SUBJECT TERMS Optical Components, Optical Theory, Remote Sensing, Quantum Optics			15. NUMBER OF PAGES 82
			16. PRICE CODE N/A
17. SECURITY CLASSIFICATION OF REPORT UNCLASSIFIED	18. SECURITY CLASSIFICATION OF THIS PAGE UNCLASSIFIED	19. SECURITY CLASSIFICATION OF ABSTRACT UNCLASSIFIED	20. LIMITATION OF ABSTRACT UL

NSN 7540-01-280-5500

Standard Form 298 (Rev. 2-89)
Prescribed by ANSI Std. Z39-18
298-102

"APPROVED"

Prof. V.D.Shagorodsky
Deputy Director,

NIIPP

"5" May, 1997



Photometric observations of space objects at the Northern-Caucasian station "Kosmoten"

Final report

(3 deliverable on the contract F61708-96-WO289)



Dr.V.Vygon
Superintendent,
"Kosmoten" station

19971002 085

Table of contents

Introduction.....	3
1. THE TECHNICAL FACILITIES AND OBSERVATION TECHNIQUES OF SPACE OBJECTS	4
<u>1.1. Brief description of the observation facilities and the recording hardware</u>	4
1.1.1. The HOSO channel	4
1.1.2. LOSO channel	8
<u>1.2. Brief description of observation techniques and algorithms for data processing</u>	12
1.2.1. HOSO channel	12
1.2.2. LOSO channel	18
2. METHODS AND RESULTS OF MEASUREMENT OF ATMOSPHERE CHARACTERISTICS IN THE REGION OF "KOSMOTEN" STATION LOCATION.....	28
<u>2.1. Statistics of meteorological conditions</u>	28
<u>2.2. Astronomical climate parameters</u>	30
3. PROPOSALS FOR THE SET OF OBJECTS FOR COORDINATE AND PHOTOMETRY OBSERVATIONS.....	32
4. Photometric measurements of SO and processing of measurements data definition of periodical component of SO movement relative to its center of mass.....	33
4.1. GSO light curves	33
4.2. Light curves of low orbiting space objects (LOSO).....	65
4.2.1. The object 88106.002: Lacrosse, USA	65
4.2.2. Analysis of light curves of the object 93023.001: Ferret-D, USA	65
Conclusion	82

Introduction

Basic concept of the work

At present time photometry is the only effective method of obtaining non-coordinate information about parameters of shape, reflecting surface and characteristics of non-orbital movement of high-orbit and geosynchronous space objects (SO). Regular seasonal photometric observations of SO at different phase angles will allow to define more accurately the existing and to develop new algorithms of reliable definition of the aforementioned parameters.

Using sets of SO parameters restored by photometric observations, one can form multidimensional vectors of SO non-coordinate features that are a powerful tool for identification and recognition of SO along with the coordinate information.

The present work is the first step in this direction: demonstration of possibility of obtaining at "Kosmoten" station of quality photometric information about geosynchronous SO directly containing specific features of shape, reflective surface and parameters of own (non-orbital) movement. The report contains data of photometric observations of 10 geosynchronous and 2 low-orbiting SO belonging to different classes (active, passive, rotation stabilized, etc.). There is given the description of used methods and equipment of photometric observations. According to the requirements of the Statement of Work, there are also presented the results of statistical characteristics of atmosphere in the area of disposition of "Kosmoten" station.

Usage of available and developed at "Kosmoten" station algorithms for processing of photometric measurements data, including forming vectors of SO features and their usage for identification and cataloguing of SO, and also support and maintenance of SO photometric catalogue is a separate work which can be carried out by the "Kosmoten" station specialists within a separate contract by the customer's request.

1. THE TECHNICAL FACILITIES AND OBSERVATION TECHNIQUES OF SPACE OBJECTS

1.1. Brief description of the observation facilities and the recording hardware

Functionally the "Kosmoten" optical observation station consists of three (3) autonomous channels for observation and measurements:

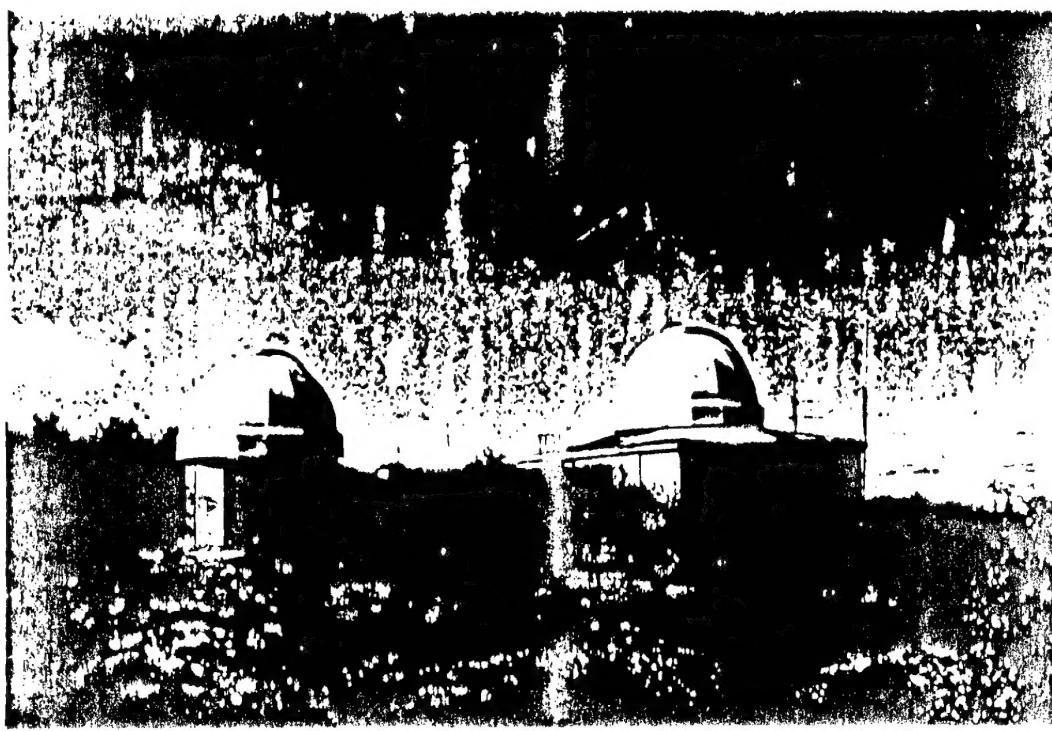
- channel for the co-ordinates and photometry observation of the high orbit space objects (HOSO channel);
- channel for the coordinates/photometry measurements and imaging the low orbit space objects (LOSO channel);
- channel for the laser range finding of space objects (LRSO channel).

The LRSO channel has not yet been put into operating mode and therefore it is not a subject of scrutiny in this report.

The general view of the "Kosmoten" station is shown in Fig.1.1. In the foreground in the tower-like pavilion the LRSO channel telescope is seen. The left dome houses the HOSO channel telescope and the right dome - the LOSO channel telescope.

1.1.1. The HOSO channel

The simplified block diagram of the channel for observing high orbit space objects (HOSO channel) is shown in Fig. 1.2.



KOSMOTEN station (sight from side BTA)

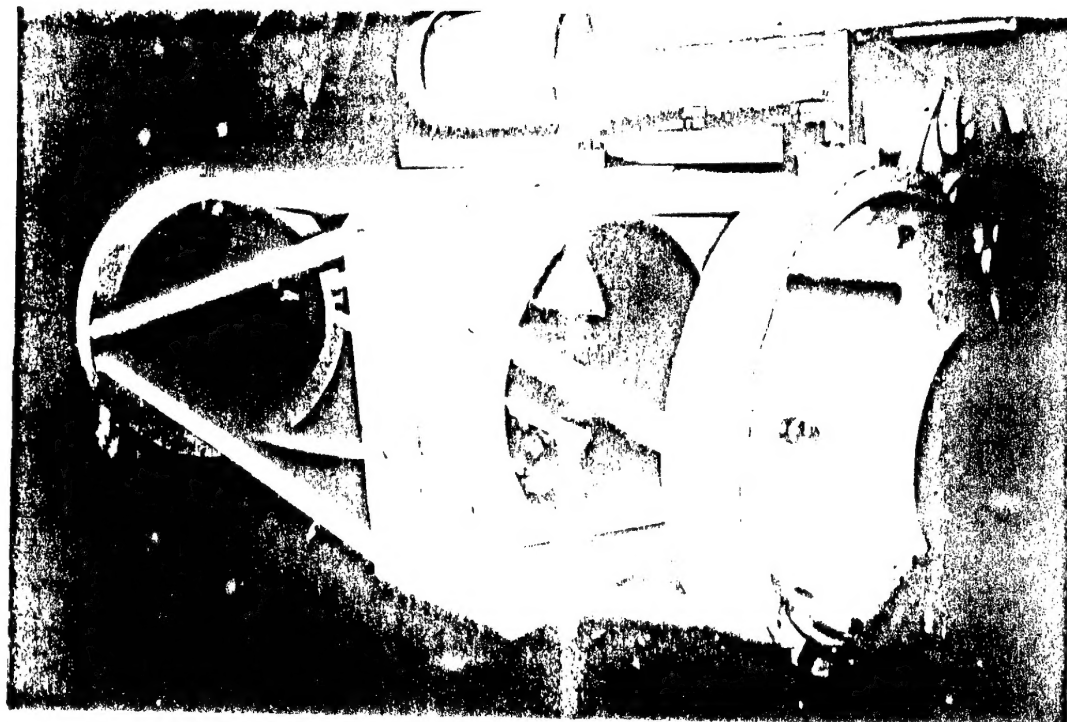
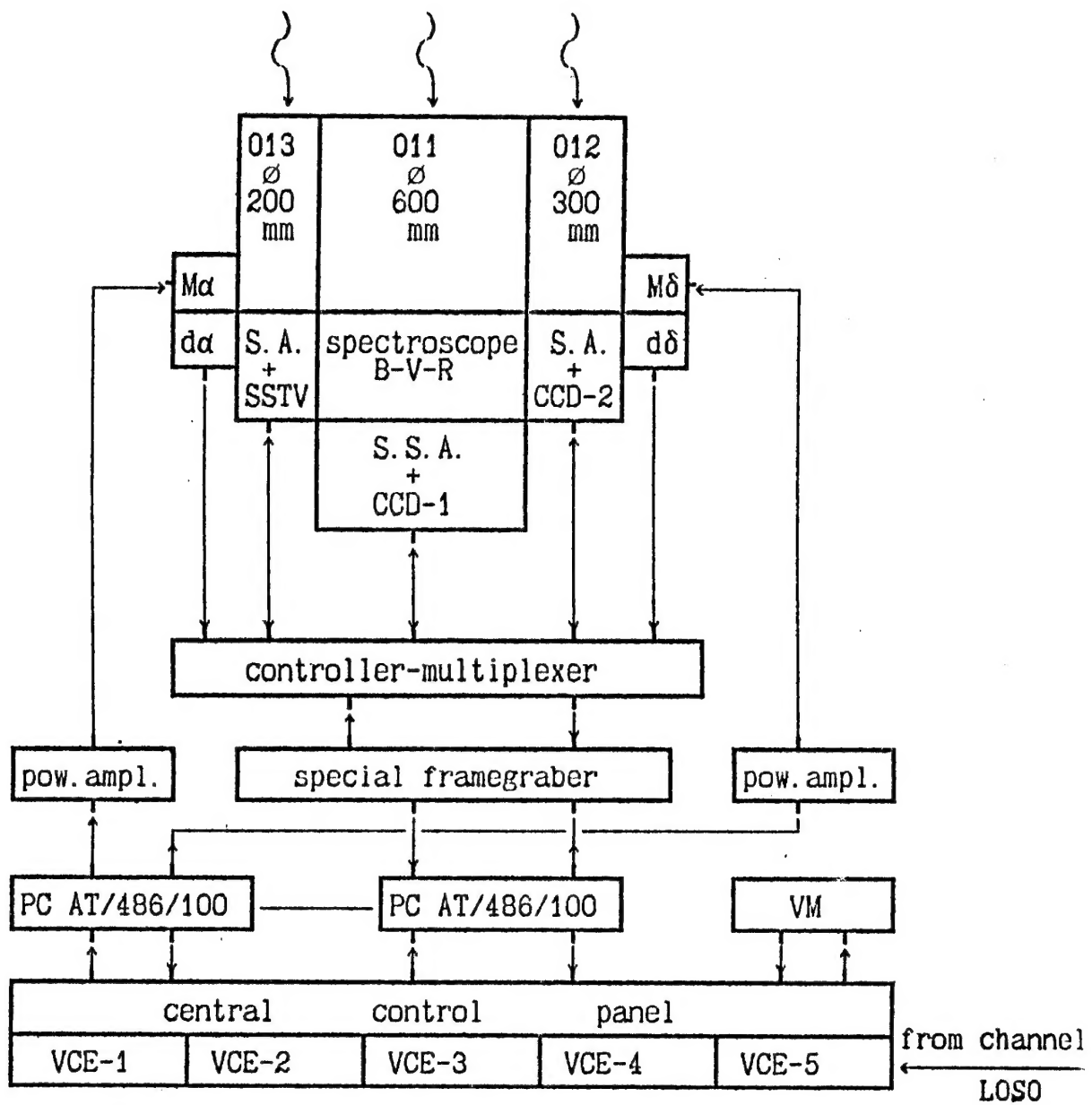


Fig. 1.1

CHANNEL LOSO



Parameters:

1. Sensitivity : subchannel 011 - $17^m.0$ (for measurements)
 (at 1 TV cadr) subchannel 012 - $15^m.5$ (for detection)
 subchannel 013 - $14^m.5$ (for control)
2. Velocity of tracking $< 2'1,s$
3. Precision of measuring angle coordinates $< 1''$
4. Precision of photometry (after treatment) $< 5\%$

Fig. 12

The main measuring sub-channel is a 600 mm objective lens of a ZEISS-600 telescope with a TV photodetector D-213 (assembled on the basis of TV tube LI-703) in its focal plane. Immediately in front of the TV photodetector device (PDD) there is a unit of changeable filters which shape the standard B,V, R colorimetric spectral bands. The TV signal from the D-213 is applied to a special preliminary processing device (PPD) where it is digitized and its parameters are measured at the given threshold level. The adaptive tracking gate formed therein measures the signal parameters at the digital level number of 256. When making the photometry measurements of space objects the size of the adaptive gate is set automatically so that it is equal to the image being measured at the level of 0.5 of its amplitude. The size of the measuring field being $10^{\circ} \times 10'$ and the pixel number of the PPD being 512*512 the photometry measurement of the space object with luminance not less than 15^m is performed in the gate of $3'' - 10''$ size (depending on the luminance of an object being measured). When making photometry measurements of space objects under 15^m the software is used to shape a tracking gate (PPD does not ensure a reliable shaping of the adaptive gate by the hardware) of $10'' \times 10''$ size while PPD is used only to measure amplitude and the video signal area in the software gate.

The measured data are recorded by ..PC which is connected to PPD through a special interface. All the read-out signals on PPD are rigidly synchronized with the starting instant of the frame scanning ($F_k=50$ Hz, progressive standard) and correspond to the absolute readings of the time instants. The accuracy of the absolute time locking per a single reading in each TV frame (taking into account the geometric position of an image being measured in the TV frame) is min. 100 ms.

In addition to the measurements of amplitude and video signal area in a gate the measurement of the image gravity center in each TV frame is made in PPD. Depending on the luminance of the object being measured the accuracy in measuring the image gravity center in a single TV frame with reference to the fixed center of the TV raster is $0.5'' - 2''$. An introduction of the appropriate co-ordinates metric into the TV raster provides a possibility to measure the angular co-ordinates of the slowly moving SO (mainly the geostationary SO) with a certain accuracy. At present, however, the co-ordinates measurements are actually not made in the sub-channel 011 with PPD (only some separate control measurements of geostationary space objects -GSSO-being scanned photometrically); measuring co-ordinates of any object is performed with the aid of a special device - the frame-grabber - the TV frame adder (TVFA) when realizing the astrometric method in real time.

Digitization (7 operating digits) of the full TV frame in real time is made by TVFA both for the progressive standard video signal and the usual cross-line broadcast standard. TVFA allows to store up to 500 digitized frames, ensures displaying (in real time) of the digitized image on a separate remote monitor and is provided with the built-in modes for external control: digitizing at a given threshold level, changing the digitizing scale, subtracting the constant (maintained by software) signal level, arranging a flexible exchange mode with PC. Maximum rate of recording by PC RAM of AT-486 type is up to 7 frames per second.

The built-in storage system for the analogous signals on the LI-703 TV tube target ensures, when TVFA is used, penetrability of the sub-channel (in moonless nights and under good weather conditions) up to 18.5^m within a storage period of 1.6 - 2.0 s. This particular variant is used both for measuring the weak slowly moving GSSO and detecting "debris/garbage" on the geostationary orbits, small planets and extra-atmospheric asteroids in the meteoritic streams (in vicinity of a corresponding radiant). TVFA is connected to a separate PC AT-486 and therefore the operation of TVFA for detecting and measuring co-ordinates can be carried out simultaneously with the TV photometry of space objects performed with the help of PPD and another PC.

Sub-channel 012 is designed for detecting and measuring the co-ordinates of fast objects (up to $1^{\circ}/s$) flying through the operating field in transit. The sub-channel is assembled on the basis of the high-speed (1:3) lens of 300 mm in diameter (the operating clear aperture = 280 mm) and the output is fed to TVFA. The operating field of view in the sub-channel is $2^{\circ} \times 2^{\circ}$. Penetrability of the sub-channel in a moonless night (outside of the Milky Way) is up to 15.6^m for one TV frame.

Sub-channel 013 is the auxiliary one and is used for the flexible identification/comparison of the objects in the small measuring field $W_3=10' \times 10'$ with the ones in the field of detection $W=2^{\circ} \times 2^{\circ}$. The operating field of view of the sub-channel 013 is $W_2=35' \times 35'$ with TV photodetector being a combination of EP10+LI-702. Penetrability of the sub-channel - up to 14^m .

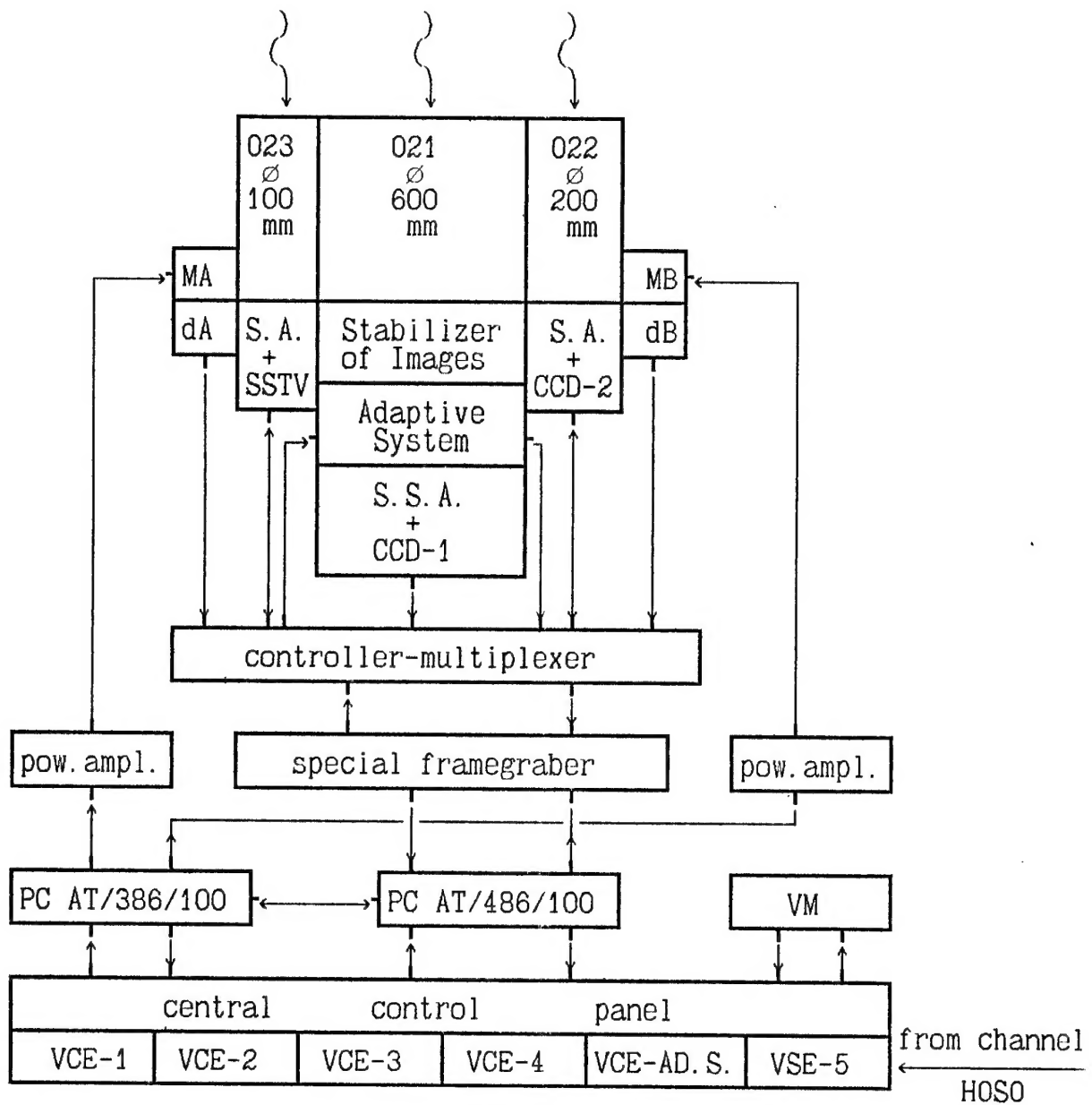
The HOSO channel is provided with the controlled drives ensuring the telescope axis of sight traveling along the whole upper hemisphere without dead zones (German equatorial mounting). The maximum speed of the telescope programmable driving - up to $5^{\circ}/s$; when driven from point to point - up to $40^{\circ}/s$.

In addition the remote monitor (RM) is installed at the central control panel (CCP) of the HOSO channel. Video signals from the medium field of the LOSO are applied to RM and this is very convenient for the synchronous operation of two telescopes (HOSO and LOSO channels) for tracking the same objects.

1.1.2. LOSO channel.

The simplified block diagram of the channel for observing the low orbit space objects is shown in Fig.1.3.

CHANNEL LOSO



Parameters:

1. Sensitivity : subchannel 021 - $10^m.0$ (registration of images)
(at 1 TV cadr) subchannel 012 - $13^m.5$ (TV photometry, tracking)
subchannel 013 - $11^m.5$ (detection and control)
2. Velocity of tracking $\leq 3^{\circ}1_s$
3. Precision of measuring angle coordinates $< 5''$
4. Precision of photometry $< 10\%$
(at subchannel 022)
5. Stabilization of images $< 0.3''$
6. Real resolution (with adaptive system for atmosphere - $2''$)

Fig. 1.3

The LOSO channel has been designed on the basis of the telescope with alt-alt (horizontal) mounting; the mirror diameter of the main objective lens being 600 mm. The diffraction objective lens is assembled on the basis of the classical Cassegrainian scheme with Nasmyth output and operating area along the whole external hemisphere. It has insignificant "dead" zones (two semi-cones in the South and North with $\sim 25^\circ$ at the vertex and a cone axis inclination over horizon $\sim 12^\circ$).

Currently the LOSO channel is the set of three structurally independent (but bound by program/algorithms) information sub-channels and the system for controlling the telescope drives.

The main sub-channel (021) - for recording pictures and analyzing the spatial structure of SO - consists of:

-main objective lens of 600 mm in diameter;

-optical and mechanical path (OMP) ensuring (without loosing the diffraction quality) the shaping of the equivalent telescope focus (at the input of the recording TV PDD) ~ 80 - 160 m (depending on the type of the terminal micro-objective) including in its turn the following:

- image stabilization circuit (SC);

- wave-front correction adaptive circuit (AC);

- additional circuit of the TV correction for controlling the telescope drives in the auto-tracking mode;

- TV PDD with the system of the digital and analogous registration of the TV images.

The image stabilization circuit assembled on the basis of the classic collimation scheme (two autonomous electro-dynamic scanners with flat mirrors for two corresponding axes of the image plane) ensures the stabilization of gravity center in distributing intensity of the optical image at the vertex of the glass pyramid with mirror facets by way of the standard processing of the signals from four (4) photomultipliers (which receive optical signals from the relevant pyramid facets) and produces the necessary error signals (adding\difference circuit) which are fed to the electro-dynamic scanners. The quasi-automatic (after applying a necessary calibration command) compensation of the background level and adjustment of the photomultipliers electronic paths transmission factors are provided in the stabilization circuit as well. Currently, the circuit (taking into account the losses of light in OMP) ensures the image stabilization factor not less than 60 (ratio of an average oscillations amplitude of the image gravity center on the image field with the switched-off circuit to an average oscillations amplitude with the switched-on circuit) for oscillations amplitudes $<1'$ with <5 Hz and luminance of SO not less than $6''$ (the quality of stabilization is improving with the amplitude and initial oscillations frequency being reduced). The stabilization quality data shown in Fig.1.3 refer to the stabilization of the star image gravity center disturbed by the atmospheric turbulence in 0-15 Hz frequency band.

The adaptive circuit (developed by A.B.Alexandrov's team, OKB"Raduga") has been designed on the basis of the flexible (diam.60 mm) mirror with 32 control components in the operating zone. 100-channel photomultiplier (PM with MCP and slit -10×10 elements- anode) is used as a photo transducer. Each controllable (bimorph piezoengine) element of the flexible mirror adjusts an average wave-front inclination at the certain section of the telescope mirror input pupil. The longitudinal radiation modulation (with subsequent phase detection at each PM channel) is used for reducing the effect of noise and for improving reliability in selection of signals from separate components of the input pupil phase plane. Unfortunately, the significant losses of light (modulator, PM, shaping optics, adaptive mirror, etc.) occurs in a part of OMP including the adaptive circuit. Therefore, the adaptive circuit is effective in operation only with regard to the rather bright objects. In particular, at the atmospheric size of star image at the level of 0.5 in $2''$ (luminance not less than $2.5''$) the switching-on of the adaptive circuit reduces the image size (at the same level) down to $0.5''$.

The additional circuit of the TV correction ($\sim 8\%$ of the main objective lens luminous flux in OMP is pinched off with the aid of a transparent flat glass plate and applied to the semi-format CCD camera with EP-10 tube at the input and subsequently the error signal is shaped along two axes between the TV raster center and the center of target mark) is designed to enhance the tracking quality in the mode of the target TV-autotracking. The quality of tracking is enhanced due to applying the high frequency for shaping the error signal (and the relevant control signal to the telescope drives) - 25 Hz and increasing slope of the direction finding characteristics on account of using (for the formation of the error signal) relatively small field of view W24 $\sim 6'' \times 6''$. Holding a target in the vicinity of the field center W24 ($\pm 1'$) ensures the reliable operation of the stabilization circuit which in its turn is the necessary condition for the adaptive circuit operation in the mode of tracking SO.

The updated (as to control functions) CCD camera of SONY company (576*764 pixels) interfaced (through the special micro-objective for transferring images, "Lepton" company, Zelenograd) with the MCP light intensifier (Image Converter Tube /ICT/ of the 2-d generation with the US MCP plate, CKB"Geofizika") is used as TV PDD. The special frame-grabber installed on the TV PDD has helped

to employ the program-controlled mode of storage (up to 300 s) and gating (in 100 ms -10 ms band), controlling the gain mode, digitizing (8 digits) and recording the digitized image on PC LD and RAM with simultaneous controlling on the remote monitor. The response of such a system turns out to be rather high: illuminance of the ICT input window at $\sim 4 \times 10^{-5}$ lx ensures the signal/noise ratio in the output video signal on the resolution element not less than 5.

In addition, the TV camera analogue video signal is recorded on UOMATIC video recorder with 4.8 MHz frequency band.

Size of the image subchannel operating field:

-without adaptive circuit	$\sim 44'' * 56''$
-with adaptive circuit	$\sim 11'' * 14''$

The TV tracking and photometry sub-channel consists of:

- Cassegrainian objective lens, diam.150 mm;
- TV PDD D-213V (on the basis of LI-703 TV tube);
- frame-grabber VS-54;
- PC AT / 486;
- interfacing bus with the control circuit of the telescope drives.

TV PDD D-213V is the updated PDD D-213 (developed by NPO "Astrofizika") forming the complete TV signal in the broadcast (cross-line) standard to ensure the normal operation with the frame-grabber VS-54 ("Videoscan" company, Moscow).

Penetrability of the sub-channel is $\sim 13.5''$ in moonless night. Special feature of the sub-channel operation is its software on PC AT / 486 (see the next section) which process TV signals both on the frame-grabber board and directly in PC.

The sub-channel operating field of view is $\sim 90'' * 110''$.

Structurally, the objective 022 and PDD unit are mounted on the telescope mullion of the main objective 021 with the accuracy of co-alignment in the order of $\pm 20''$ (misalignment might be a chance occurrence in connection with temperature and dynamic deformations of the structure elements). The control unit of the TV PDD is installed at the CCP and provides a possibility for an observer to adjust response and switch-on/switch-off the automatic gain control (AGC) /the PDD AGC is not engaged in the photometry mode and usually used occasionally for TV tracking objects like UFO under condition of the high background noise/.

Detection and astroorientation sub-channel consists of:

- objective MT-1000 (lens 023 on the block diagram);
- TV PDD on the basis of TV tube LI-702;
- separate channel of XS-54 frame-grabber (having its own software on AT/486);
- PPD unit of the TV tracking circuit.

This is the cylindrical structure: PDD photodetecting unit 023 is mounted on the outer central part of the objective 021 (external shadow area of the secondary mirror unit on objective 021).

Operating field of view of the channel $\sim 7.5^0 * 8.5^0$;

Penetrability $\sim 9.5''$.

The PPD unit structurally being a part of CCP is designed for shaping the tracking gate and the error signal between the target mark and TV raster center in the mode of coarse autotracking the target by TV circuit. The frame-grabber and AT/486 are the same as the ones used for the sub-channel 022; only PDD on the subchannel 023 is connected to another input of the frame-grabber which (on command from PC) engages one PDD or another (but not simultaneously).

The main task of the sub-channel - automatic or semi-automatic (following the operator's command) detection of the moving target at the background of the "immobile" stars and effective astroorientation in the observed star picture in the course of the procedures for calibrating the transducers of telescope and the photometry sub-channel.

Drives control system consists of :

- reduction drives (on the basis of the step-engines ShD-4 with wave reducer);
- transducers of the telescope axis elevation angle (16-digit output);

-devices of converting PC control codes in the control signals for the telescope engines (including units for controlling technical condition of any component in the electro-drives control system).

-two controlling PC (AT/386 and EC-1841 with the set of ADC and DAC units for converting the input and output signals);

-CCP which includes in addition to the indicators (showing the health of the system) the controls (and appropriate electronic units) of semi-automatic mode for tracking gate and telescope movement velocity vector on both axes.

Functionally the drives control system of the telescope consists of four (4) circuits:

- control program circuit (controlling signals to drives are sent from PC according to the shaped target indication polynomial taking into account the 'a priori' data);

- circuit 1 of the TV correction and tracking (controlling signals to drives are sent on the basis of the 022,023 sub-channels error signals shaped in PPD unit);

- circuit 2 of the TV correction and tracking (controlling signals to drives are sent on the basis of the 022,023 sub-channels error signals shaped in the frame-grabber and PC AT/486);

- circuit 3 of the fine TV correction (controlling signals to drives are adjusted taking into account the error signals from TV camera field W24 of 021 sub-channel).

Such system of controlling (with corresponding SW) allows to ensure the tracking accuracy (in spite of the fact that quality of wave reducers is not up to the mark - spring effect, worn-out gear generation-and principally discrete motion of the step-engine shaft) up to 1' at a target speed up to 30'/s which is quite acceptable for a reliable operation of the image stabilization circuit in sub-channel 021.

At present the activities are going on at "Kosmoten" station on replacing the reduction drives with the step-engines by the new (momentum) DMS-3 engines with 22-digits elevation transducers which should increase the tracking accuracy up to 10" at the speed of up to 60"/s.

1.2. Brief description of observation techniques and algorithms for data processing

1.2.1. HOSO channel

The HOSO channel realizes two modes of photometry:

-mode of the tracking gate with the telescope stopped (TSM);

-mode of the tracking gate during the programmed tracking of SO (TTM).

Photometry in TSM mode is performed on objects moving with the sped of <1'/s. Otherwise the TTM mode is used.

From the methodological point of view the photometry process consists of two phases: preliminary photometry calibration of the measuring channel and actual photometry of SO.

The idea of photometry calibration is in the following:

A special Photometry Guide Star Catalog is included in the program-algorithms support (SW) of HOSO channel. Each box 5°*5° in the catalog has 7 to 9 reference stars of G-F spectral class with luminance in the range of 9"- 15".

For each selected (or current if a slow moving object is tracked) axis of sight direction of telescope PC display indicates on command "C" -calibration- the group of photometry stars (being nearest to the selected direction) with the program implementing the star tracking mode. The images on star pictures in W1-W3 fields and PC display are compared and the reference stars to be selected are identified. The identification may be carried out both in the fully automatic and combined (with operator's participation) modes. In practice however the fully automatic mode is used extremely rarely due to two reasons: W3 measuring field does not cover all the stars of the selected group; in the field of detection W1 (and monitoring field W2) not all stars of the selected group (due to weather or background noise conditions) can be reliably detected with their amplitudes and coordinates fixed. That is why an operator usually feeds sequentially the reference stars in W3 field following the program which marks the necessary stars in the indicated image on the catalog field. Time of measuring (with the aid of PPD) the intensity of each star is 2 s (averaging on 100 TV frames). As a result of the preliminary calibration measurements the three (3) data files are produced: star magnitude data files m_1, m_2, \dots, m_N , the corresponding data files of the average intensity $\langle I_1 \rangle, \langle I_2 \rangle, \dots, \langle I_N \rangle$ and the data files of errors in measuring intensity d_1, d_2, \dots, d_N ($d_j = \sqrt{1/99 * \sum (I_{js} - \langle I_j \rangle)^2}$) in a single TV frame. The calibration curves $m = f_m(\langle I_j \rangle)$ and $60_m = f_{60_m}(\langle I_j \rangle)$ are automatically formed on the basis of the received data files. Before carrying out photometry measurement of SO the program is to be provided with 3 parameters: photometry measurement interval (dt - duration of a single implementation- usually in the interval of 10s - 5 min.), data picking-up frequency ($F \leq 15$ Hz) and time for the storage of a single measurement

($t \leq 1/F$). Actually, t given the program determines a number of the sequential frames N_F , which are used for averaging intensity being measured I_{KO} : $N_F = E(t/0.02)$, where $E(x)$ - whole part of x . Thus, each measured value of intensity $I(t) = 1/N_F \sum I_k$ at interval t corresponds to star magnitude $m = f_m(I(t))$ and measurement error $d_m = f_s(I(t)) \sqrt{N_F/100}$. As a result of the SO photometry measurements (for a single implementation) the PC disk stores three (3) data files $\{m_j\}, \{I_j\}, \{d_{mj}\}$, $j=1,2,\dots,E(dT/4F)$.

One of the most important tasks of photometry is to restore the true curve of the SO luminance (the change in intensity of the recorded radiation of SO illuminated by the Sun due to its specific motion and nature of the reflecting surface) from the primary implementation, distorted by intensity fluctuations due to atmospheric turbulence and peculiarities of photorecording. If the optical signal being registered is rather strong (for W3 measuring field of HOSO channel it corresponds to the equivalent luminance of the source not less than 15^m) the video signal fluctuations in connection with the photo-recording process can be ignored (in comparison with the level of fluctuations attributed to intensity fluctuations of the optical signal being recorded). This is especially important while observing SO at high zenith angles ($Z > 70^\circ$) when intensity fluctuations are actually saturated and may reach 100%. It is interesting that the classic method of compensating the influence of atmospheric turbulence, due to the increased time in storing a single measurement or averaging the data file of a single measurement, in this particular case is ineffective because the data spectrum of the SO brightness curve is intercepted to a considerable extent (or even fully overlapped) by the fluctuation spectrum attributed to atmospheric turbulence.

In September-October 1996 a new method of restoring the SO brightness curves under strong atmospheric turbulence was offered (V.G.Vygon) and successfully tested at "Kosmoten" station in tracking GSSO. The idea of the method is in the following. Intensity of radiation at the input of Photometer due a multiplication nature of noise connected to atmospheric turbulence can be described in the following form:

$$I(t) = I_0(t) \cdot x(t), \quad (1)$$

where $I_0(t)$ - regular function of intensity change due to a rotation of a satellite;

$x(t)$ - random modulating function attributed to the effect of atmospheric turbulence.

Taking into account that the square of spectrum module of any function is the Fourier transform of its autocorrelation function it is possible to put it down as:

$$\begin{aligned} |G(\omega)|^2 &\sim \int_{-\infty}^{\infty} \exp(i\omega\tau) d\tau \int_0^T I_0(t) I_0(t+\tau) \xi(t) \xi(t+\tau) dt = \\ &\sim \int_{-\infty}^{\infty} \exp(i\omega\tau) d\tau \cdot \int_0^{T_0} I_0(t) I_0(t+\tau) \cdot \sum_{i=1}^N \xi(t-iT_0) \xi(t-iT_0+\tau) dt = \\ &N \int_{-\infty}^{\infty} \exp(i\omega\tau) d\tau \cdot \int_0^{T_0} I_0(t) I_0(t+\tau) \rho(\tau) dt = \\ &\sim \int_{-\infty}^{\infty} g_o(\tau) \rho(\tau) \exp(i\omega\tau) dt = \text{fft}[g_o(\tau) \cdot \rho(\tau)], \end{aligned} \quad (2)$$

where $g_o(\tau) = \int_0^{T_0} I_0(t) I_0(t+\tau) dt$; $G(\omega) = \text{fft}[I(t)]$ - Fourier transform.

For obtaining (2) we have used the periodicity of the regular process $I_0(t)$: $I_0(t \pm iT_0)$, $i=1,2,\dots$, T_0 - period of $I_0(t)$ change and stationarity of the chance process $x(t)$: $r(t) = \langle x(t) x(t+\tau) \rangle$

Ratio (2) shows that the square Fourier-spectrum module received in the experiment of photometry implementation $I(t)$ is the Fourier transform of the autocorrelation function product $g_o(t)$ of regular process $I_o(t)$ and correlation function $r(t)$ of the random stationary process $x(t)$.

Correlation function $r(t)$ can always be determined independently obtaining the photometry implementation from the star in the vicinity of the observed satellite. Therefore we may say that together with the initial realization $I(t)$ we have (as to the direction of sighting) the corresponding $r(t)$.

If now the square spectrum module of the non-distorted luminance curve $I_o(t)$ is denoted through $|G_o(w)|^2$ then evidently:

$$|G_o(\omega)|^2 = \text{fft} \left[\frac{\text{ifft}[|G(\omega)|^2]}{\rho(\tau)} \right] \quad (3)$$

here $\text{ifft}(G)$ - reverse Fourier transform.

Ratio (3) is the algorithm of obtaining the non-distorted Fourier-spectrum module of the true luminance curve $I_o(t)$ from which all the components of a satellite dynamics revealed.

As a first approximation of the restored luminance curve it is possible to use the restored spectrum module $G_o(w)$ and spectrum phase $G(w)$:

$$I_{o1}(t) = \text{ifft} \left[\frac{G(\omega)}{|G(\omega)|} \times |G_o(\omega)| \right] \quad (4)$$

As the actual experiments on photometry measurements of satellites under heavy atmospheric turbulence prove the ratio (4) gives good results at $T > 10\zeta T_o$.

The typical examples of the method described above are shown in Fig.1.4, 1.5.

FILE = 50036.12

Nkosc = 500360

Nkonor = 51918

Day = 27

Month = 8

Year = 1996

Nkoint = 0

(IMEWS, p_t)

phase = 42.1

Lg = 69.5Vector at t0:

hg = 31.2 **a** = 42165.553

ten = 51 **e** = 0.001

m1 = 11.95 **In** = 1.381

m2 = 15.84 **OM** = 80.829

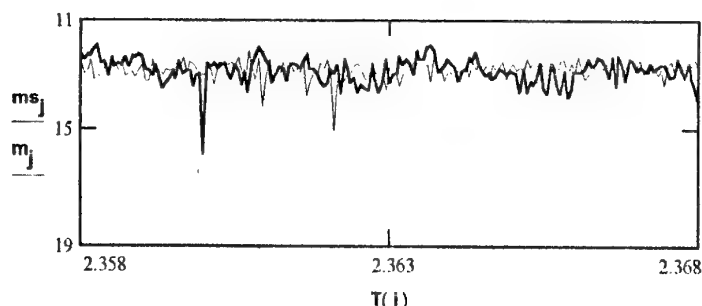
t0 = 2.358 **w** = 55.831

tm = 2.368 **u** = 314.448

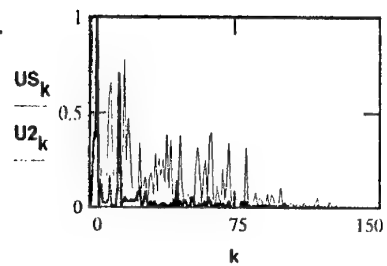
dT = 36.84 **n** = 8

F = 5 Gc

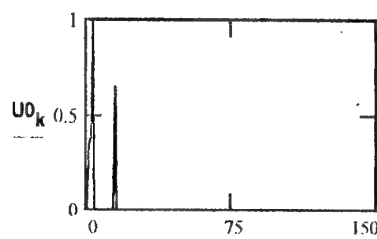
np = 5



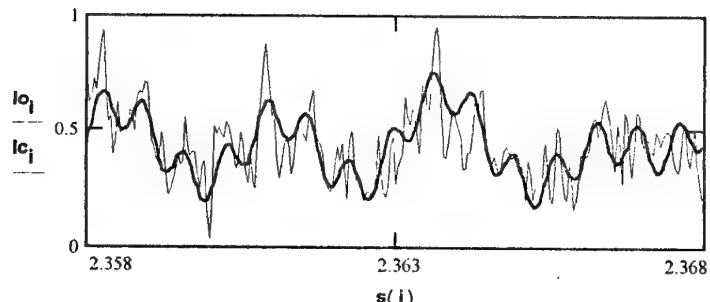
Initial curve of brightness (m; st.mag.)
and curve of brightness from the star(ms)



FFT from intencity of the star(US);
restored spectrum of the object(U2)



Restored and smoothed spectrum
of the intencity of object(U0)s



Initial (Io) and restored (Ic) curves of brightness
(Intensity at relative units)

T1 = 9.446 s

T2 = 2.481 s

T3 = 0 s

T4 = 0 s

T5 = 0 s

Tm = 9.446 s

Fig. 1.4

FILE = 7424.04

Nkosc = 7424

Nkonor = 51925

Day = 27

Month = 8

Year = 1996

Nkoint = 0

(?????, p_t)

phase = 56.4

Lg = 335.Vector at t0:

hg = 8.2 a = 42166.139

ten = 2.8 e = 0

m1 = 13.56 ln = 1.793

m2 = 23 OM = 74.144

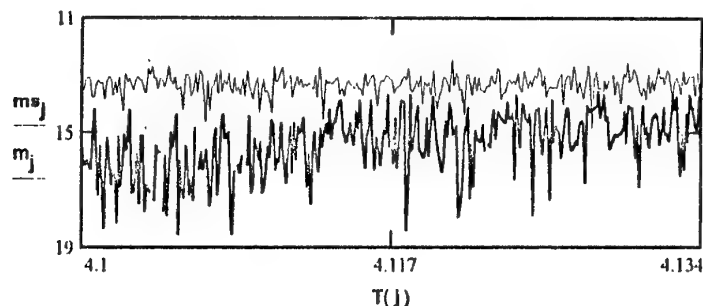
t0 = 4.1 w = 41.662

tm = 4.134 u = 253.816

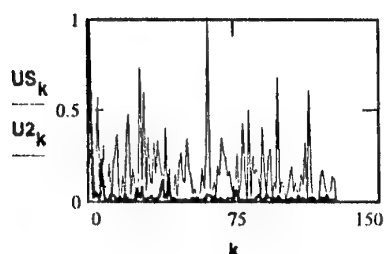
dT = 121.52 n = 8

F = 2.5 Gc

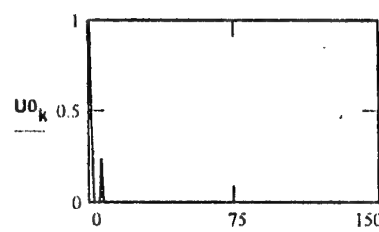
np = 5



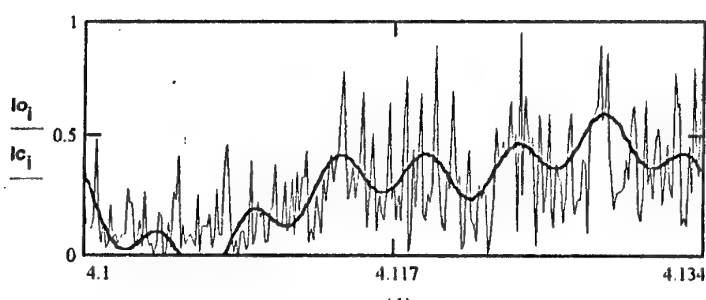
Initial curve of brightness (m; st.mag.)
and curve of brightness from the star(ms)



FFT from intencity of the star(US);
restored spectrum of the object(U2)



Restored and smoothed spectrum
of the intencity of object(U0)s



Initial (Io) and restored (Ic) curves of brightness
(Intensity at relative units)

T1 = 17.612 s
T2 = 17.612 s
T3 = 0 s
T4 = 0 s
T5 = 0 s
Tm = 121.52 s

Fig. 1.5

In particular, Fig.1.4 depicts the restoration of a luminance curve of the well-known US geostationary reconnaissance spacecraft IMEWS. In the upper part of the figure it shows the initially recorded intensity curves of the object (m_j , bold line) and of the star (m_{S_j} , thin line) in star magnitudes at the time interval $dT=37s$ and data pickup frequency $F=5$ Hz. Though the altitude of the object over horizon was rather high ($hg=31.2^0$) the intensity fluctuation level due to atmospheric turbulence was so significant (amplitude changes of the star luminance) that it became comparable with the changes in the object luminance.

To the left of the middle pictures on Fig.1.4 the Fourier-spectrum module of the star luminance curve (U_{S_k} , thin line) and the restored module of the SO luminance curve (U_{2_k} , bold line) in accordance with the superimposition of the above algorithm are shown. To the right of the middle picture the restored module of SO spectrum with threshold cut-off of low amplitude is shown:

$$U_{O_k} = \begin{cases} U_{2_k} & \text{for } U_{2_k} \geq \max(U_{2_k})/5 \\ 0 & \text{for } U_{2_k} < \max(U_{2_k})/5 \end{cases}$$

One can see that two main spectral components of the SO rotation with periods $T_1 \sim 10$ s and $T_2 \sim 2.5$ s are highlighted absolutely vividly and they unquestionably correspond to the type of form and rotation of IMEWS SO.

The bottom picture shows (intensity in relative units) the initial (recorded I_o , thin line) and restored according to spectrum U_{O_k} (I_c , bold line) the SO luminance curves.

Even more impressive results have been obtained regarding object 0447424 (this the internal number of the station catalog). This the Russian stationary satellite at 335^0 longitude (25^0 W). It is observed by Kosmoten station at 8.2^0 altitude, i.e. rather low for usual optical observations: no matter what is the condition of atmosphere the intensity fluctuations level is close to 100%. Satellite 0447424 is the 3-axis stabilized system, i.e. previously its luminance curve did not show any characteristic changes due to its own motions in the orbit. In August 1996 the situation changed (actually we do not know when exactly the changes occurred with SO 0447424- one of the recurrent curve was made in August 1996): the luminance curve restored from background noise (see 1-5) show distinctly the periodic components of its own motion-rotation. Actually it means that either the mode of stabilization changed or (what is the most probable reason) the stabilization function failed and the SO became "dead" i.e. inoperative.

1.2.2. LOSO channel

Each set of observations (in this particular case we mean one night of observation including the evening semi-set and morning semi-set) consists of four (4) phases:

- testing (checking the condition) and tuning the hardware;
- calibration of the transducers of the telescope axes angle position;
- preliminary photometry calibration of sub-channel 022;
- carrying out the observation of space objects and obtaining the relevant (being characteristic for the given SO type) measured data.

1.2.2.1. Methods of getting prepared for observations

The first 3 phases are of preliminary nature (for tuning) and are fulfilled immediately after the LOSO channel equipment has been switched on.

As a rule, a checking of the drives system (including the dome drives) is carried out simultaneously and takes max. 5min. Some discrepancies might occur sometimes when checking the automatic tracking of the dome visor slit center in the telescope axis of sight direction. Such discrepancies are caused by the temperature and geomagnetic anomalies at the time of the testing which effect the radio-electromagnetic method (realized on LOSO channel) of determining a position of the dome visor center in relation to the telescope axis of sight (original method of S.F.Bondar, "Kosmoten"). Therefore at the initial phase of observations it is necessary sometimes to adjust a position of the transducer antennas at the telescope input ring.

The most difficult part is to test and tune the modes of the stabilization circuit (SC) and the adaptive circuit (AC). The difficulties are attributed to the following: the initial switch-on and tuning of LOSO channel modes are carried out in twilight (especially unpleasant are the evening twilight when time for checking and adjusting is very insignificant) when the background noise is changing rapidly. That is why we have developed special techniques (using some hardware tricks) ensuring the effective initial tuning and subsequent correction of modes when conditions are changed in the process of observation.

At present, the initial adjustment of SC requires max.3 min. while AC- 15 min. Thus, it takes about 30 min. to switch on the LOSO channel and put in operating mode.

The testing and calibration of the telescope transducers and preliminary photometry calibration are the parts of the operating mode of this channel and refer to the phase of tuning the measuring paths (in principle, if there is no time before the process of tracking a SO , the mentioned calibrations can be performed after the tracking session having entered by the program necessary corrections in the received changes on the basis of the results of subsequent calibrations. Moreover, that the controlling photometry measurements are performed in any case after each tracking session (below you shall find more details on this matter).

The telescope transducer calibrations are made in conformity with the following scheme.

The LOSO channel SW provides for two modes of calibration: the correction mode and the mode of complete calibration of transducers. The matter is that SW has the built-in preliminary calibration grid (upon the results of the special measurements) in the form of functional dependence $A=F1(bg)$; $h=F2(bg)$, where A,h - correspondingly the true (including the effect of regular refraction) azimuth and altitude of axis of sight and bg - correspondingly the readings of the transducers on the telescope horizontal and 'elevation' axes. That is why in the correction mode (if there is no time to perform complete calibration) the dependencies F1, F2 are specified as per one star: on command <SHIFT K1,<mooving to a reference star? y\n>> the program drives the telescope to the nearest star of 2^m - 5^m luminance in the area of zenith. An operator monitors the sequential appearance of the star images in the vicinity of the all fields centers (W23,W22,W24,W21). Upon the detection of the star in the field W22 a command "AC" is given and the star is drawn sequentially into the centers of fields W22,W24,W21 with an error not exceeding 5% from the size of the field (if a misalignment occurred due to some reasons an operator will manually adjust the centers of their rasters). If the star has been detected simultaneously in W22,W24,W21 fields (with the given error as to the position) the PROGRAM asks for a permission to make fixation and on a command "D" at the given moment of time makes the coordinates of stars (a,d) correspond to the readings of the telescope transducers (,<g>) averaged for the interval of 1 s. As the result of this operation the functional dependencies F1 and F2 are corrected.

The mode of complete calibration (<SHIFT K2,<Complete calibration of transducers?, y\n>>) differs from the correction mode in the following: the PROGRAMM carries out the above operation with 31

selected stars on the whole upper hemisphere (distributed roughly equally in azimuth - 6 stars for each altitude - and in altitude (in each 15°) with one star in the vicinity of zenith). The stars are selected from the basic catalogue for a certain moment of time. The whole procedure of obtaining the initial data files $\{t_j, (a_j, d_j), (b_j, g_j), j=1,2\dots31\}$ takes usually (taking into account a possible interference of an operator) max.10 min. The PROGRAM on the basis of the obtained data files makes new functional dependencies $A=F1(b,g)$; $h=F2(b,g)$, and at this point the procedure of the transducers calibrations is over. Usually the procedure of complete calibration is made after the procedure of correction. In this case it can be made in full automatic mode. Otherwise an interference (a supervision) of an operator is a must.

The preliminary photometry calibration of 022 sub-channel is performed from the software point of view in the same way as it has been described in item 1.2.1. (using the same photometry star catalogue and constructing the output calibration curves $m=f_m(\langle l \rangle)$ and $dO_m=f_s(\langle l \rangle)$). The difference here is that this calibration (since it is the preliminary one) is carried out for the zenith area. Its goal is to depict correctly the maximum range D_m in the maximal measured range DI ($I_j \sim S_k(U_{jk})$, where U_{jk} - is the amplitude of a videosignal in k-m pixel image of $j\dots$ frame). The concrete fixations to the absolute values of luminance and measurement errors are made after (or just before) the SO tracking in one, two or three characteristic points of the SO trajectory (depending on the type and angular length of the SO trajectory) as per the photometry measurements of correspondingly one, two or three reference stars.

1.2.2.2 Methods of making observations and obtaining measurements data.

The process of observing the space objects consists of 3 main phases:

- to detect the SO (on the basis of the preliminary target indications or in the mode of a free (random) search);
- to start auto-tracking of the space object in the given measuring field with the required smoothness and accuracy of tracking;
- to realize the measurement process in the mode of the auto-tracking (angular coordinates and photometry measurements, obtaining pictures).

SO detection

The mode of detecting the SO can be realized by using one of two variants:

- either it is the detection of the known SO with the known preliminary target indications in the form of a reference vector of the orbit components at the given moment of time and date; in this case the fully automatic detection mode can be realized including the programmed tracking and regular TV correction;
- or it is the detection on an unknown SO in the mode of a free search (or the object itself entered W23 field in stand-by mode and grabbed operator's attention); in this case the mode of automatic TV lock with tracking strobe and subsequent TV tracking is realized.

Detection of known SO is performed in the following way. In advance (data of reference orbit shall be entered in the controlling PC at least 5 minutes prior to calculated point of entry of SO into detection zone) using input data, a program calculates parameters of trajectory both in the form of ephemeris (t_j, A_j, h_j) and in the form of coefficients of controlling polynomial with calculation of status vector in waiting point.

4 minutes prior to object's entering detection zone, the telescope is automatically pointed to initial waiting "point". These 4 minutes are necessary, first, to bring the telescope to the waiting point from arbitrary initial position of vision axis, and second, to let the operator a possibility to estimate meteorological conditions in waiting point (and, in case of unfavorable conditions - strong background, the Moon, clouds, etc. - to let operator issue a command to re-point the telescope at the next point of trajectory) and quality of alignment of vision axis relative to dome's sleet, with possibility of operative correction. If detection point is in the near or right in the zone of expected measurements (for instance, point of SO entry is near the point of its culmination), then there will be performed a check-out calibration of SO and photometry record of signal of nearest star in the field W22.

Starting at from the moment t_0-15s (t_0 - calculated moment of entering SO in the W23 field) the Program starts search of target in the field W23. The detection is performed in PC AT/486 by comparison (registered at threshold level and stored in the PC RAM from UPO frame grabber module) of coordinates of centers of marks in series of 6 subsequent frames (during information reading from next subsequent frame the very first frame is removed after first 6 frames, so every time there is analyzed a series of 6 subsequent frames, including the last one).

For W23 field, all stars in series of 6 subsequent frames are "fixed" objects. Because of this, the Program quickly selects them using a simple criterion of spatial coincidence taking into account their vector of star velocity. Just the opposite, there are detected all non-coinciding marks in subsequent frames and they are used for building initial velocity vectors which in each frame are compared with a priori velocity vector in the given point of waiting. During building of initial vectors there is taken into account that two adjoining marks (in two subsequent frames) shall not be in a distance more than $|V \cdot dt| \pm 0.5 \cdot V \cdot dt$ (V is a priori vector of SO velocity, dt - an interval between two subsequently analyzed frames, defined from the condition: $dt \geq dr/V$, where $dr = \sqrt{dx^2 + dy^2}$ - spatial element of resolution of TV raster of detection field); and any 3 and more subsequent marks shall be in the area of a straight line L with diameter $dL = 0.02 \cdot L$. The object is detected and considered as identified if L vector built using subsequent marks conforms to the condition: $L \cdot V / (L \cdot V) \geq 0.99$ and this condition is confirmed in 4 from 5 subsequent (after 1st identification) analyzed frames (divided by interval dt).

If the condition of comparison with a priori vector V is not set, then the Program works in the mode of detection of arbitrary moving object with stopped telescope.

Sometimes there is a situation when the object in principle can not be detected in the automatic mode (amplitude of its video signal is lower than the threshold and lowering the threshold is dramatically increasing number of noise marks what makes difficult the analysis in the given time balance).

At the same time the operator can select a weak object moving in the field W23 easily enough. In this case if the object goes through the central area of detection field W23 (the operator has to solve quickly a problem of identification of SO with its velocity vector) a command for programmed tracking <Enter> is issued and the telescope starts moving along the calculated trajectory. Subsequent operations for entering the SO in smaller fields in this case are performed in the mode of manual correction until the object's light reaches the level which is sufficient for holding the tracking strobe.

Finally, there is possible a situation when nothing at all can be seen in the fields W23 and W22 (even bright stars can not be seen due to a bright background). In this case (basing on initial evaluation of background situation) the operator implements automatic mode of the "blind" programmed tracking: at the calculated moment t_0 of object's movement through the center of W23 field, the telescope automatically starts movement along the calculated trajectory, and the Program, permanently estimating background level in the sample strobe in central area, gradually lowers the threshold, permanently maintaining stable number of noise noncorrelated marks in adjoining frames (not more than 5 in a strobe) until either it finds motionless mark in 6 subsequent frames (in dt) or until operator himself detects this motionless mark and identifies it as a tracked object.

Lock and automatic tracking of SO.

After the object is detected (this or that way) in the mode of programmed tracking, in the SO area there will be formed tracking strobe (again, either automatically or by operator), which is used to measure coordinates of the SO in the raster field, will be formed an error signal and will be issued a command for programmed correction of controlling signals for elimination of spatial mismatch between position of SO and center of TV raster of the field W23. After removal of this mismatch in the field W23 (with accuracy of $\pm 5'$) the object's image is appearing in the field W22, and the Program implements the algorithm of detection of quasi-motionless object and subsequent correction of its position in the field W22. Further on, everything depends on specific situation.

If the object is relatively far (its a priori evaluated angular dimensions are smaller than $2''$) and relatively weak (visually evaluated light is not stronger than 3^m - 4^m) so attempt of getting any topical image is obviously meaningless even with enabling of adaptive circuit, then the process of correction of SO position using other fields is stopped (all further correction is periodically performed using field W22 (when noticeable difference appears - more than 10 resolution elements of W22 field) and the Program switches to implementation of measurement mode.

In the opposite case (if there is a hope to get a topical image), there is implemented detection and closing of the circuit of permanent correction in the field W24, circuit for image stabilization is enabled and as soon as stabilized image appears in the field W21 in favorable conditions (using SO light at resolution element, and quality of stabilization of its center of gravity), adaptive circuit for correction of wave fronts is enabled.

Mode of measurements and registration of images

Two types of direct measurements are performed at LOSO channel:

- measurements of SO angular coordinates;
- SO photometry measurements.

In addition, software of LOSO channel allows to perform geometry and photometry measurements of elements of registered topical images. However, these measurements are performed off-line, they depend on used software and have a special features (out of present SOW). That us why methods and results of such measurements are not included in the present report.

Measurements of angular coordinates are performed in two ways:

- using readings of sensors of telescope axes taking into account calibration surfaces $A=F1(\beta, \gamma)$, $h=F2(\beta, \gamma)$;
- using astrometry method in the field W22 with exposure time 1-40 ms (depending on SO velocity).

When working with SO of known type (which has preliminary target definitions), measurement of angular coordinates is an auxiliary one and serves rather for evaluation of quality of ephemeris calculation depending on how old reference target definitions are. In these situations measurement of angular coordinates using readings of axes sensors is quite acceptable. Accuracy of this method of measurement (with smoothening of single measurements obtained with sampling rate of 10 Hz at measurement intervals of 10 seconds with 20-second interval between them) is $2\sigma=30''$.

When working with SO of unknown type ("UFO" type or technogenic object) this accuracy can be insufficient for subsequent beginning of trajectory and identification of SO in the LOSO class from the basic catalogue. That is why for these cases the astrometric method of measurement of angular coordinates in the field W22. Depending on velocity of tracked SO (velocities along both axes are displayed at PC screen with frequency 1 Hz - averaged 10 measurements during 1 second) there will be chosen exposure time of TV frame $\tau_{exp}=\min_{\beta,y}(dl/V_{\beta,y})$ where dl - angular element of resolution of measurement field. In particular, for the field W22 with angular resolution element $dl \sim 9''$ and with maximal velocity of SO along one of axes $V=30'1/s$ we have $\tau=5$ ms. With this exposure time, stars entering the field W22 have almost no traces and therefore there is possibility to realize almost potential accuracy of astrometry method. The most trouble here is absence (simultaneously in one frame) of necessary amount (≥ 5) of sufficiently bright stars. Because of this, the operator has to carefully watch star picture in the wide field W23 and when acceptable star configuration approaches the filed W22 - to issue a command for measurement - in fact, this is command to store 4 subsequent full TV frames of the field W22 on PC's hard drive (frequency of storage of full TV frame 512x512 elements on PC's hard drive is 2 Hz). All measurements of angular coordinates are performed in the AS mode with fixation of object's image in the field W21 (what is important for measurements on sensor's axes). In the present report we, again, do not describe such measurements due to absence of corresponding requirements of the SOW.

Photometry measurements are also performed only in the AS mode (with programmed tracking with the TV correction or with the pure tracking using the signal of mismatch of TV raster) and, mainly, in the field W22. Normal photometry in the field W21, as a rule, does not work because of image shaking in the narrow field W21 with disabled image stabilization circuit. If the object noticeably changes its light (and exactly these objects are of the most interest), then SC holds it badly and there is an additional quasi-random modulation of the signal due to object's shaking in the field W21. However, the photometry sometimes is performed in the field W21: when problem of obtaining of topical image is solved simultaneously with the problem of photometry with registration of digital image on the PC.

Before issue of the command for photometry of the SO, the Program asks to set SO number, frequency of registration of single measurements and photometry interval. Frequency of sampling of initial photometry information can be set in the range 1-25 Hz (all photometry curves given in the next section were obtained at frequency $F_{Ph}=25Hz$). Maximum photometry interval of SO with $F_{Ph}=25Hz$ is 5 minutes (this is related to limited abilities of RAM of used PC). If the object is relatively far and is present in the work zone of tracking more than 5 minutes, it is possible to continue photometry after dumping RAM to the PC's hard drive.

After completion of photometry tracking of the SO, there is performed the photometry recording of signals of reference stars (with approximately same digital readings as for the SO at the same locations) around the point of photometry beginning, SO culmination point, and point of photometry end (with short arc and minor changes of height $<10^\circ$ one 30-second check record of one G-F - class star is sufficient).

When performing photometry of fast objects in AS mode, there is a problem of entering stars in the photometry strobe. Even with strobe dimensions of $18'' \times 18''$ (3x3 resolution elements of the field W22), frequency of entering outside stars in the tracking strobe with SO velocity up to $30'1/s$ is about 1 star per 10 seconds what can lead to errors in the further interpretation of obtained light curve. Solution of this problem is to subtract at the moment t from the signal obtained in the tracking strobe, the signal

obtained at the moment $t-\tau$ in the measurement area of the tracking strobe which center at the moment $t-\tau$ is located at the distance $V\cdot\tau$ from the center of the tracking strobe containing SO image. However, in practice it is more comfortable to fix radius of location of the center r_c of forestall strobe relative to the center of the tracking strobe, and to calculate delay interval τ and position of the center of forestall strobe on the circle with the radius r_c depending on vector V of SO velocity. Thus, if to denote integral of video signal in the measurement strobe of given size read at the moment t , as $J(t)$, than the corresponding photometry signal shall be recorded in the RAM:

$$J_{ph}(t) = J(t) - J_c(t-\tau), \text{ where}$$
$$\tau = \tau(t) = r_c/V(t),$$

and position of the center of forestall strobe at the moment $t-\tau$ is defined relative to the vector r_0 - the center of measurement strobe at the same moment of time $t-\tau$ by the vector $r_c = r_0 + V\cdot\tau$.

Note, that this simple algorithm by the way automatically solves background problem during photometry measurements.

Fig. 1.6-1.9 show light curve of the object 92023001 (Ferret-D) at the interval (Fig. 1.6) and also separate fragments of this curve (1.7-1.9) with the frequency of information sampling 25 Hz. Careful observer (however, it is not our task!) having wish and corresponding algorithm can, using this data, define not only periodical components of own movement, but also orientation and some parameters of shape.

FILE = 92023.310
Nkonor = 0
Nkusr = 920230
Nkoint = 92023.001

(Ferret-d, USA)

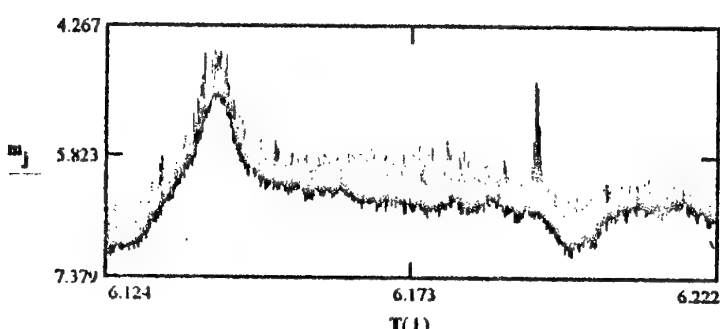
Day = 4

Month = 12 Year = 1996

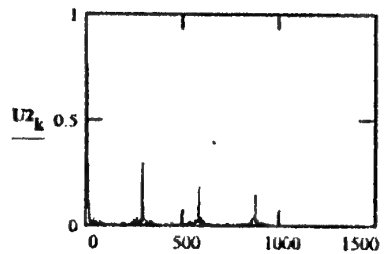
$\Delta m_{\text{apr}} \approx 2.5$ $\Delta m_{\text{mirror}} = 1.4909$ $\Delta m_{\text{izm}} = ???$

R0 = 2119

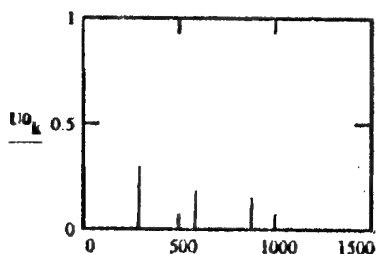
Rm = 1070



Initial curve of brightness (m; st. mag.)



FFT from intensity of the object

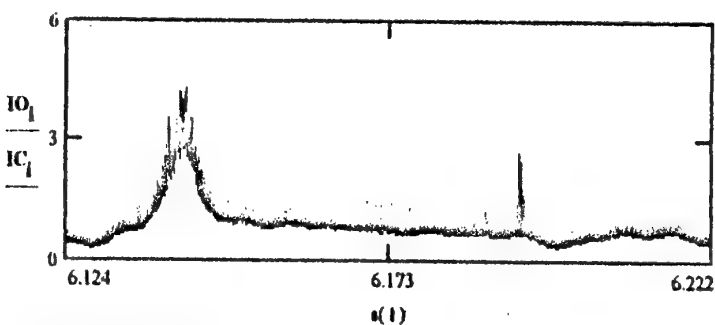


Restored and smoothed spectrum of the intensity of object

Vector at 100=6h07m27s

Az = 165 M00 = 18.72
 $\varphi_0 = 115.1$ $\varphi_m = 96$
 $b_g = 15.4$ $a = -7174.3417$
 $t_m = 21.7$ $e = 0.0015$
 $m1 = 4.5266$ $In = 85.0092$
 $m2 = 7.12$ $OM = 163.383$
 $t0 = 6.1242$ $w = 96.6205$
 $ts = 6.2217$ $u = 27.2805$
 $dT = 351.0s$ $n = 11$
 $F = 25$ Gc
 $mp = 8$

$U0m = 0.7907$
 $U01 = 0.7907$
 $U02 = 0.3107$
 $U03 = 0.1615$
 $U04 = 0.2962$
 $U05 = 0.181$
 $U06 = 0.1495$
 $U07 = 0$
 $U08 = 0$

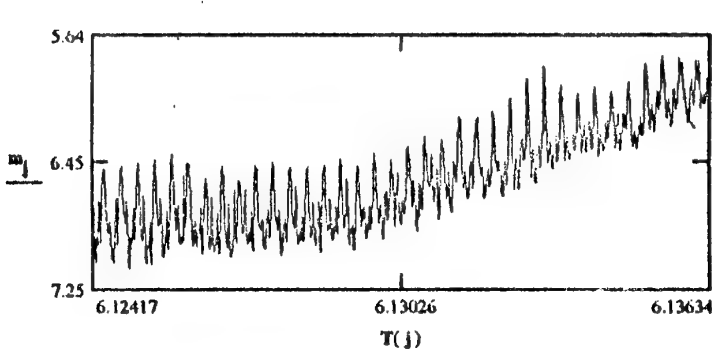


Tm = 111.454
T1 = 111.454
T2 = 43.3432
T3 = 27.0062
T4 = 1.2023
T5 = 0.6001
T6 = 0.4001
T7 = 0.4001
T8 = 0.4001

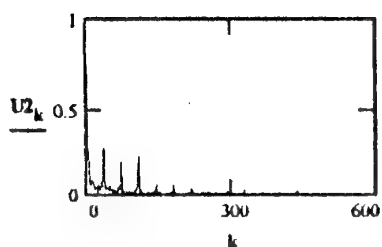
Initial (IO) and restored (IC) curves of brightness (intensity at relative units)

Fig. 1.6

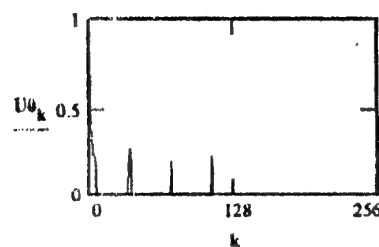
FILE = 92023.31- | Nkonor = 0 Day = 4 Month = 12 Year = 1996
 Nkosr = 920230 (Ferret-d, USA)
 Nkoint = 92023.001 $\Delta m_{\text{apr}} = 1.2$ $\Delta m_{\text{mirror}} = 1.4909$ $\Delta m_{\text{icm}} = 0.2$
 R(t0)=2119km R(tm)=1843km Vector at t00=7h07m27s
 Az=165° M00 = 18.72
 φ0=115.1 φm=115.4
 hg=15.4 a = 7174.3417
 ten = 21.7 e = 0.0015
 n1 = 5.7703 ln = 85.0092
 n2 = 7.12 OM = 163.383
 t0 = 6.1242 w = 96.6205
 tm = 6.1363 u = 27.2805
 dΓ = 43.84s n = 10
 F = 25 Gc
 np = 6



Initial curve of brightness (m; st.mag.)

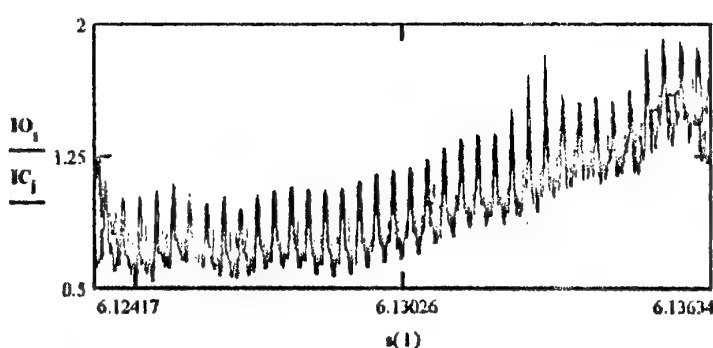


FFT from intencity of the obj.(U2)



Restored and smoothed spectrum of the intencity of object(U0)

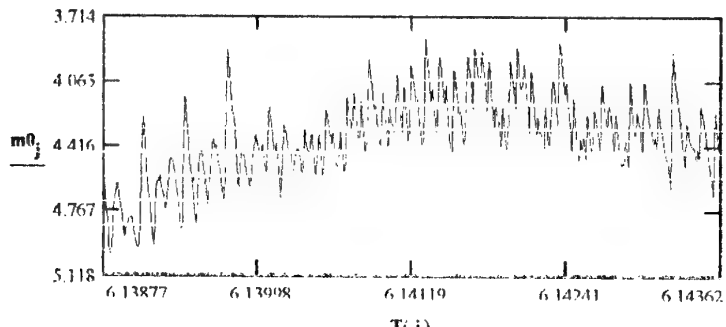
U0m = 0.3228
 U01 = 0.2392
 U02 = 0.2763
 U03 = 0.1984
 U04 = 0.2307
 U05 = 0
 U06 = 0
 U07 = 0
 U08 = 0



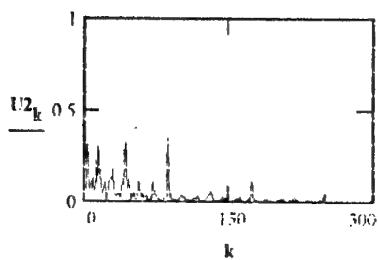
Initial (IO) and restored (IC) curves of brightness (Intensity at relative units)

Tm = 14.6133 s
 T1 = 8.5126 s
 T2 = 1.1817 s
 T3 = 0.6005 s
 T4 = 0.4022 s
 T5 = 0.4022 s
 T6 = 0.4022 s
 T7 = 0.4022 s
 T8 = 0.4022 s

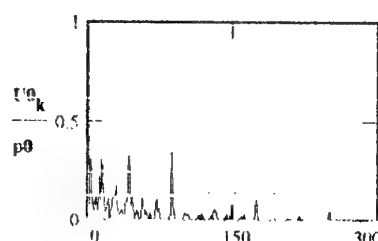
Fig. 1.7

Pic = 920233004
 FILE = 92023300 Nkonor = 0.00000 Day = 4 Month = 12 Year = 1996
 Nkosc = 920230 (Ferret-D, USA) Am_apr = 0.13 Am_mirror = 0.13 Am_mes = 0.36
 Nkoint = 92023.001
 R0 = 1798.1 Rm = 1694.9 Vector at
 Az0 = 163.1 Azm = 161.7 100=06h07m27s
 h0 = 19.2 hm = 21.5 φ0 = 115.5 φm = 115.6

 m0j = 4.416 m1 = 3.83 In = 85.009
 3.714 m2 = 5.00 OM = 163.383
 4.065 t0 = 6.13877 w = 96.620
 4.767 tm = 6.14362 n = 27.281
 5.118 dT = 17.5 s n = 9
 F = 25 Gc np = 50 p0 = 0.143

Initial curve of brightness (m; st. mag.)

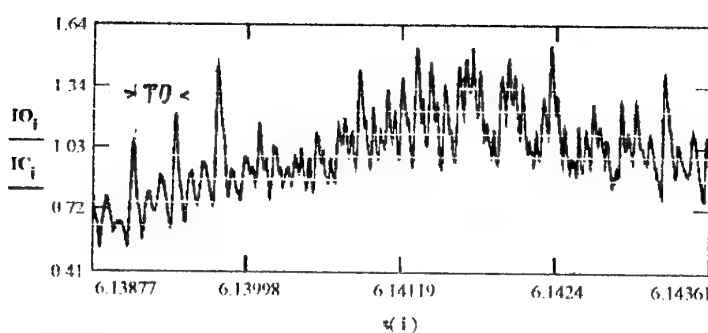


FFT from intencity of the obj.(U2)



Restored and smoothed spectrum of the intencity of object(U0)

U0m = 1.000
 U01 = 0.312
 U02 = 0.226
 U03 = 0.307
 U04 = 0.180
 U05 = 0.327
 U06 = 0.346
 U07 = 0.000
 U08 = 0.000



Initial (IO) and restored (IC) curves of brightness (Intensity at relative units)

Tm = 0.20 s
 T1 = 5.55 s
 T2 = 1.33 s
 T3 = 1.17 s
 T4 = 0.58 s
 T5 = 0.41 s
 T6 = 0.20 s
 T7 = 0.20 s
 T8 = 0.20 s
 T0 = 1.2 s

N
1925 T

Fig. 1.8

Pic = 920233010
FILE = 92023300
Nkhor = 920230
Nkint = 92023.001

Nkhor = 0.00000
(Ferret-D, USA)

Day = 4

Month = 12

Year = 1996

Am_apr = 0.06 **Am_mirror** = 0.06

Am_mes = 0.31

R0 = 1685.5
Az0 = 161.6
h0 = 21.7

Rm = 1639.7
Azm = 160.9
hm = 22.8

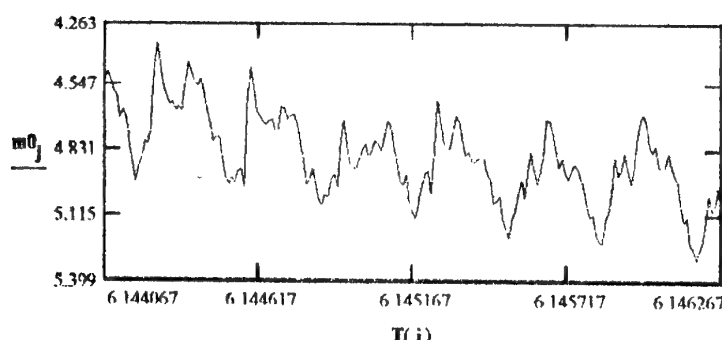
Vector at
t00=06h07m27s

phi0 = 115.6 **phi_m** = 115.6
M00 = 18.02 **a** = 7174.342
e = 0.001464

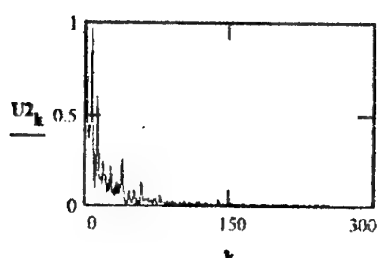
m1 = 4.36 **In** = 85.009
m2 = 5.30 **OM** = 163.383

t0 = 6.14407 **w** = 96.620
tm = 6.14627 **u** = 27.281

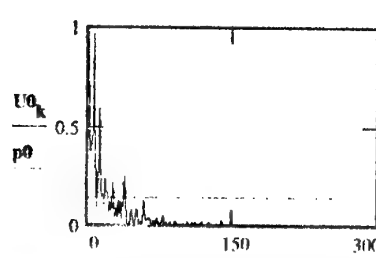
dT = 7.9 s **n** = 9
F = 25 Gc
np = 50 **p0** = 0.143



Initial curve of brightness (m; st.mag.)

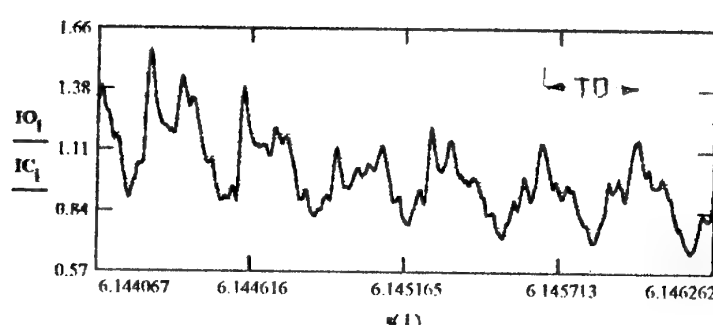


FFT from intencity of the obj.(U2)



Restored and smoothed
spectrum of the intencity of
object(U0)

U0m = 1.000
U01 = 0.969
U02 = 0.261
U03 = 0.603
U04 = 0.166
U05 = 0.245
U06 = 0.179
U07 = 0.220
U08 = 0.255



Initial (IO) and restored (IC) curves of brightness (Intensity at relative units)

Tm = 1.13 s
T1 = 1.11 s
T2 = 0.71 s
T3 = 0.61 s
T4 = 0.47 s
T5 = 0.42 s
T6 = 0.37 s
T7 = 0.29 s
T8 = 0.20 s
TO = 1.2 s

N
1787 T
O

Fig. 1.9

Methods of registration of topical images.

As was already mentioned earlier, registration of SO images both on VM and in digital form on the PC shall be performed with necessarily enabled image stabilization circuit. So, before each tracking of the SO, where image of finite size is expected, the following operations are performed:

- stabilization circuit is calibrated for background level and for expected SO light in the region of the SO culmination;
- average size (and its fluctuations) of star image (also in the region of culmination) is evaluated with current condition of turbulent atmosphere in the field W21 both with enabled SC and without it (to evaluate influence of SC on the size of real resolution element); evaluation is performed by recording and operative analysis of corresponding digital images; SC modes are corrected according to the results of analysis;
- maximum level of signal which is at the limit of saturation of video signal (according to values of corresponding digitizing) is evaluated to maintain sensitivity level of photo receiving device which will not allow losses of resolution due to saturation of the video signal and which will provide maximal dynamic range across the frame during registration of the image while SO tracking;
- operator stores the picture of star image on the monitor, which corresponds to this utmost signal level (dynamic range of visible signal at monitor is noticeable less than the range of TV photo receiving device with CCD array; so when controlling picture using the monitor only one can easily make a mistake and lose some information by reducing sensitivity at seeming in the monitor saturation of video signal);
- there is evaluated possibility of use of AC at current astronomical climate conditions, background conditions and expected SO light (taking into account what was said before about possibility of use of AC for practical observations of SO, there were no corresponding conditions during the whole period of work; this quite characterizes efficiency of use of AS in the existing technological variant; it is interesting that in the USA, where first reports about use of AC for observations of astronomy objects appeared, there is no reliable information about efficient use of AC for satellite observations either).

During SO tracking (with its reliable holding in the field W21 by stabilization circuit) the operator continuously checks maximal level of signal both in the monitor and by digital indication of the PC, and selects optimal level of sensitivity for obtaining of maximal number of image details (sometimes even sacrificing resolution of one part of the image in order to obtain invisible in other way details of the other part). At present time there is no any acceptable criterion of getting maximum informative image in the condition of noticeable turbulence and limited dynamic range of photo receiving device. Due to this, the role of subjective perception of image quality by observing operator is very important.

Image registration in the form of recording analog TV signal at video recorder is performed continuously during the whole tracking of the SO; storage on the PC's hard drive of digital image is performed (according to previously selected registration mode) by operator's commands.

After completion of tracking of SO once again (taking into account the real level of measured signal of the SO) there is performed recording on the video recorder and registration of separate digital images of a star with light close to the SO in the region of the SO culmination.

2. METHODS AND RESULTS OF MEASUREMENT OF ATMOSPHERE CHARACTERISTICS IN THE REGION "KOSMOTEN" STATION LOCATION

3 ways of monitoring of atmosphere conditions are used at the station:

- everyday twenty-four-hour measurement of meteorological parameters: temperature, pressure, humidity, velocity and direction of wind, intensity of clouds and haze;
- periodical (two-three times a night) measurements of average dimensions of star images (at the level of 0.5 of video signal amplitude);
- special study of turbulence characteristics of atmosphere using both "Kosmoten" station facilities and original methods and equipment of other researchers.

2.1. Statistics of meteorological conditions.

Fig. 2.1. shows histogram of month-by-month distribution of amount of observational astronomy hours (average number of night hours of clear weather per month; clouds - not stronger than number 3) in the period 1980-1996.

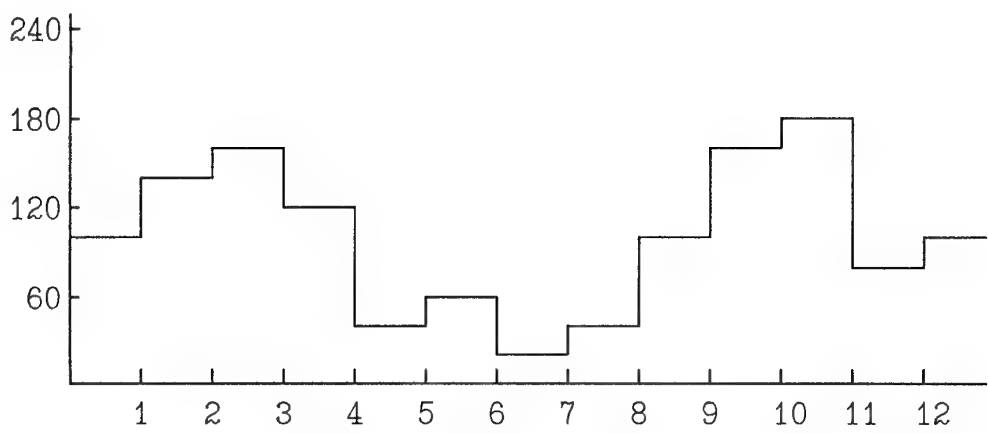


FIG. 2.1.

From the histogram it is seen that the most favorable with amount of clear nights period are January-March and September-October.

It is clear that this data is rather conditional and strongly depends on global atmosphere phenomena related to change of solar activity, movements of the Earth's crust, volcanic activities and so on, though it is difficult to find any correlation relation to them (it was noticed that in 1-2 years after the minimum of solar activity, meteorological conditions for astronomy observations are noticeably worse). For instance, in November-December 1993 (according to the histogram this time is rather unfavorable) there were 45 observational nights!, and for the same period in 1996 - only 16. In average, it is accepted that in this place the real observation time is about 50% of the total possible time of night astronomy observations.

2.2. Astronomical climate parameters

On "Kosmoten" station 3 main parameters characterizing condition of astronomical climate are used: coefficient of optical transparency in B, V, R bands (in zenith in clear night), average (per night) value of turbulent optical factor $I(h_0)$ $I(h_0) = \int_{h_0} Cn^2(z)dz$, $Cn^2(h)$ - structural characteristics of the refraction factor at the height h), daily change of turbulent optical factor $I(h_0,t)$.
By many-year measurements, average values of transparency coefficient are:

- in the band B ~ 0.75
- in the band V ~ 0.78
- in the band R ~ 0.82

Special studies were devoted for measurement of turbulent optical factor (TOF) in the region of "Kosmoten" station:

1978-79 - group of A. Makarov, Institute of Atmospheric Optics, Tomsk - photoelectric method;
1984 - group of P. Sheglov, GAISH, Moscow - photoelectric method and interferometric methods;
1983, 1994 - group of M. Kallistratova, Institute of Atmospheric Physics, Moscow - radio acoustic method.
1992 - 1993 - group of V. Vygon, "Kosmoten" station - TV method.

Photoelectric method is based on measurement of shaking spectrum of the center of gravity of the image of the Polar star in the focal plane of small aperture (3-5 cm) lens in frequency range 0.1-1.5 Hz. Interferometric method (A. Tokovinin, GAISH) is based on measurement of radius of coherence of a wave front using photographs of interference bands obtained by interferometer based on obtaining interference picture from a star with sliding light incidence on Lloyd mirror. Measurements were also performed using the Polar star and Zeiss-600 telescope.

Radio acoustic method is based on permanent registration and subsequent analysis of sound signal dispersed by the atmosphere with vertical radiation of sounding pulse.

TV method is based both on measurements of amplitude spectrum of center of gravity shaking of star image in telescope's focal plane, and on measurements of spectrum of fluctuations of dimensions of the star image at the level of 0.5 of amplitude in the field of view 20"x20" with different sets of input apertures (20-60 cm). This method allows to work with the stars of all upper hemisphere and, therefore, to additionally detect anisotropy of TOF.

Fig. 2.2. shows typical averaged profile of $C_n^2(h)$ which is typical for location of "Kosmoten" station in comparison with similar data for Haleakala mount (Maui, Hawaii), White Sands (New Mexico, USA), Maidanak mount, Uzbekistan.

It is seen in the figure that type of change of all curves versus height $C_n^2(h)$ is close enough, though numeric values for "Kosmoten" station are slightly than for Haleakala mount.

Fig. 2.3. shows histogram of average values (for the observation period 1983-84 and 1992-93) of daily change of TOF (I , $m^{-1/3}$)

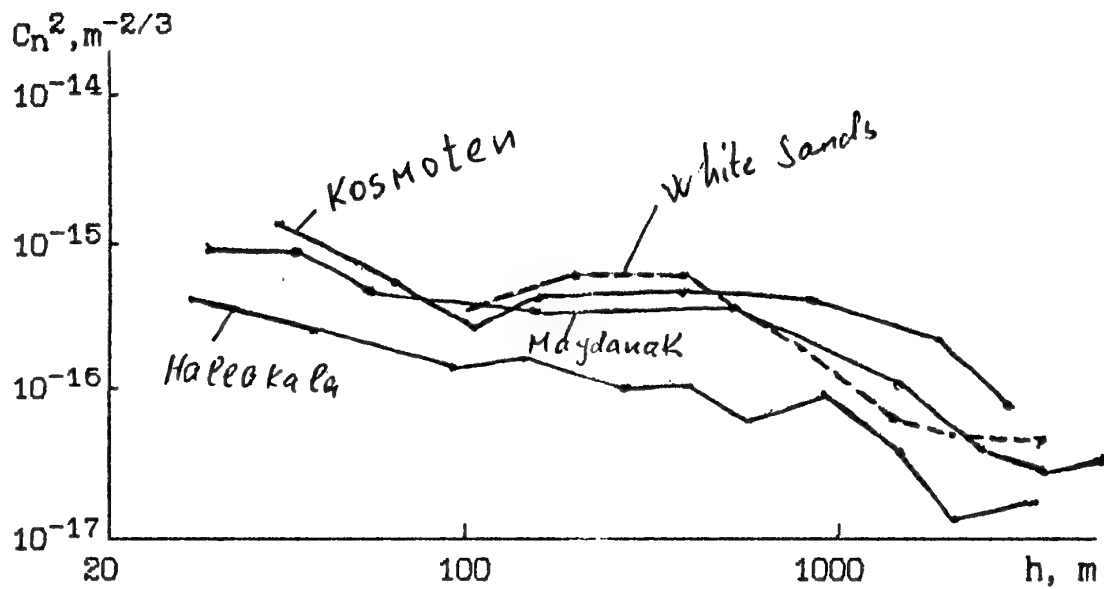


Fig. 2.2

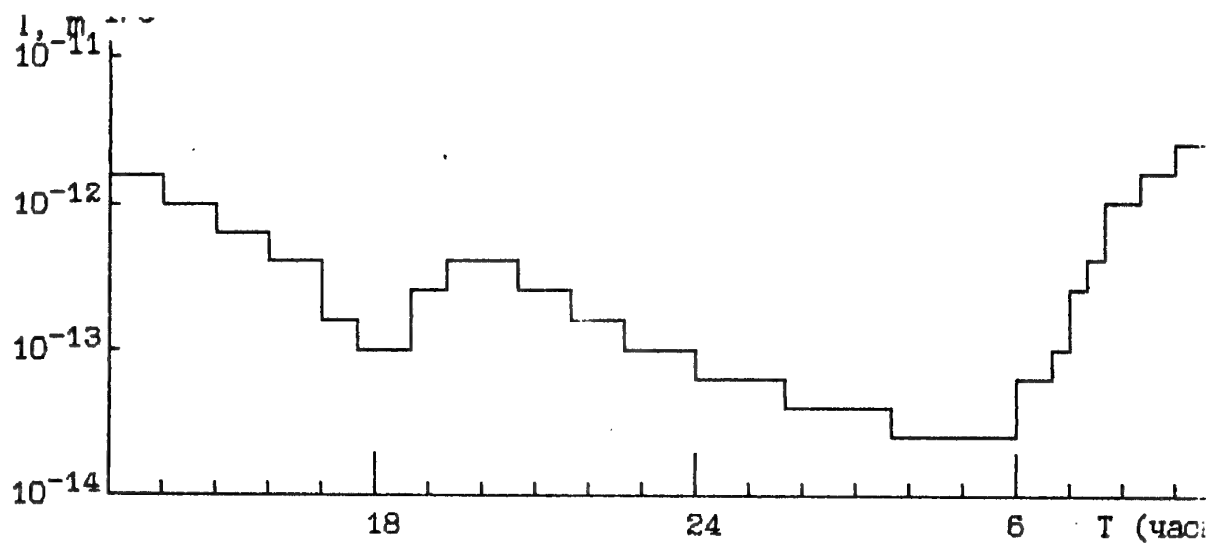


Fig. 2.3

In the figure it is seen that the best conditions for image quality distorted by atmosphere turbulence, are 1-2 hours prior to the beginning of astronomy twilight. This is true for Fall-Winter and Spring-Summer observation periods.

3. PROPOSALS FOR THE SET OF OBJECTS FOR COORDINATE AND PHOTOMETRY OBSERVATIONS.

10 objects (according to the SOW) are proposed for observations: 8 geostationary object and 2 low-orbit ones. All of them have very specific fast periodical change of light.

International ID of the object	Name	Launch country	Spacecraft type
1. 93013004	"Cosmos"	Russia	geosynchronous
2. 84101001	Galaxy-3	USA	geosynchronous
3. 82058001	Westar-5	USA	geosynchronous
4. 90064001	Gorizont-20	Russia	geosynchronous
5. 91080002	Imews-16	USA	geosynchronous
6. 89101001	Cosmos 2054	Russia	geosynchronous
7. 87096001	Cosmos 1897	Russia	geosynchronous
8. 83065001	Galaxy-1	USA	geosynchronous
9. 92023001	Ferret-D	USA	Low-orbit
10. 88106002	Lakros	USA	Low-orbit

With this one shall take into account that the range of stable work of "Kosmoten" station for geosynchronous spacecraft is within: 105° Eastern Longitude - 25° Western Longitude (Border range: 110° ... -30°).

4. Photometric measurements of SO and processing of measurements data definition of periodical component of SO movement relative to its center of mass.

This section contains photometry results of 11 SO, including 9 geosynchronous SO (GSO) and 2 low-orbiting SO (LOSO). Light curves of 2 more GSO were given in materials of the Deliverable 2. According to the requirements of the Statement of Work, only periodical components of Fourier spectrum characterizing special features of SO rotation around its center of mass are picked out.

4.1. GSO light curves

Periodical component can be simply picked out for 9 of 11 GSO light curves, which can be a reliable feature for SO identification during operative measurements. At the same time for 2 SO, in spite of obvious presence of light changes, reliable picking out of periodical light changes is a problem. However, we intentionally give data for these objects just to show variety of options one can face in the course of classification of SO photometry results. Besides, the absence of obvious periodical changes in some realizations says about methodical error of obtaining and evaluation of photometry data: it is absolutely clear that to obtain reliable non-coordinate characteristics of SO the long enough sequences of photometric realizations are necessary in order to cover the most possible number of different SO phases (relative to the Sun and to the observer). This is why the attempt to introduce in the set of features the components of Fourier spectrum obtained from one-two realizations can lead to a wittingly false result. Because of this, the results given in this report can be considered as illustrations to the method of photometric analysis and value of photometric information.
Below there are given the concrete results of GSO photometry obtained at "Kosmoten" station in the period from October 1996 through March 1997 with usage of the equipment and methods described in the materials of the Deliverable 2. All information is given along with the full coordinate information what allows to easily check authenticity of the presented results by means of direct measurements at the Customer's facilities. Orbital vectors were obtained by linking trajectories basing on coordinate measurements data at not less than 3 orbits for each GSO. Initial identification of GSO was done by comparison of the obtained orbital vector with the data of GSO basic catalogue. The subsequent more accurate definition of the initial identification was performed already taking into account selected specific features of SO.

The object 93013004: Cosmos ?, SL/12 R/B (2), CIS

Fig. 4.1 and 4.2 show light curves of the 93013004 object. In the figure there is clearly seen a periodical structure with two basic periods: $T_1=9.39$ s and $T_2=4.70$ s. - first two harmonics of the Fourier - spectrum. The specified period (direct measurement of number of oscillations at the given interval) is $T_0=9.36$ s. It is interesting that the second harmonics has the considerably greater intensity. From the point of view of values T_1 and T_2 , curves in fig. 4.1 and 4.2 are practically identical (though they were obtained with the interval of 4 days). However, ratio of intensities of their spectral components differ in more than 2 times. This situation is very often and it is very illustrative: it says that one cannot introduce such photometric feature of SO as ratio of spectral components (though it would be very convenient!) for addition to the vector of features for SO recognition and identification (as well as the feature related to the absolute values and ratio of maximal and minimal amplitude of light changes). The stable feature are absolute values T_1 and T_2 . At the same time, all energy characteristics are very unreliable.

According to the SO number, this is a fourth fraction in the launch 93013. So, it easily can be a last freely rotating stage of a launch vehicle: it is very typical for the USSR launches - to leave junk in orbit (the launch was not long ago - just 4 years, the functional object could still work, and this one is freely drifting from the East to the West).

FILE = 19570101

Nkosc = 195701

Nkonor = 22624

Day = 11

Month = 11 Year = 1996

Nkoint = 93013.004

(Cosmos-?, SL-12
R/B(2), CIS, d-t)

Ag = 116.1 hg = 13.7

Lg = 102.0

phase = 24.7

Vector at t0:

a = 42812.6592

ten = 9.9 e = 0.00141

m1 = 11.25 fm = 1.35765

m2 = 12.75 OM = 74.11614

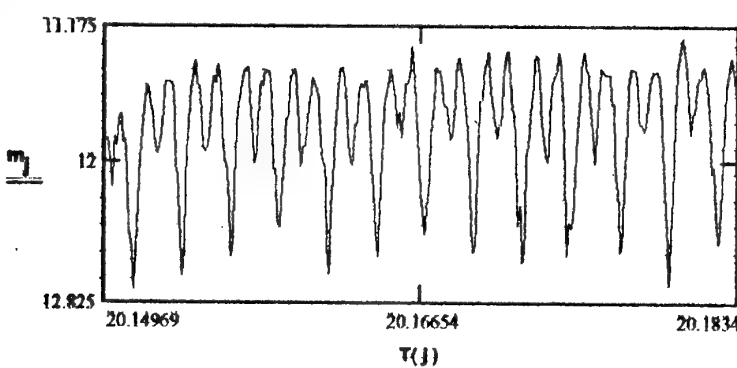
t0 = 20.14969 w = 201.30656

tm = 20.1834 u = 330.85936

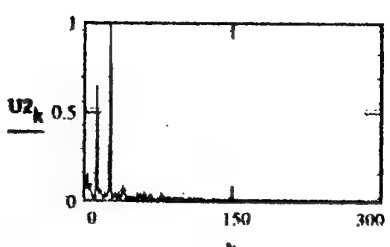
dT = 121.36 s n = 9

F = 2.5 Gc

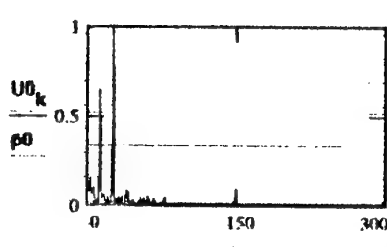
np = 30



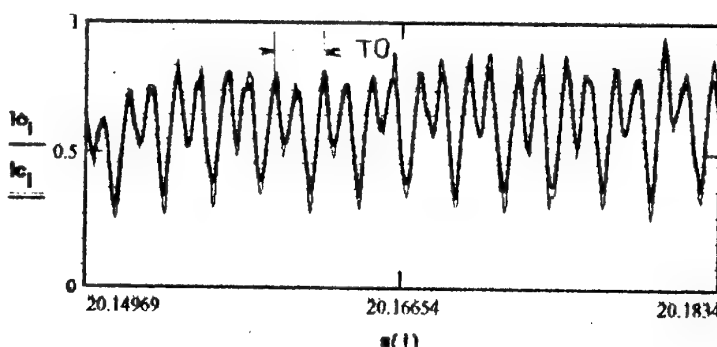
Initial curve of brightness (m; st.mag.)



FFT from intencity of the obj. (U2)



Restored and smoothed spectrum
of the intencity of object (U0)



Initial (Io) and restored (Ic) curves of brightness
(Intensity at relative units)

T1 = 9.34 s
T2 = 4.67 s
T3 = 0.00 s
T4 = 0.00 s
T5 = 0.00 s
T6 = 0.00 s

Tm = 4.67 s
F = 2.5 Gc
dT = 121.36 s
T0 = 9.32 s

Fig. 1

FILE = 19570102

Nkosc = 195701

Nkonor = 22624

Day = 15

Month = 11 Year = 1996

Nkolnt = 93013.004

(Cosmos-?, SL-12
R/B(2), CIS, d-t)

Ag = 149.7 hg = 34.1 Lg = 66.3

phase = 30.7

Vector at t0:

$$\mathbf{a} = 42810.631507$$

$$ten = 18.4 \quad e = 0.001453$$

$$m1 = 10.64 \quad ln = 1.373222$$

$$m2 = 13.35 \quad OM = 74.078136$$

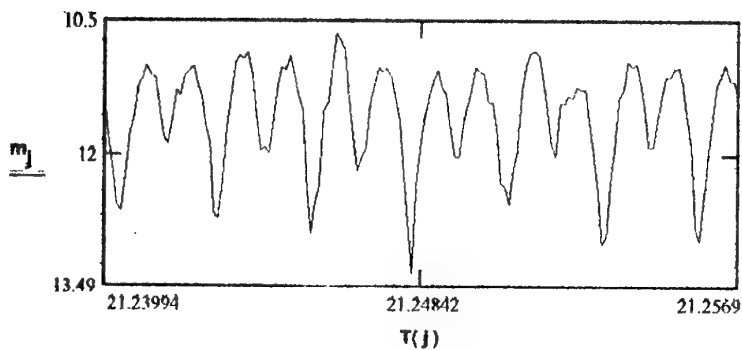
$$t0 = 21.239944 \quad w = 197.70228$$

$$tm = 21.2569 \quad u = 318.342208$$

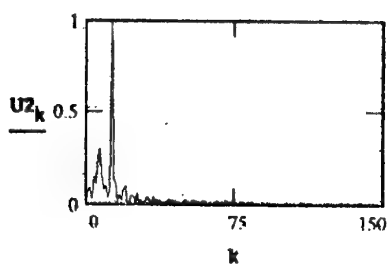
$$dT = 61.04 \text{ s} \quad n = 9$$

$$F = 2.5 \text{ Gc}$$

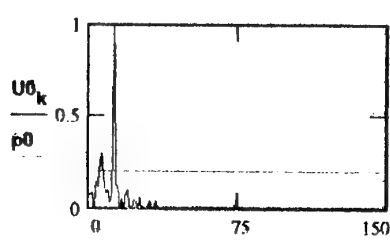
$$np = 30$$



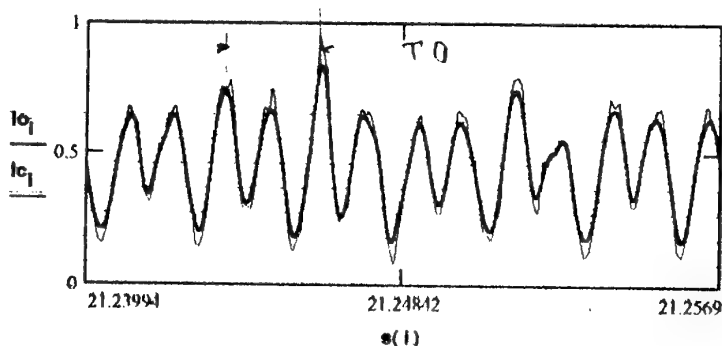
Initial curve of brightness (m; st. mag.)



FFT from intencity of the obj. (U2)



Restored and smoothed spectrum
of the intencity of object (U0)



Initial (Io) and restored (Ic) curves of brightness
(Intensity at relative units)

T1 = 9.39 s
T2 = 4.70 s
T3 = 0.00 s
T4 = 0.00 s
T5 = 0.00 s
T6 = 0.00 s
Tm = 4.70 s
F = 2.5 Gc
dT = 61.04 s
T0 = 9.36 s

Fig. 1.1

The object 82058001: Westar-5, US.

Light curves of this object are given in fig. 4.3 and 4.4. Time interval of obtaining data in these figures is more than 4.5 months. With their forms, these curves look like the previous object but values of periodical components are completely different here. In fig. 4.3 there is only one reliably seen component $T_0=1.72$ s, and at the same time in fig. 4.4 there are three reliably seen components: $T_0=1.76$ s, $T_2=0.86$ s, $T_3=0.46$ s. Absence of more high-frequency components in fig. 4.3 can be explained by the fact that photometry was performed with the sampling rate $F=2.5\text{Hz}$, and in fig. 4.4 value $F=5\text{Hz}$. However, some increase of the main period T_0 (by 0.04 s) drags attention; it can not be explained by measurement errors: the object is confidently drifting towards the East and velocity of its rotation relative to the center of mass is decreasing. The lifetime of the object launched in 1982 is, to all appearances, over, and it is now inoperative (in fact it is turned into debris). Here again the reliable feature is a period T_0 (doublet: main component with a small peak), and also the doublet $T_3=0.87$ s. Again, energy characteristics do not carry any useful information deserving to be included in the vector of SO features.

FILE = 19570302

Nkoer = 195703

Nkonor = 13269
(Westar-5, US, p-t)

Day = 16

Month = 11 Year = 1996

Nkoint = 82058.001

Ag = 150.2

hg = 36.8

Lg = 65.0

phase = 43.5

Vector at t0:

a = 42462.67473

ten = 29.3 e = 0.00152

m1 = 12.88 ln = 3.80057

m2 = 23 OM = 65.90684

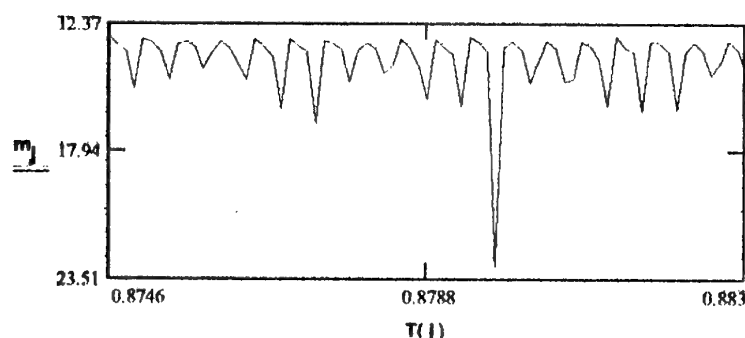
t0 = 0.87464 w = 7.90512

tm = 0.89116 u = 20.00789

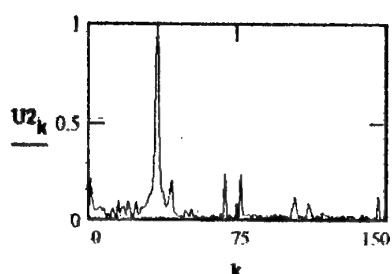
dT = 59.48 s n = 10

F = 2.5 Gc

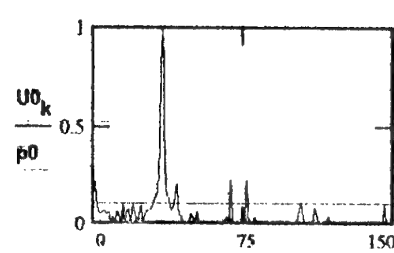
np = 30



Initial curve of brightness (m; st.mag.)

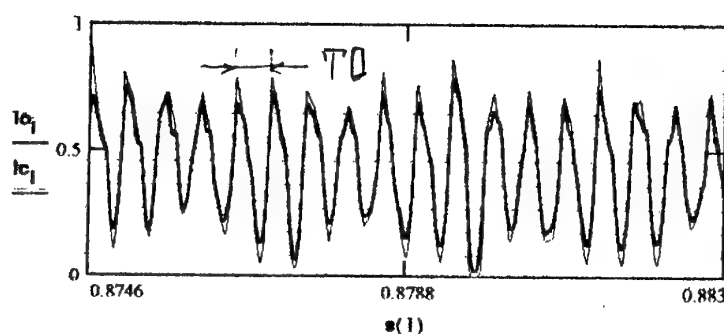


FFT from intencity of the obj. (U2)



Restored and smoothed spectrum of the intencity of object (U0)

U01 = 1
U02 = 0.20404
U03 = 0.22637
U04 = 0.22172
U05 = 0.10939
U06 = 0
U0m = 1



Initial (Io) and restored (Ic) curves of brightness
(Intensity at relative units)

T1 = 1.72 s
T2 = 1.43 s
T3 = 0.87 s
T4 = 0.78 s
T5 = 0.57 s
T6 = 0.00 s
Tm = 1.72 s
F = 2.5 Gc
dT = 59.48 s

T0 = 1.72 s

Fig. 4.3

FILE = 30301.06

Nkosr = 30301

Nkonor = 13269
(Westar-5, US, p-t)

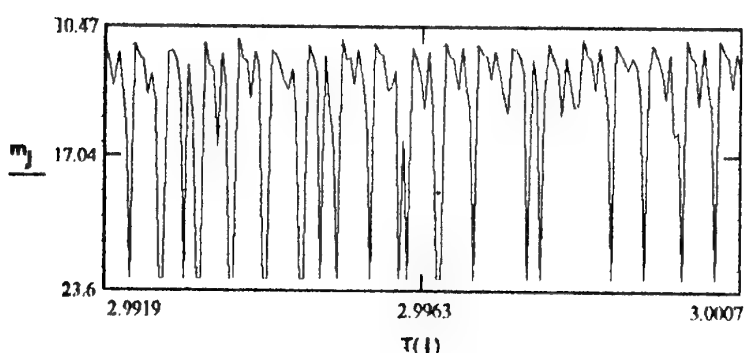
Day = 4

Month = 3

Year = 1997

Nkolmt = 82058.001

Ag = 222.2 hg = 35.2 Lg = 8.1 phase = 10.1 Vector at t0:



a = 42463.36794

ten = 0.2 e = 0.00175

m1 = 11.07 ln = 4.0214

m2 = 23 OM = 65.77371

t0 = 2.99189 w = 0.34685

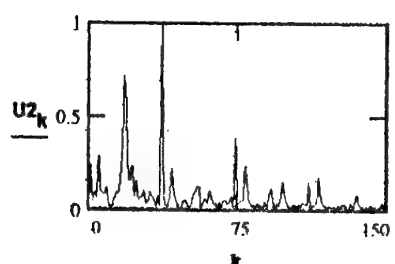
tm = 3.00069 u = 107.41815

dT = 31.7 s n = 10

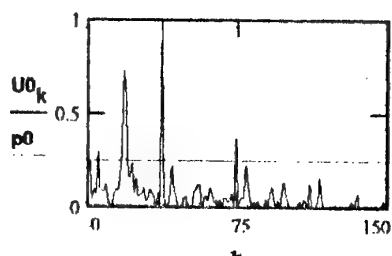
F = 5 Gc

np = 30

Initial curve of brightness (m; st.mag.)

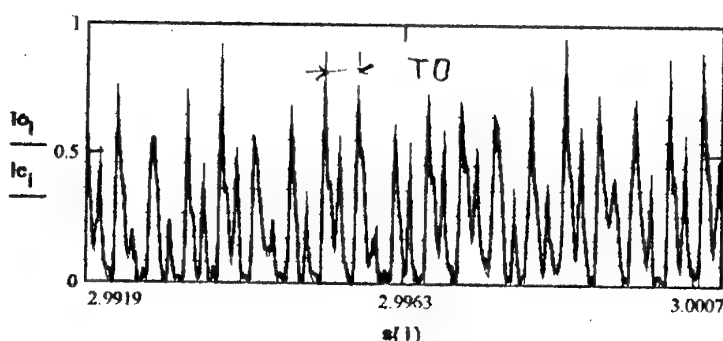


FFT from intencity of the obj. (U2)



Restored and smoothed spectrum
of the intencity of object (U0)

U01 = 0.29041
U02 = 0.72374
U03 = 1
U04 = 0.36997
U05 = 0
U06 = 0
U0m = 1



T1 = 5.76 s
T2 = 1.77 s
T3 = 0.86 s
T4 = 0.43 s
T5 = 0.00 s
T6 = 0.00 s
Tm = 0.86 s
F = 5 Gc
dT = 31.7 s

T0 = 1.76 s

Initial (Io) and restored (Ic) curves of brightness
(Intensity at relative units)

Fig. 1.1

The object 83065001: Galaxy-1, US.

Light curves - in fig. 4.5 and 4.6. By the style of intensity change at light curves we refer this object to a group of pulsing SO (unlike the previous two that were referred to a group of just variable SOs). The object will be referred to a pulsar group (in our classification) if:

- intensity in a flash is at least ten times greater than intensity between flashes;
- intensity flashes are observed at all phases of the SO.

If one carefully looks at both light curves, it is seen that the reliable (stable) features of the SO are:

- two first spectral components $T_0=2.32$ s and $T_2=1.16$ s;
- each line of Fourier-spectrum is at least a doublet;
- half-width of the main flash $\tau=0.28$ s;
- range of half-widths of flashes is $d\tau=0.14$ s.

At rotation period $T=2.32$ s the value $\tau=0.28$ s corresponds to a turn of SO along its rotation axis to an angle $43^\circ \pm 10^\circ$, and for the shortest flash - $21^\circ \pm 8^\circ$, what corresponds to a superposition of the mirror and diffusion components and almost clearly mirror one. So, the feature of the object can be the acceptance of the fact that the object is a polyhedron, and in this specific case - a tetrahedron (4 clear enough peaks at the interval T_0 in the upper picture in fig. 4.6).

Again, this object is abandoned, because it is drifting towards the East, and its type of rotation is an inheritance of a functional task in its past active life (for instance, monitoring of space, or search and detection in the mode of radiotechnical survey).

FILE = 30201

Nkosr = 302

Nkonor = 14138
(Galaxy-1, US, p-t)

Day = 5

Month = 2

Year = 1997

Nkolmt = 83065001

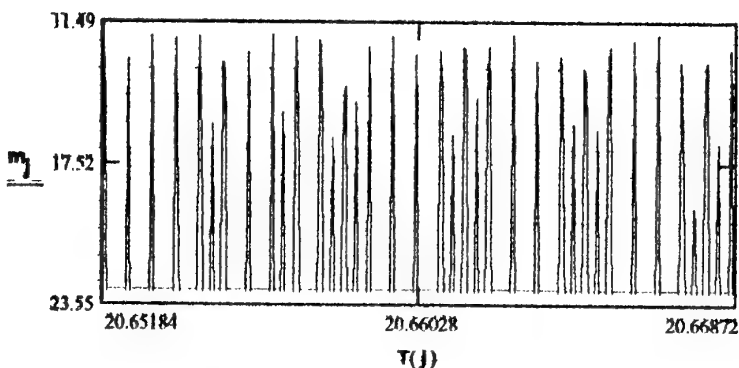
Ag = 38.2 hg = 40

Lg = 38.2

phase = 61.8

Vector at t0:

a = 42210.32667



ten = 50.7 e = 0.00027

m1 = 12.04 ln = 2.42333

m2 = 23 OM = 74.07917

t0 = 20.65184 w = 50.00129

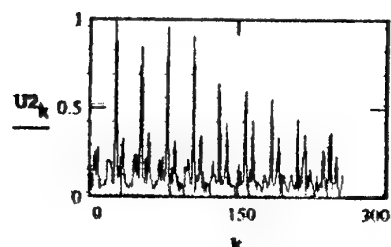
tm = 20.66872 u = 7.17538

dT = 60.78 s n = 9

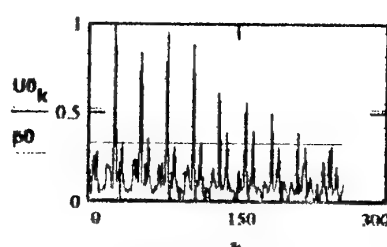
F = 5 Gc

np = 30

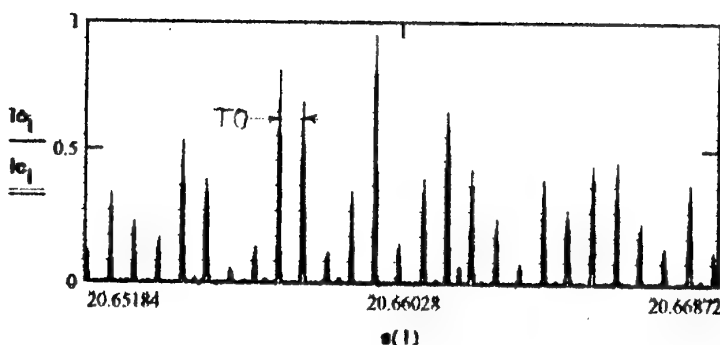
Initial curve of brightness (m; st.mag.)



FFT from intencity of the obj. (U2)



Restored and smoothed spectrum of the intencity of object (U0)



T1 = 2.32 s
T2 = 1.16 s
T3 = 1.02 s
T4 = 0.77 s
T5 = 0.58 s
T6 = 0.54 s
Tm = 2.32 s
F = 5 Gc
dT = 60.78 s
T0=2.32s

Initial (Io) and restored (Ic) curves of brightness
(Intensity at relative units)

Fig. 1.5

FILE = 30203

Nkosc = 302

Nkonor = 14158

Day = 6

Month = 2

Year = 1997

Nkoint = 83065001

(Galaxy-1, US, p-t)

Ag = 38.1 + hg = 42.2

Lg = 38.1

phase = 20.7

Vector at t0:

a = 42210.94351

ten = 6

e = 0.00029

m1 = 9.35

In = 2.42402

m2 = 23

OM = 74.09237

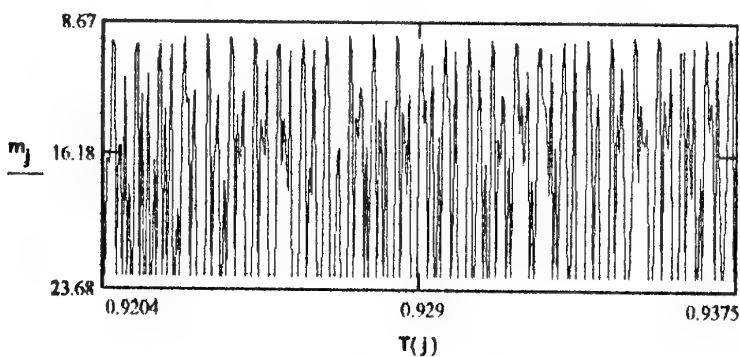
t0 = 0.92039 w = 47.44201

tm = 0.93755 u = 71.29345

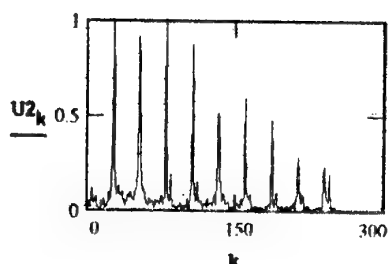
dT = 61.78 s n = 9

F = 5 Gc

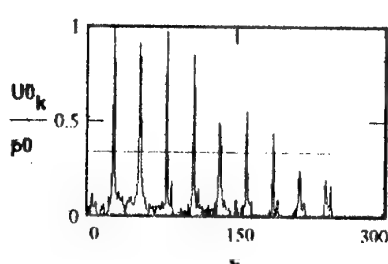
np = 30



Initial curve of brightness (m ; st.mag.)

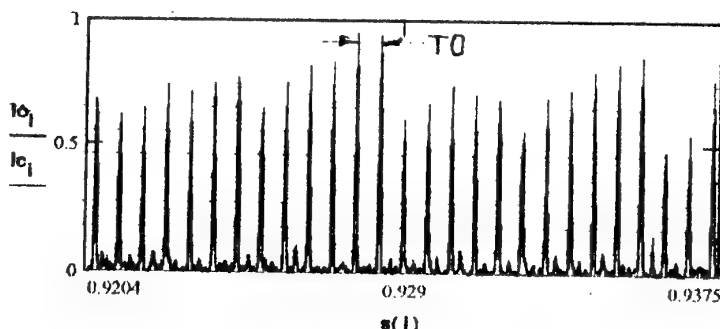


FFT from intensity of the obj. (U_2)



Restored and smoothed spectrum of the intensity of object (U_0)

**U01 = 1
U02 = 0.91276
U03 = 0.97443
U04 = 0.85053
U05 = 0.49168
U06 = 0.55416
U0m = 1**



Initial (I_0) and restored (I_c) curves of brightness (Intensity at relative units)

**T1 = 2.31 s
T2 = 1.17 s
T3 = 0.78 s
T4 = 0.58 s
T5 = 0.47 s
T6 = 0.39 s
Tm = 2.31 s
F = 5 Gc
dT = 61.78 s
T0 = 2.326**

Fig. 4.6.

The object 86097001: Cosmos 1897, USSR

Light curves are shown in fig. 4.7 and 4.8. They were selected as the most typical from a number of curves for this object.

Comparison of both figures shows that the general form of light curve can strongly change depending on sight phase. First three harmonics: $T_0=94$ s, $T_2=47$ s and $T_3=23$ s are constant (the main period of Fourier-spectrum didn't appear in fig. 4.7 just because of insufficient length of realization). An additional feature (beside periodical components) for this object is half-width of the sharpest peak which has the same value at both figures: $\tau=1.5\pm0.3$ s. It is clear that this is a purely mirror component and that it can serve not only as an additional SO feature but also as a starting point for definition of the main kinetic momentum vector of SO.

The object is slowly drifting towards the East and, likely, is not active (additional measurements are needed). Anyway, it can be excellently selected by its light curve at an interval >200 s.

FILE = 500365.04

Nkosr = 500365

Nkonor = 18575
(Cosmos 1897, USSR, p-t)

Day = 26

Month = 2

Year = 1997

Nkoint = 87096.001

Ag = 78.8

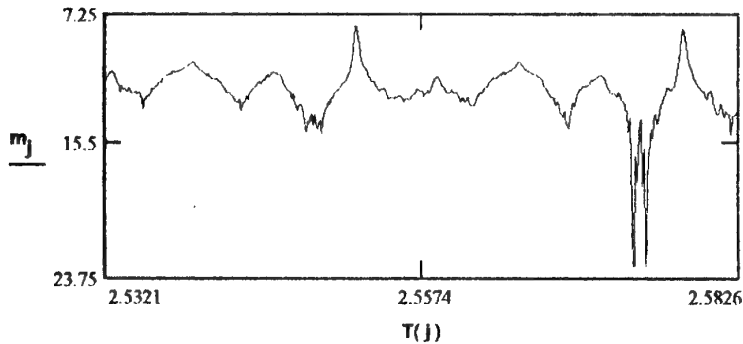
hg = 28.1

Lg = 83.0

phase = 74.0

Vector at t0:

a = 42179.84411



ten = 60.1

e = 0.00048

m1 = 8

In = 6.2268

m2 = 23

OM = 54.87948

t0 = 2.53213

w = 223.53319

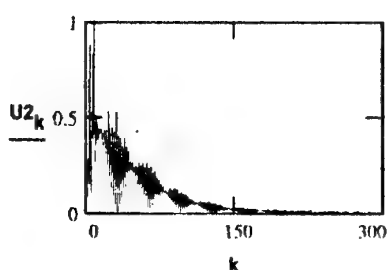
tm = 2.58258 u = 172.78737

dT = 181.64 s n = 10

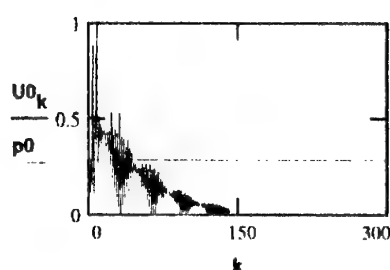
F = 2.5 Gc

np = 30

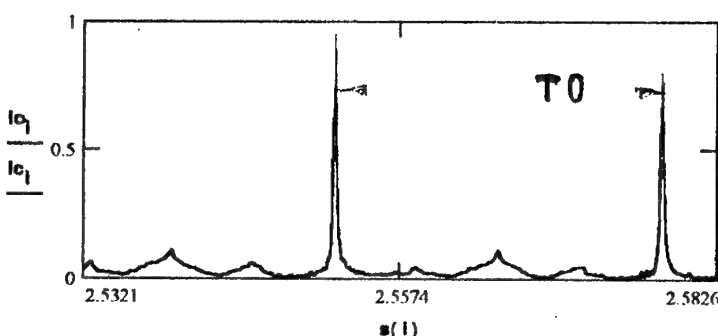
Initial curve of brightness (m; st. mag.)



FFT from intencity of the obj. (U2)



Restored and smoothed spectrum of the intencity of object (U0)



T1 = 46.57436 s

T2 = 31.04957 s

T3 = 22.705 s

T4 = 19.12 s

T5 = 15.79478 s

T6 = 13.45481 s

Tm = 22.705 s

F = 2.5 Gc

dT = 181.64 s

T0=94s

Initial (I_0) and restored (I_c) curves of brightness
(Intensity at relative units)

Fig. 1.7.

FILE = 500365.05

Nkosc = 500365

Nkonor = 18575

Day = 27

Month = 2

Year = 1997

Nkoint = 86097.001

(Cosmos 1897, USSR, d-t)

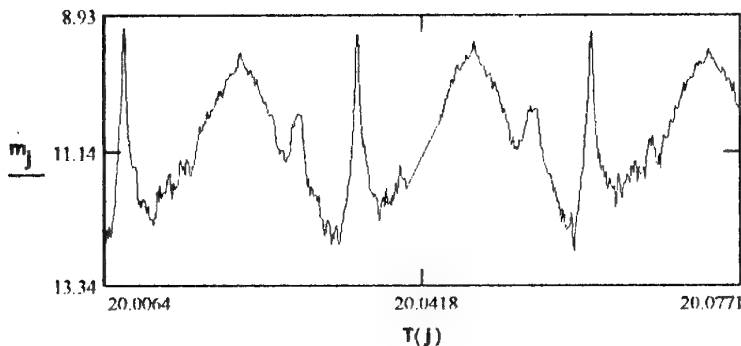
Ag = 128.2 hg = 33.1

Lg = 82.6

phase = 26.6

Vector at t0:

a = 42179.07854



ten = 20.8

e = 0.00049

m1 = 9.13

In = 6.22868

m2 = 13.14

OM = 54.85134

t0 = 20.00636

w = 227.20984

tm = 20.07715

u = 76.33762

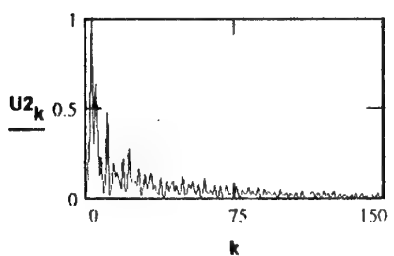
dT = 254.84 s

n = 10

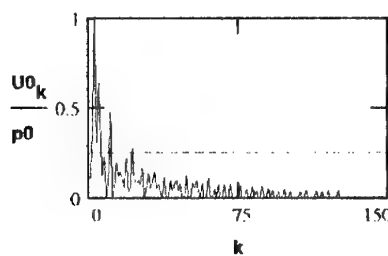
F = 2 Gc

np = 30

Initial curve of brightness (m; st. mag.)

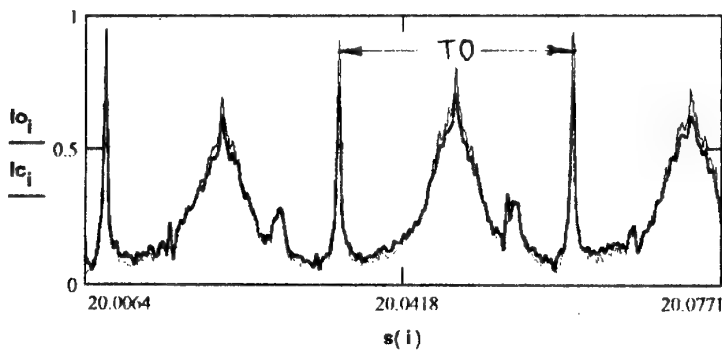


FFT from intencity of the obj. (U2)



Restored and smoothed spectrum
of the intencity of object (U0)

U01 = 1
U02 = 0.63558
U03 = 0.47465
U04 = 0.27311
U05 = 0
U06 = 0
U0m = 1



Initial (Io) and restored (Ic) curves of brightness
(Intensity at relative units)

T1 = 94.38519 s

T2 = 52.54433 s

T3 = 23.37982 s

T4 = 11.63653 s

T5 = 0 s

T6 = 0 s

Tm = 94.38519 s

F = 2 Gc

dT = 254.84 s

T0 = 94 s

Fig. 43

The object 89030.001: Raduga-23, USSR

Light curves are shown in fig. 4.9 - 4.11 These curves are illustrative in two respects:

- first, they clearly say that it is unreasonable to rely on Fourier-analysis only for evaluation of characteristics of own movement and for pointing out the specific features of SO: on our opinion, initial curves are much more informative (from the point of the final set of definitive features) than their Fourier-spectra;

- and second, they are just nice and simply identify the type of an object even without coordinate information.

4 periodical components are seen immediately, without breaking down into spectrum: $T_0=136$ s, $T_2=68$ s, $T_3=34$ s, $T_4=17$ s. All other spectral components seen in the figures U_{0k} are just combination frequencies of these components.

However, object's shape is so specific that already at half-an-hour interval (compare fig. 4.9 and 4.10) light curve's form changes very strongly. And if one compares forms of curves 4.9 and 4.10 than (without numeric evaluation) one can think these curves belong to different SO!

Again, one of characteristics can be half-width of the main peak of light curve which is 1.8 s. So, purely mirror reflection also takes place here. A set of a big number of mirror points for this object (not less than 6 per period) gives a reach information for definition of parameters of SO shape and vectors of symmetry axes and different types of rotation, but this is already outside of the frames of the present work.

FILE = 30303.07

Nkosc = 30303

Nkonor = 19928

Day = 8

Month = 3

Year = 1997

Nkoint = 89030.001

(Raduga-23, USSR, d-t)

Ag = 200.1

hg = 43.4

Lg = 27.0

phase = 30.3

Vector at t0:

a = 42163.98472

ten = 19.4

e = 0.00162

m1 = 9.66

In = 4.9916

m2 = 13.14

OM = 58.80812

t0 = 23.39319

w = 281.29843

tm = 23.46023

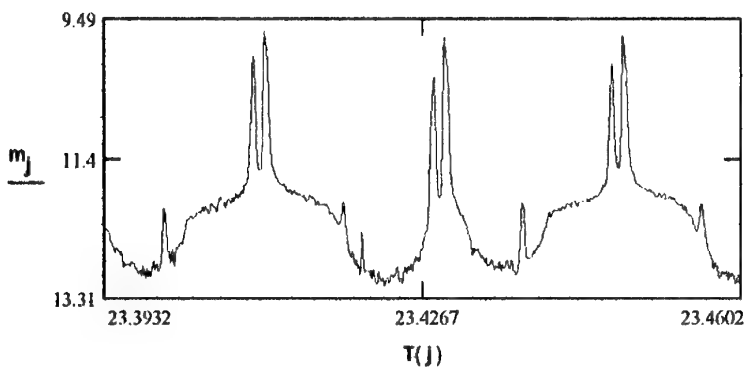
u = 82.24989

dT = 241.34 s

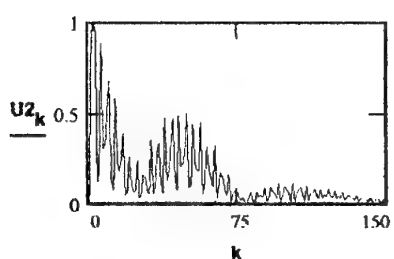
n = 10

F = 2.5 Gc

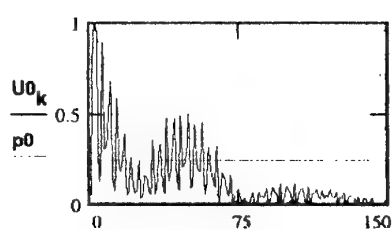
np = 30



Initial curve of brightness (m; st.mag.)

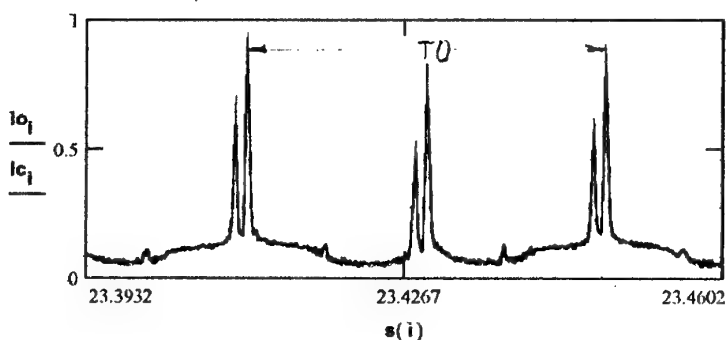


FFT from intencity of the obj. (U2)



Restored and smoothed spectrum
of the intencity of object (U0)

U01 = 1
U02 = 0.89126
U03 = 0.67659
U04 = 0.58853
U05 = 0.39683
U06 = 0.26719
U0m = 1



Initial (Io) and restored (Ic) curves of brightness
(Intensity at relative units)

T1 = 68.95 s
T2 = 33.06 s
T3 = 22.77 s
T4 = 17.88 s
T5 = 13.79 s
T6 = 11.77 s

Tm = 68.95 s
F = 2.5 Gc
dT = 241.34 s

$T0 = 135.7$ s

Fig 4.9

FILE = 3030308

Nkosr = 30303

Nkonor = 19928

Day = 9

Month = 3

Year = 1997

Nkolmt = 89030.001 (Raduga -23, USSR, d-t)

Ag = 200

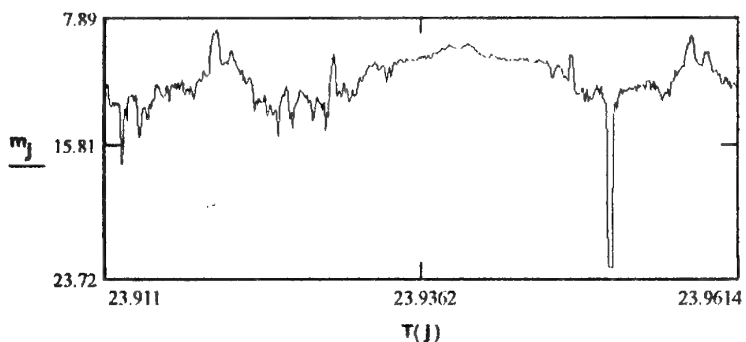
hg = 43.4

Lg = 27.0

phase = 22.5

Vector at t0:

a = 42163.73555



ten = 11.6

e = 0.00163

m1 = 8.61

In = 4.99176

m2 = 23

OM = 58.78945

t0 = 23.911

w = 280.3938

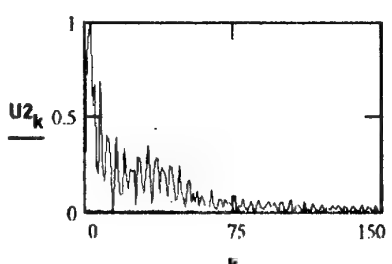
tm = 23.96141 u = 91.04576

dT = 181.48 s n = 10

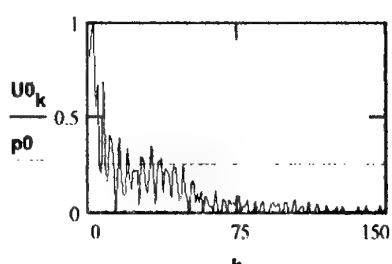
F = 2.5 Gc

np = 30

Initial curve of brightness (m; st. mag.)

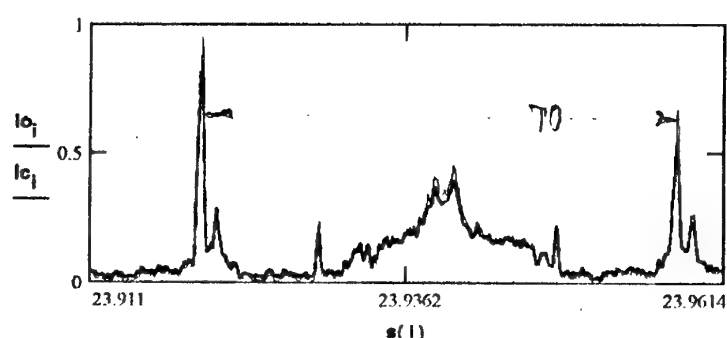


FFT from intencity of the obj. (U2)



Restored and smoothed spectrum
of the intencity of object (U0)

U01 = 1
U02 = 0.67188
U03 = 0.68574
U04 = 0.40071
U05 = 0.3876
U06 = 0.33047
U0m = 1



Initial (Io) and restored (Ic) curves of brightness
(Intensity at relative units)

T1 = 65.99273 s
T2 = 34.24151 s
T3 = 23.87895 s
T4 = 17.28381 s
T5 = 11.70839 s
T6 = 9.30667 s
Tm = 65.99273 s
F = 2.5 Gc
dT = 181.48 s

T0=135.7s

Fig. 1.10

FILE = 30303.13

Nkosr = 30303

Nkonor = 19928

Day = 14

Month = 3

Year = 1997

Nkoint = 89030.001

(Raduga -23, USSR, p-t)

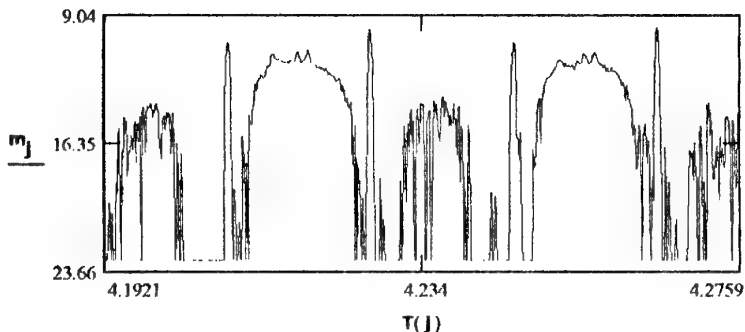
Ag = 198.8 hg = 40

Lg = 27.1

phase = 43.2

Vector at t0:

a = 42162.94143



ten = 35.5

e = 0.00171

m1 = 9.7

In = 4.99885

m2 = 23

OM = 58.69283

t0 = 4.19214

w = 279.18445

tm = 4.27588

u = 159.4362

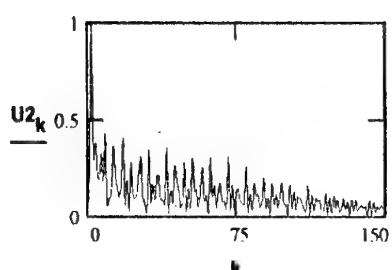
dT = 301.44 s

n = 10

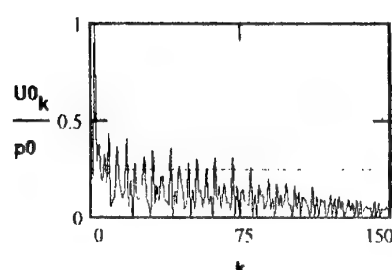
F = 2 Gc

np = 30

Initial curve of brightness (m; st. mag.)



FFT from intencity of the obj. (U2)



Restored and smoothed spectrum
of the intencity of object (U0)

U01 = 1

U02 = 0.37937

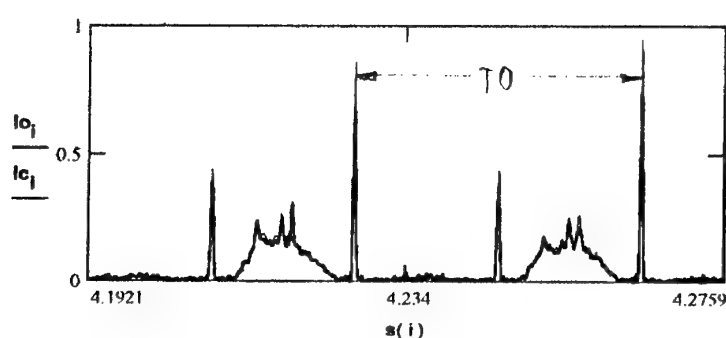
U03 = 0.32604

U04 = 0.43247

U05 = 0.36666

U06 = 0.40819

U0m = 1



T1 = 137.01818 s

T2 = 68.50909 s

T3 = 45.67273 s

T4 = 33.86966 s

T5 = 23.18769 s

T6 = 17.22514 s

Tm = 137.0181 s

F = 2 Gc

dT = 301.44 s

T0 = 135.7 s

Initial (I_o) and restored (I_c) curves of brightness
(Intensity at relative units)

Fin. L. A.

The object 90002.002: Leasat-, US.

Light curve is shown in fig. 4.12. The object was selected as an example of a situation when especially Fourier-spectrum (unlike the previous case) almost simply defines that the SO belongs to a given class. The spectrum contains 2 information components: $T_0=1.96$ s and the third harmonics $T_2=0.66$ s. Numeric values of the coordinate vector show absence of any noticeable drift. The high degree of regularity of light curve change (in combination with the absence of drift) says that the object is likely active and stabilized by rotation. The special feature of this object is rather small light changes (not greater than $0.3''$ relative to its average magnitude). This says about purely diffusion dissipation of solar radiation (at least for this phase of aspect) and presence of one informational scanning element with scanning period of ~ 2 s.

FILE = 500363.02

Nkosr = 500363

Nkonor = 20410

Day = 26

Month = 2 Year = 1997

Nkoint = 90002.002

(Leasat-5, US, d-t)

Ag = 137.8

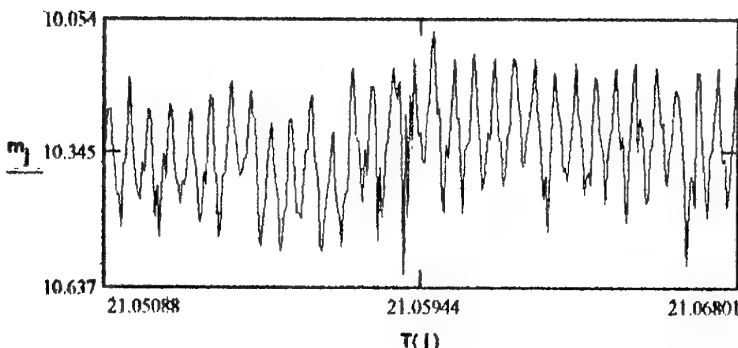
hg = 34.5

Lg = 75.1

phase = 20.7

Vector at t0:

a = 42165.416



ten = 12.7 e = 0.000254

m1 = 10.08 ln = 3.649929

m2 = 10.61 OM = 24.793

t0 = 21.050878 w = 124.477

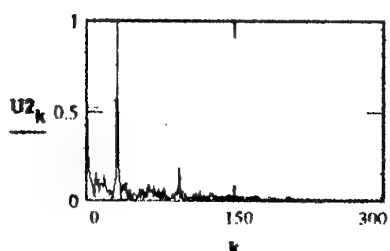
tm = 21.068006 u = 114.129

dT = 61.66 s n = 9

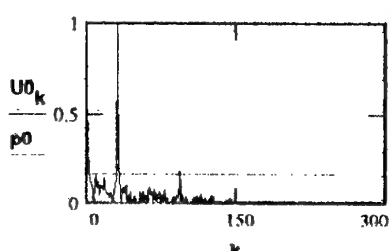
F = 5 Gc

np = 30

Initial curve of brightness (m; st. mag.)

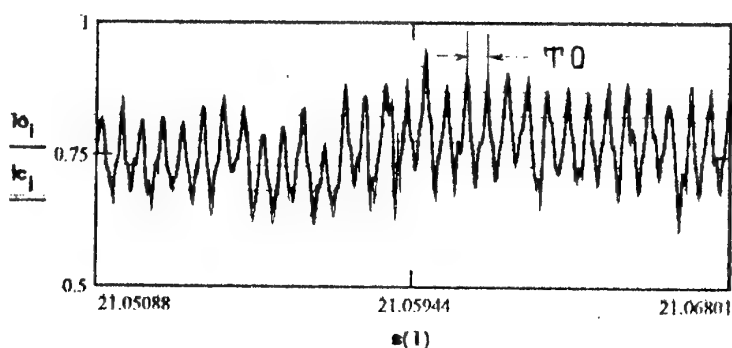


FFT from intencity of the obj. (U2)



Restored and smoothed spectrum
of the intencity of object (U0)

U01 = 1
U02 = 0.18307
U03 = 0
U04 = 0
U05 = 0
U06 = 0
U0m = 1



T1 = 1.98 s
T2 = 0.66 s
T3 = 0.00 s
T4 = 0.00 s
T5 = 0.00 s
T6 = 0.00 s

Tm = 1.98 s
F = 5 Gc
dT = 61.66 s

T0 = 1.96 s

Initial (Io) and restored (Ic) curves of brightness
(Intensity at relative units)

Fig. 4.12

The objects 90054.001: Gorizont-20, USSR, and 84101.001: Galaxy-3, USA

Light curves are shown in fig. 4.13 - 4.15 With this, the fig. 4.14 shows smoothed intensity curve $I_c = I_c(t)$ according to the type of spectrum UO_k . These curves are given as an example of objects with the variable light but without reliably pointed out periodical components. In other words, there is no any stable quantitative characteristics of object's change and its belonging to any class. This means that one shall continue collection of photometric data of such type of objects with possible increase of observation intervals (for 90054) and sampling rate (for 84101) with further usage of atmospheric distortions compensation method described in the section 2 of the present report.

FILE = 3030401

Nkosc = 30304

Nkonor = 20659

Day = 8

Month = 3

Year = 1997

Nkoint = 90054.001

(Gorizont 20, USSR, p-t)

Ag = 203

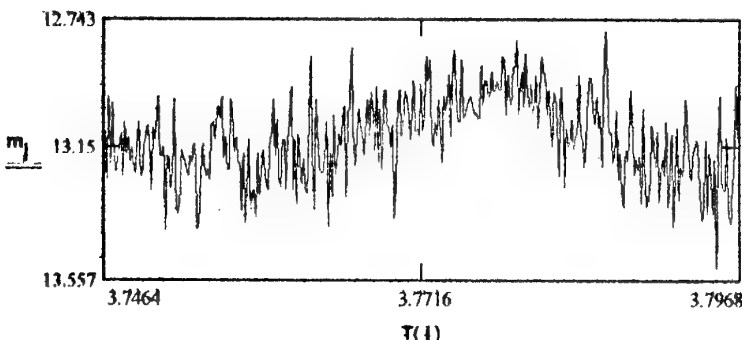
hg = 40.1

Lg = 24.0

phase = 33.5

Vector at t0:

a = 42166.558



ten = 25.6

e = 0.000136

m1 = 12.78

In = 3.941277

m2 = 13.52

OM = 65.375

t0 = 3.746358

w = 27.466

tm = 3.796781

u = 137.388

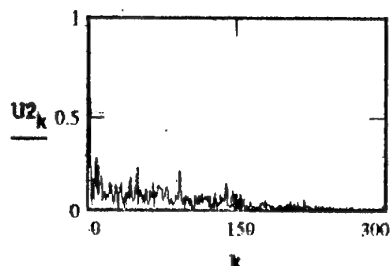
dT = 181.52 s

n = 10

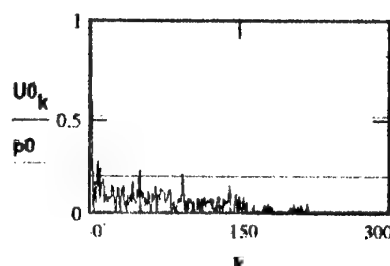
F = 2 Gc

np = 30

Initial curve of brightness (m; st.mag.)



FFT from intencity of the obj. (U2)



Restored and smoothed spectrum
of the intencity of object (U0)

U01 = 0.282347

U02 = 0.242849

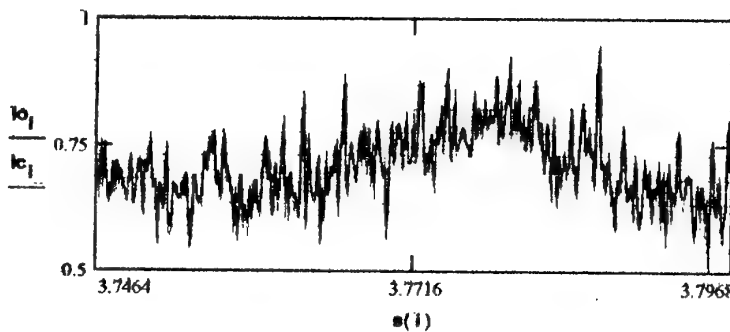
U03 = 0.229433

U04 = 0.20856

U05 = 0

U06 = 0

U0m = 1



T1 = 22.14 s

T2 = 18.91 s

T3 = 3.66 s

T4 = 1.96 s

T5 = 0.00 s

T6 = 0.00 s

Tm = 181.52 s

F = 2 Gc

dT = 181.52 s

Initial (Io) and restored (Ic) curves of brightness
(Intensity at relative units)

Fig. 4.13

FILE = 3030401

Nkosc = 30304

Nkonor = 20659

Day = 8

Month = 3

Year = 1997

Nkoint = 90054.001

(Gorizont 20, USSR, p-t)

Ag = 203

hg = 40.1

Lg = 24.0

phase = 33.5

Vector at t0:

a = 42166.558

ten = 25.6 e = 0.000136

m1 = 12.78 ln = 3.941277

m2 = 13.52 OM = 65.375

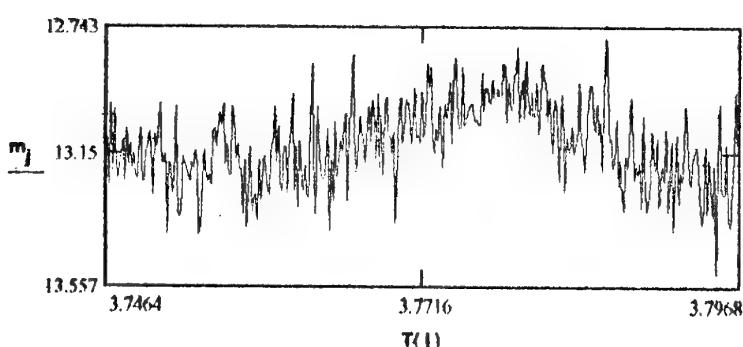
10 = 3.746358 w = 27.466

tm = 3.796781 u = 137.388

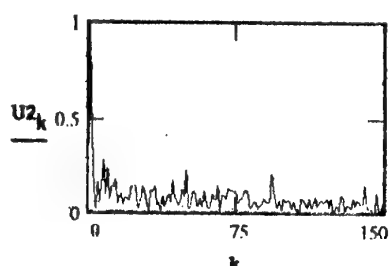
dT = 181.52 s n = 10

F = 2 Gc

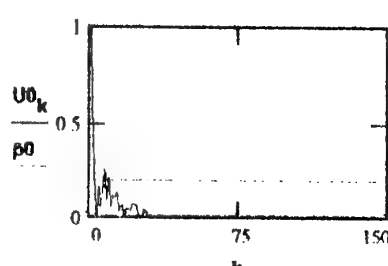
np = 30



Initial curve of brightness (m; st.mag.)



FFT from intencity of the obj. (U2)



Restored and smoothed spectrum
of the intencity of object (U0)

U01 = 0.258912

U02 = 0.211935

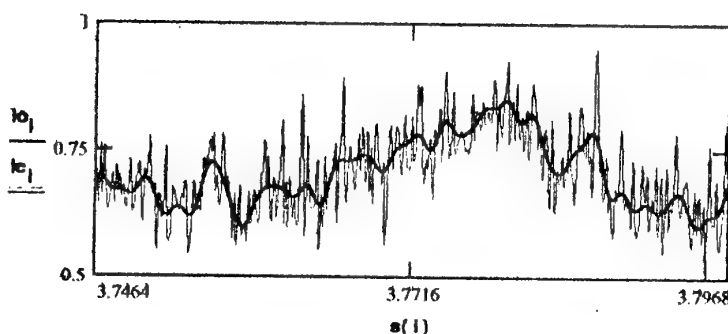
U03 = 0

U04 = 0

U05 = 0

U06 = 0

U0m = 1



T1 = 22.14 s

T2 = 18.91 s

T3 = 0.00 s

T4 = 0.00 s

T5 = 0.00 s

T6 = 0.00 s

Tm = 181.52 s

F = 2 Gc

dT = 181.52 s

Initial (Io) and restored (Ic) curves of brightness
(Intensity at relative units)

Fig. 1. 1.

FILE = 218940

Nkosc = 218940

Nkonor = 15308

Day = 16

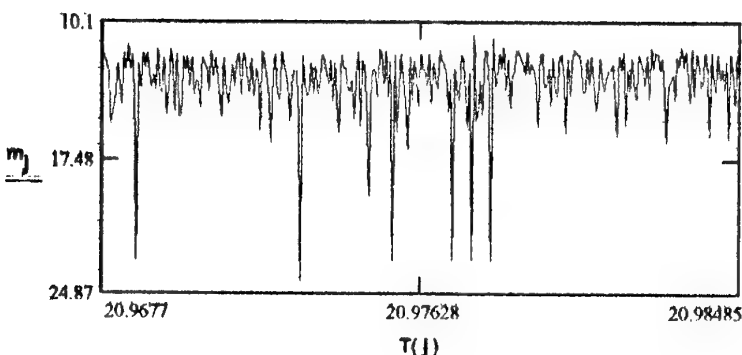
Month = 10 Year = 1996

Nkoint = 84101.001

(Galaxy-3, US, d-t)

Ag = 189.22 hg = 37.8 Lg = 34.1 phase = 55.3 Vector at t0:

a = 42286.923



ten = 44.2 e = 0.000922

m1 = 10.77 ln = 1.393471

m2 = 24.2 OM = 79.316

t0 = 20.9677 w = 102.457

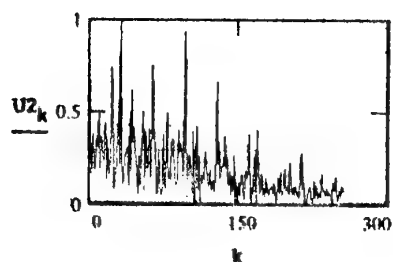
tm = 20.98485 u = 250.621

dT = 61.74 s n = 9

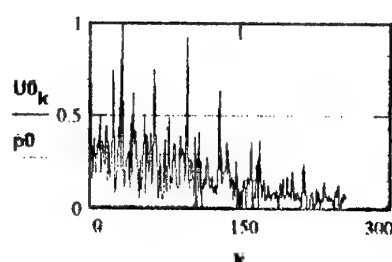
F = 5 Gc

np = 30

Initial curve of brightness (m; st.mag.)



FFT from intencity of the obj. (U2)



Restored and smoothed spectrum of the intencity of object (U0)

U01 = 0.740145

U02 = 0.542656

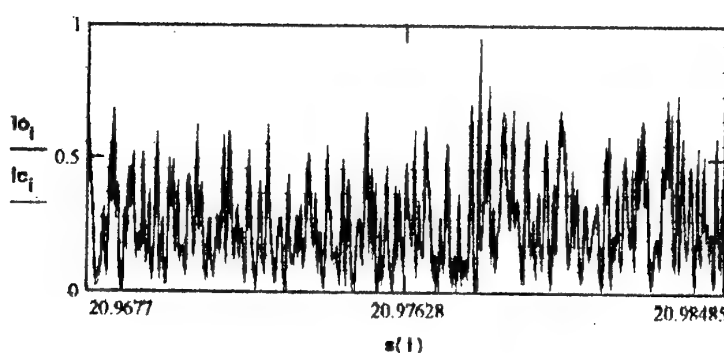
U03 = 1

U04 = 0.61845

U05 = 0.502411

U06 = 0.744723

U0m = 1



**Initial (Io) and restored (Ic) curves of brightness
(Intensity at relative units)**

T1 = 2.74 s

T2 = 2.09 s

T3 = 1.93 s

T4 = 1.45 s

T5 = 1.13 s

T6 = 0.97 s

Tm = 1.93 s

F = 5 Gc

dT = 61.74 s

Fig. 4.15

The object 91080.002: Imews-2-16, USA

This object's light curves are shown in fig. 4.16 - 4.24. This is one of the most favorite object for specialists dealing with photometry of GSO. The attention to this satellite is because, on one hand, its light curve's form is a very typical one (for some phases of aspect) and on the other hand - because this curve can be almost simply interpreted by known geometry form and type of satellite stabilization. So, we will stop on it in more detail.

Nine figures given below (4.16. - 4.24.) illustrate change of the Imews object light curve for different phases of aspect and different phase angles.

A priori it is known from different literature sources that Imews satellite is a cylindrical body with 4 panels of solar batteries at one butt and with asymmetrical informational scanning element (photo receiver of far infrared range). With this, the satellite rotation is used both for its orientation's stabilization and for scanning of determined area of the Earth surface by the photo receiver. Period of rotation of the satellite around the main symmetry axis, as it is seen from figures, is with high accuracy: $T_0 = 10 \text{ s} \pm 0.05 \text{ s}$. The four solar panels are symmetrically located relative to rotation axis what is clearly seen in fig. 4.18, 4.19, 4.21. The aforementioned asymmetrical scanning element is also clearly seen in these figures (small peaks divided by the interval T_0). Really, the spacecraft structure (of course, only its form directly influencing the light curve) is much more complex. This is seen, for instance, in fig. 4.16 and 4.17. Both solar arrays ($T=2.5 \text{ s}$) and main rotation period T_0 are seen there, but there also is a number of other peaks witnessing about presence of other diffusion reflecting functional elements (this can be a subject for independent analysis). It is interesting that these additional elements are appearing better in the absence of a strong masking mirror component from the solar arrays. By the way, the width of mirror glare from an array at the level 0.5 is $\sim 0.65 \text{ s}$, what corresponds to an angle $\sim 24^\circ$ of turn around the axis. This turn angle, in combination with the approximately known orientation of arrays relative to their rotation axis and relative to the Sun at mirror point, basically allows to define dimensions and useful area of these arrays, and therefore to evaluate energy potential of the satellite (this is a topic for a separate work).

Light curves at figures 4.18. and 4.19. are separated by an interval of only 13 minutes. However, it is clearly seen how character of mirror flashes from the arrays changed during these 13 minutes: though aspect phase and phase angle changed only by 3 degrees, this appeared to be enough for disappearance of couple symmetry of flashes, and all flashes became approximately equal (in terms of imposition of weak modulation of intensity with non-obvious period).

Fig. 4.22 - 4.24 show light curves of 3 consequential phases: approach the Earth's shade (4.22), shade entry (4.23) and shade exit (4.24). These figures are interesting because they show dynamics of orientation change of solar arrays planes right before the entry to the Earth shadow and confirm that the satellite is active.

The given set of figures shows that separate light curves of Imews satellite (fig. 4.17, 4.22 for example) can be of little use for recognition and determination of functional state of a satellite, and one shall use long rows of measurements covering a big set of aspect phases and phase angles.

FILE = 500360.06

Nkosc = 500360

Nkonor = 50036
(Imews-2-16 , US, p-t)

Day = 29

Month = 5

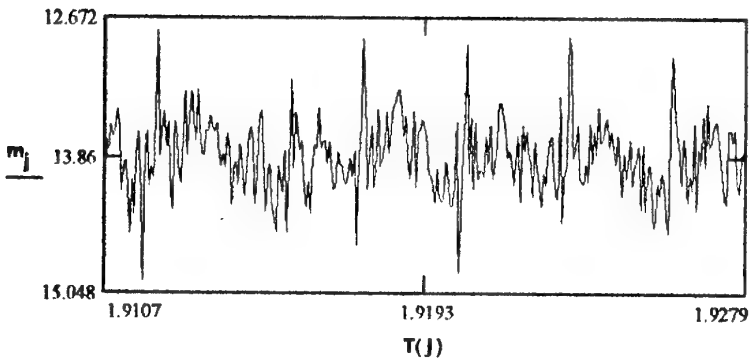
Year = 1996

Nkolnt = 0

hg = 31.6 Lg = 69.6 phase = 44.3

Vector at t0:

a = 42163.155



ten = 47.8 e = 0.000829

m1 = 12.78 ln = 1.168912

m2 = 14.94 OM = 79.942

t0 = 1.910728 w = 46.601

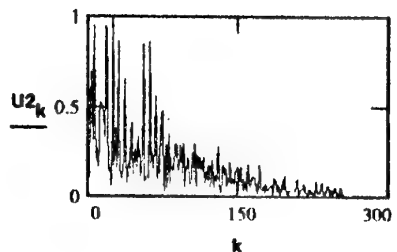
tm = 1.927889 u = 220.075

dT = 61.78 s n = 9

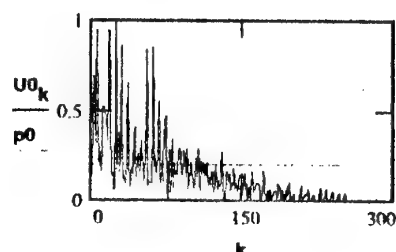
F = 5 Gc

np = 30

Initial curve of brightness (m; st. mag.)

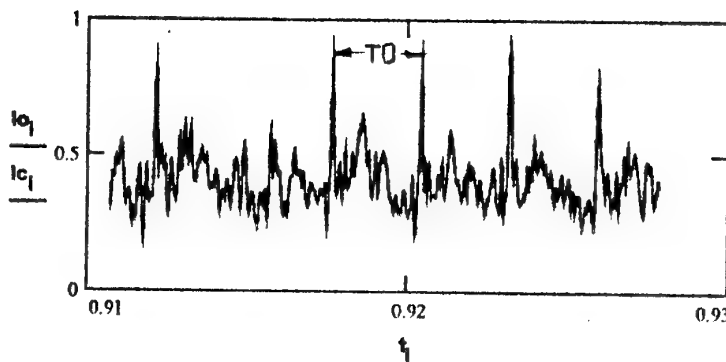


FFT from intencity of the obj. (U2)



Restored and smoothed spectrum
of the intencity of object (U0)

U01 = 0.697388
U02 = 0.951848
U03 = 0.270565
U04 = 0.527111
U05 = 0.94925
U06 = 1
U0m = 1



Initial (Io) and restored (Ic) curves of brightness
(Intensity at relative units)

T1 = 21.01 s
T2 = 9.96 s
T3 = 6.94 s
T4 = 4.83 s
T5 = 3.53 s
T6 = 2.51 s

Tm = 2.51 s
F = 5 Gc
dT = 61.78 s

T0=9.94s

FILE = 50036.12

Nkosc = 500360

Nkonor = 21805
(Imnews-2-16 , US, p-t)

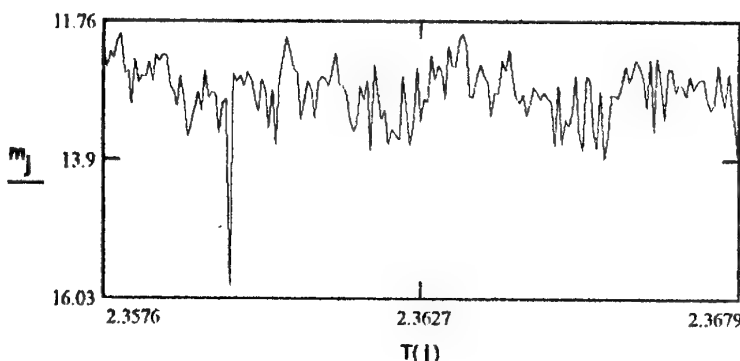
Day = 27

Month = 8

Year = 1996

Nkoint = 0

hg = 31.4 Lg = 69.4 phase = 61.9 Vector at t0:



$a = 42165.553$

$t_{en} = 51 \quad e = 0.000813$

$m_1 = 11.95 \quad l_n = 1.380759$

$m_2 = 15.84 \quad OM = 80.829$

$t_0 = 2.357617 \quad w = 55.831$

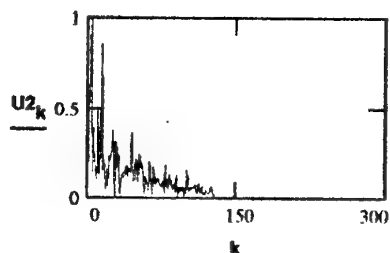
$t_m = 2.36785 \quad u = 314.448$

$dT = 36.84 \text{ s} \quad n = 8$

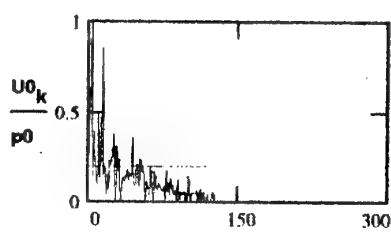
$F = 5 \text{ Gc}$

$np = 30$

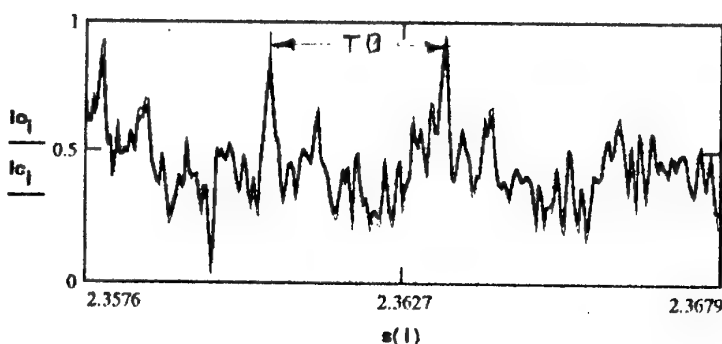
Initial curve of brightness (m; st.mag.)



FFT from intencity of the obj. (U2)



Restored and smoothed spectrum of the intencity of object (U0)



$T_1 = 9.96 \text{ s}$

$T_2 = 5.94 \text{ s}$

$T_3 = 3.38 \text{ s}$

$T_4 = 2.49 \text{ s}$

$T_5 = 2.11 \text{ s}$

$T_6 = 1.71 \text{ s}$

$T_m = 9.96 \text{ s}$

$F = 5 \text{ Gc}$

$dT = 36.84 \text{ s}$

T0=10.0s

Initial (I_o) and restored (I_c) curves of brightness
(Intensity at relative units)

Fig. 4.17

FILE = 500360.16

Nkosr = 500360

Nkonor = 21805

Day = 15

Month = 12 Year = 1996

Nkolnt = 91080.002

(Imews-2-16 ,US, p-t)

hg = 33.6

Lg = 70.1

phase = 86.1

Vector at t0:

a = 42164.039

ten = 71.7 e = 0.000719

m1 = 9.57 ln = 1.595427

m2 = 14.89 OM = 78.558

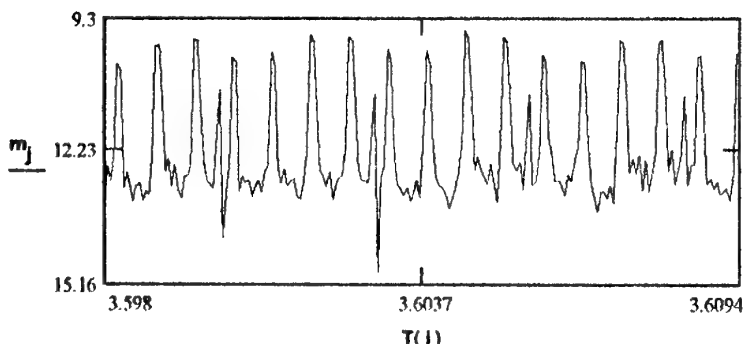
t0 = 3.598033 w = 64.883

tm = 3.60935 u = 84.451

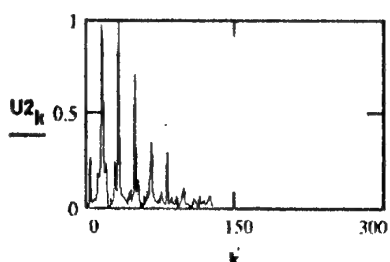
dT = 40.74 s n = 8

F = 5 Gc

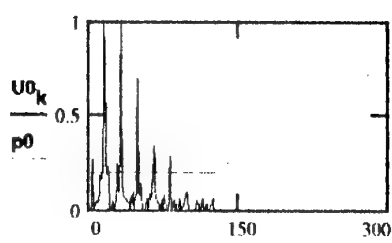
np = 30



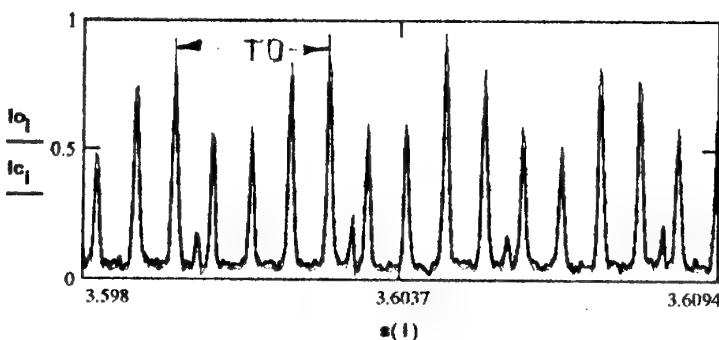
Initial curve of brightness (m; st.mag.)



FFT from intencity of the obj. (U2)



Restored and smoothed spectrum of the intencity of object (U0)



Initial (Io) and restored (Ic) curves of brightness
(Intensity at relative units)

T1 = 10.03 s
T2 = 2.51 s
T3 = 2.05 s
T4 = 1.41 s
T5 = 1.25 s
T6 = 0.84 s
Tm = 1.25 s
F = 5 Gc
dT = 40.74 s

T0=10.0s

Fig. 4.18

FILE = 500360.18

Nkoar = 500360

Nkonor = 0

Day = 15

Month = 12 Year = 1996

Nkolnt = 91080.002

(Imews-2-16 , US, p-t)

hg = 33.6 Lg = 70.1

phase = 89.3

Vector at t0:

a = 42163.944

ten = 75 e = 0.000716

m1 = 9.47 ln = 1.595429

m2 = 13.25 OM = 78.558

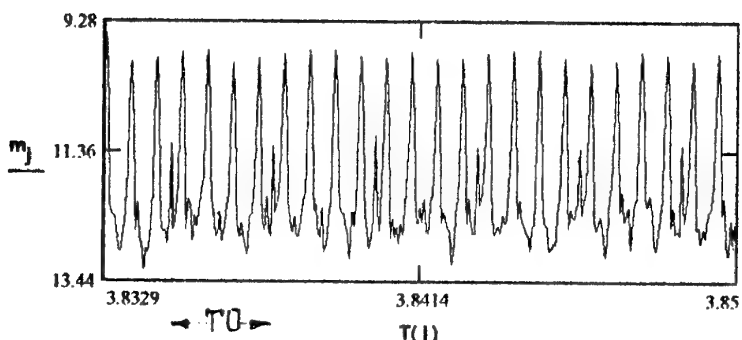
10 = 3.832872 w = 64.902

tm = 3.850006 u = 87.987

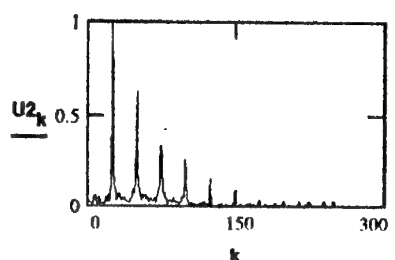
dT = 61.68 s n = 9

F = 5 Gc

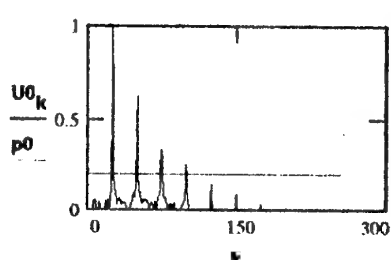
np = 30



Initial curve of brightness (m; st. mag.)

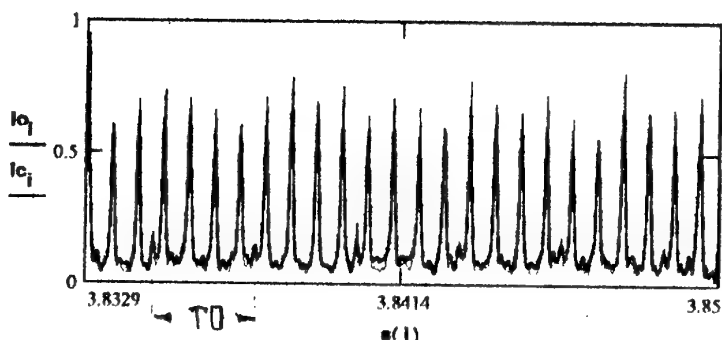


FFT from intencity of the obj. (U2)



Restored and smoothed spectrum of the intencity of object (U0)

U01 = 1
U02 = 0.627313
U03 = 0.332292
U04 = 0.251566
U05 = 0
U06 = 0
U0m = 1



Initial (Io) and restored (Ic) curves of brightness (Intensity at relative units)

T1 = 2.50 s
T2 = 1.24 s
T3 = 0.84 s
T4 = 0.63 s
T5 = 0.00 s
T6 = 0.00 s
Tm = 2.50 s
F = 5 Gc
dT = 61.68 s
T0=10.0s

Fig. 6-14
(

FILE = 500360.31

Nkosr = 500360

Nkonor = 21805

Day = 3

Month = 3

Year = 1997

Nkoint = 91080.002

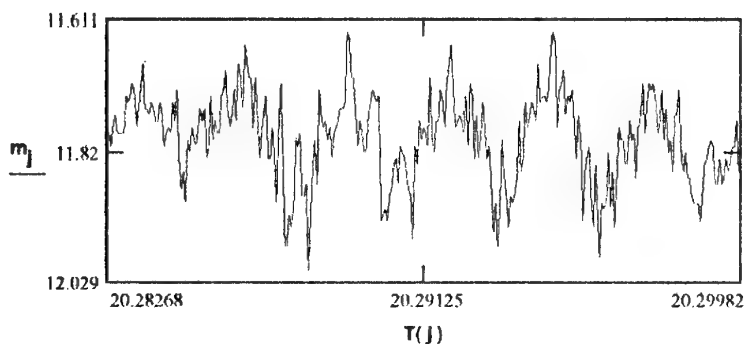
(1mews-2-16 , US, d-t)

hg = 33.7

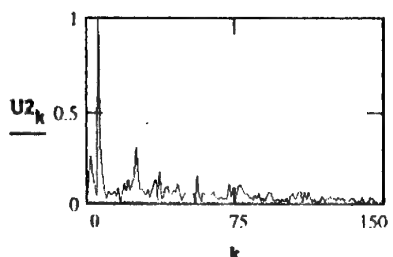
Lg = 69.5

phase = 33.0

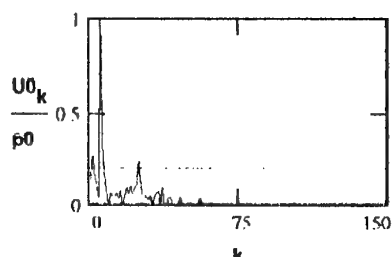
Vector at
t00=19h00m00s



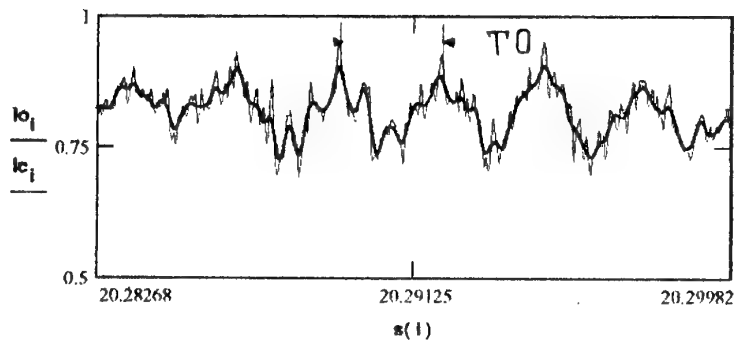
Initial curve of brightness (m; st.mag.)



FFT from intensity of the obj. (U2)



Restored and smoothed spectrum
of the intensity of object (U0)



Initial (Io) and restored (Ic) curves of brightness
(Intensity at relative units)

T1 = 26.82 s

T2 = 10.08 s

T3 = 2.51 s

T4 = 0.00 s

T5 = 0.00 s

T6 = 0.00 s

Tm = 10.08 s

F = 5 Gc

dT = 61.68 s

$T0=10.0s$

Fig. 4.20

FILE = 500360.36

Nkoer = 500360

Nkonor = 21805

Day = 4

Month = 3

Year = 1997

Nkoint = 91080.002

(Imews-2-16 ,US,d-t)

hg = 32.8

Lg = 69.6

phase = 82.7

Vector at
t00=01h00m00s

a = 42166.08

ten = 70 e = 0.000592

m1 = 9.5 ln = 1.761151

m2 = 13.67 OM = 79.521

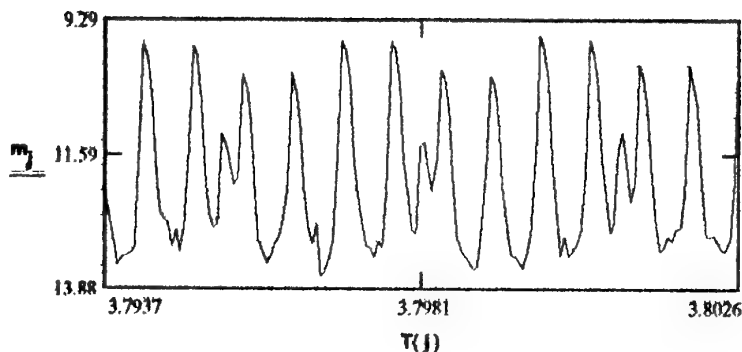
t0 = 3.793744 w = 46.768

tm = 3.80255 u = 121.783

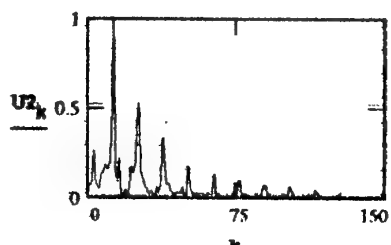
dT = 31.7 s n = 8

F = 5 Gc

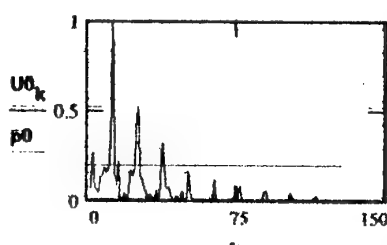
np = 30



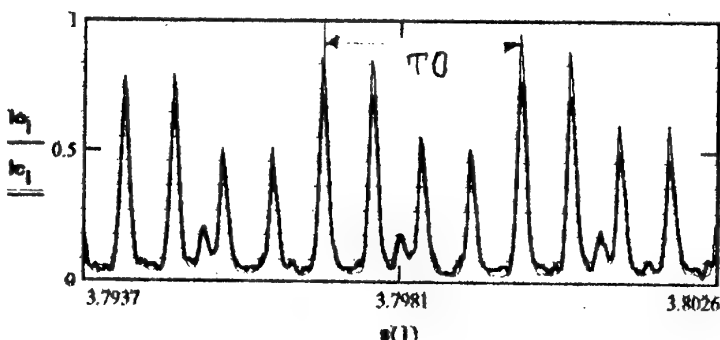
Initial curve of brightness (m; st.mag.)



FFT from intensity of the obj. (U2)



Restored and smoothed spectrum
of the intensity of object (U0)



Initial (Io) and restored (Ic) curves of brightness
(Intensity at relative units)

T1 = 10.06 s
T2 = 2.49 s
T3 = 2.03 s
T4 = 1.24 s
T5 = 0.85 s
T6 = 0.00 s
Tm = 2.49 s
F = 5 Gc
dT = 31.7 s

T0=10.0s

Fig. 4.24

FILE = 500360.37

Nkosr = 500360

Nkonor = 21805

Day = 6

Month = 3

Year = 1997

Nkoint = 91080.002

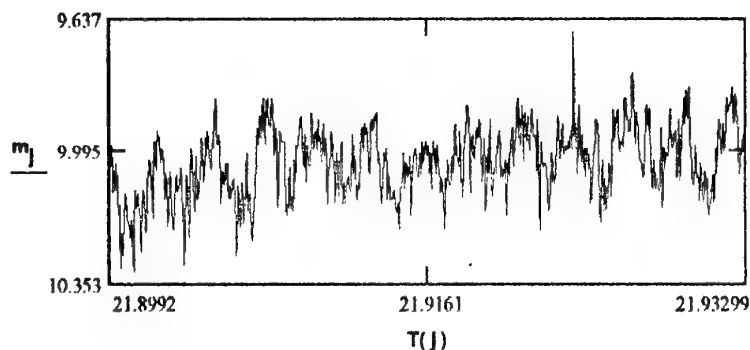
(Imews-2-16 , US, d-t)

hg = 34

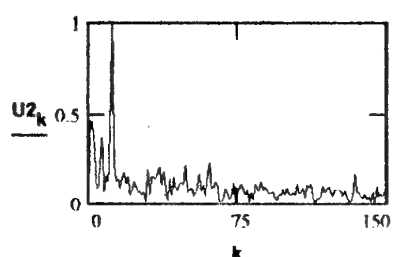
Lg = 69.5

phase = 12.2

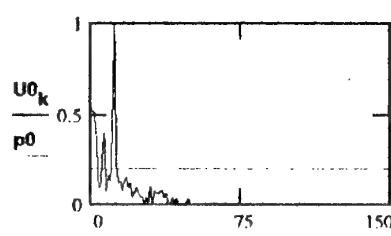
Vector at
t00=21h30m00s



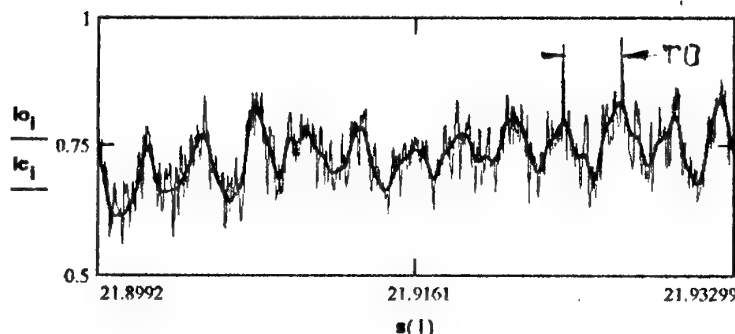
Initial curve of brightness (m ; st.mag.)



FFT from intencity of the obj. (U_2)



Restored and smoothed spectrum
of the intencity of object (U_0)



Initial (I_o) and restored (I_c) curves of brightness
(Intensity at relative units)

$T_1 = 17.02$ s

$T_2 = 10.01$ s

$T_3 = 0.00$ s

$T_4 = 0.00$ s

$T_5 = 0.00$ s

$T_6 = 0.00$ s

$T_m = 10.01$ s

$F = 5$ Gc

$dT = 121.66$ s

$T_0 = 10.0$ s

Fig. 4. C 11

FILE = 500360.38

Nkosr = 500360

Nkonor = 21805

Day = 6

Month = 3 Year = 1997

Nkolmt = 91080.002

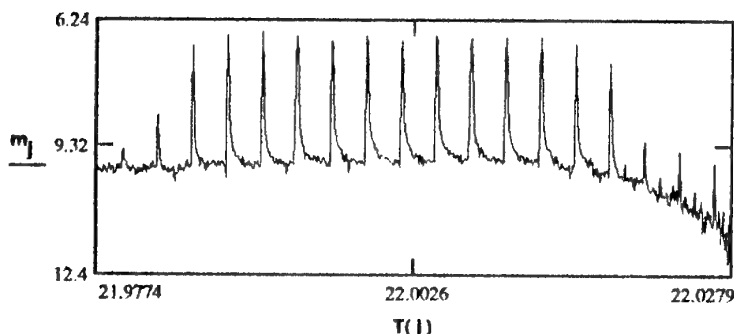
(Imews-2-16 , US, d-t)

hg = 34

Lg = 69.5

phase = 11.4

Vector at
t00=21h30m00s



Initial curve of brightness (m; st.mag.)

a = 42168.112

ten = 0.6 e = 0.000683

m1 = 6.52 ln = 1.767733

m2 = 12.12 OM = 79.64

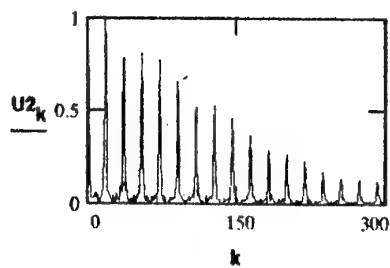
t0 = 21.977394 w = 50.9

tm = 22.027872 u = 71.895

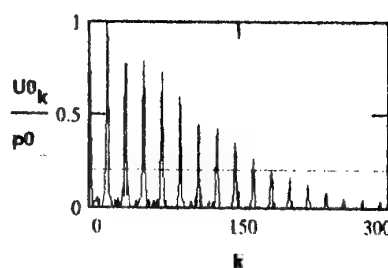
dT = 181.72 s n = 10

F = 5 Gc

np = 30

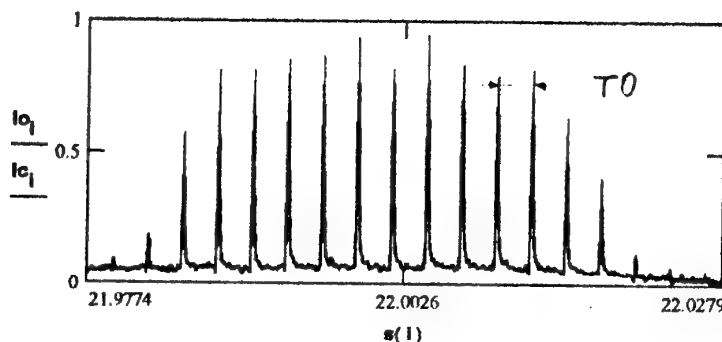


FFT from intencity of the obj. (U2)



Restored and smoothed spectrum
of the intencity of object (U0)

U01 = 1
U02 = 0.776211
U03 = 0.786249
U04 = 0.727234
U05 = 0.594099
U06 = 0.446553
U0m = 1



Initial (Io) and restored (Ic) curves of brightness
(Intensity at relative units)

T1 = 10.01 s
T2 = 4.94 s
T3 = 3.33 s
T4 = 2.51 s
T5 = 2.01 s
T6 = 1.66 s
Tm = 10.01 s
F = 5 Gc
dT = 181.72 s

T0=10.0s

Fig. 4.13

FILE = 500360.39

Nkosc = 500360

Nkonor = 21805

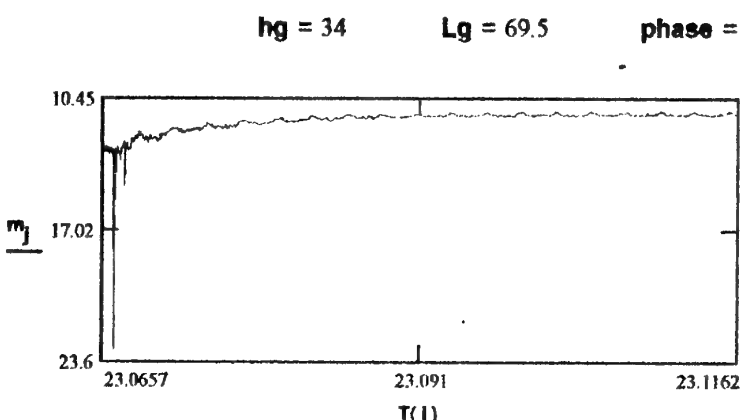
Day = 6

Month = 3

Year = 1997

Nkoint = 91080.002

(Imews-2-16 , US, d-t)



Vector at
t00=21h30m00s

a = 42168.112

ten = 0 e = 0.000683

m1 = 11.05 ln = 1.767733

m2 = 23 OM = 79.64

t0 = 23.065706 w = 50.9

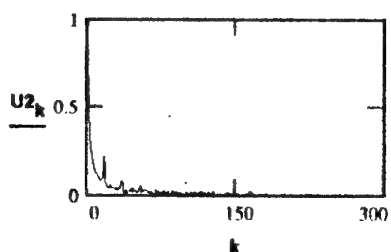
tm = 23.1162 u = 71.895

dT = 181.78 s n = 10

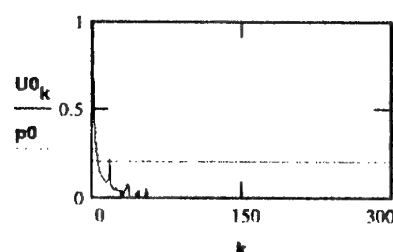
F = 5 Gc

np = 30

Initial curve of brightness (m; st.mag.)

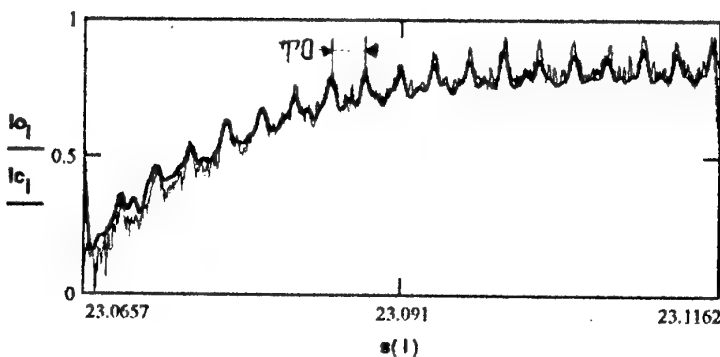


FFT from intencity of the obj. (U2)



Restored and smoothed spectrum
of the intencity of object (U0)

U01 = 0.214253
U02 = 0
U03 = 0
U04 = 0
U05 = 0
U06 = 0
U0m = 1



T1 = 10.02 s
T2 = 0.00 s
T3 = 0.00 s
T4 = 0.00 s
T5 = 0.00 s
T6 = 0.00 s
Tm = 158.07 s
F = 5 Gc
dT = 181.78 s

T0=10.0s

Initial (Io) and restored (Ic) curves of brightness
(Intensity at relative units)

Fig. 1.24

4.2. Light curves of low orbiting space objects (LOSO).

Below there is given the data of photometric observation of two low-orbiting objects: 88106.001: Lacrosse, USA and 92023.001: Ferret-D, USA.

4.2.1. The object 88106.002: Lacrosse, USA

Light curves are given in fig. 4.25.0 - 4.25.2

About the satellite 88106 it is only known that this USA object of a special purpose has a system for three-axis stabilization. That is why its light curve shall be smooth enough with the specific drops and slopes depending on aspect phase and phase angle dependent of reflections from different structure elements. However, the situation appears to be different. Fig. 4.25.0 shows change of 88106 light obtained for one session in December 1996. Here we even can hardly say about any smoothness of light change. The curve contains both clearly visible relatively slow changes (~ 10 s) and rather fast oscillations, not to say about separate flashes. These oscillations can be easily tracked at some parts 1, 2 of the curves shown in fig. 4.25.1 and 4.25.2. There are clear periodical changes with specific values of $T \sim 1-2$ s and $T_m \sim 10$ s. This obviously says about presence of some internal movements in the spacecraft structure.

4.2.2. Analysis of light curves of the object 93023.001: Ferret-D, USA

In the present section we will give a detailed description (but in first approach) of the light curves of a spacecraft.

4.2.2.1. Preliminary classification of light curves

The 92023.001 spacecraft has inclination of about 85° . This is why its visible motion is either from the South to the North (S-N) or from the North to the South (N-S). The most number of obtained light curves is related to the S-N type passes. Non-coordinate information containing in these curves we will conditionally call "bottom view". The information containing in the light curves obtained during passes of N-S type we will call "top view". This terminology is appropriate for spacecraft with at least one pointed out direction (for instance, rotation axis in case of stabilization by rotation, or an axis of the main kinetic momentum) remaining unchanged in the geocentric coordinate system in any point of the spacecraft orbit. In addition to two defined groups (S-N, N-S), it is possible to define the following subgroups:

S-N:WaWs - observed part of the spacecraft trajectory (Wa) and the Sun illuminating it (Ws) are in the Western (W) hemisphere (relative to the observing station);

S-N:WaOs - trajectory is in the West, the Sun is in the East;

S-N:OaWs - trajectory is in the East, the Sun is in the West;

S-N:OaOs - trajectory is in the East, the Sun is in the East.

Similar subgroups are defined for the group of curves N-S. From general considerations it is clear that the most likeness will have light curves of the same subgroup, and observed differences of light curves in different subgroups are related namely with different observation conditions of the spacecraft. From the same consideration, the most qualitative difference of light curves will be in the groups N-S and S-N.

4.2.2.2. Analysis goals

Analysis of the 92023001 spacecraft is performed for the solution of the following problems:

Determination of the specific periodical components of the spacecraft motion relative to the center of mass.

Reliable information about presence and intensity of these components will allow to make a conclusion about type of spacecraft stabilization in orbit.

Pic = 88106.100

FILE = 88106.100

Nkonor = 0.00000

(Lacross-2, USA)

Day = 4

Month = 12

Year = 1996

Nkosr = 881060

Nkoint = 88106.002

$\Delta m_{apr} = 1.07$

$\Delta m_{mirror} = 1.49$

$\Delta m_{mes} = 2.85$

R0 = 1792.5

Rk = 728.2

Rm = 905.0

Az0 = 240.4

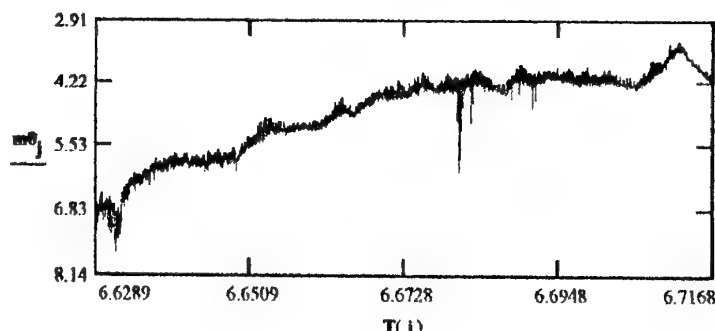
$\phi_0 = 44.7$

Azm = 381.6

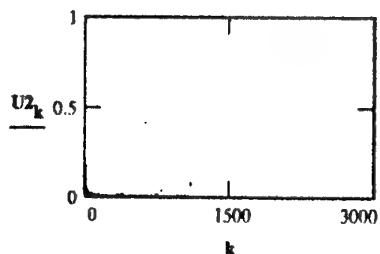
h0 = 14.3

hk = 64.1

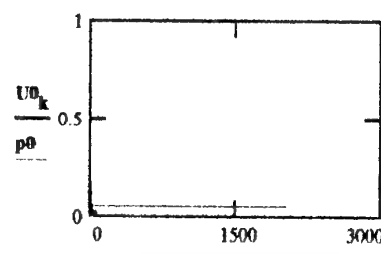
hm = 44.4



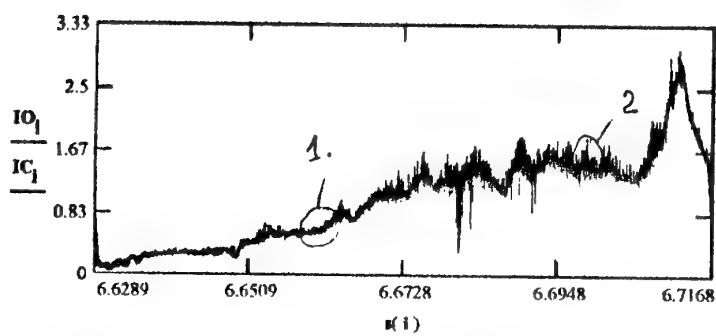
Initial curve of brightness (m; st.mag.)



FFT from intensity of the obj. (U2)



Restored and smoothed spectrum of the intensity of object(U0)



Initial (IO) and restored (IC) curves of brightness (Intensity at relative units)

$U_{0m} = 0.349$
 $U_{01} = 0.052$
 $U_{02} = 0.050$
 $U_{03} = 0.060$
 $U_{04} = 0.061$
 $U_{05} = 0.000$
 $U_{06} = 0.000$
 $U_{07} = 0.000$
 $U_{08} = 0.000$

$T_m = 105.47$ s
 $T_1 = 22.36$ s
 $T_2 = 18.5$ s
 $T_3 = 15.82$ s
 $T_4 = 13.18$ s
 $T_5 = 13.18$ s
 $T_6 = 13.18$ s
 $T_7 = 13.18$ s
 $T_8 = 13.18$ s

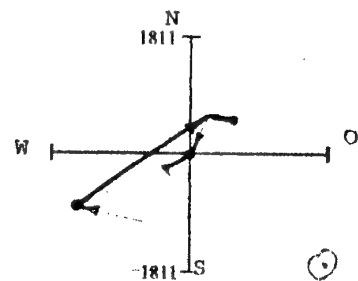


Fig. 4.25.0

Pic = 88106.104
FILE = 88106.100
Nkonor = 881060
(Lacross-2, USA)
Nkoint = 88106.002

R0 = 1227.0
Az0 = 247.4
h0 = 28.1

Nkonor = 0.00000
(Lacross-2, USA)

Day = 4

Month = 12

Year = 1996

Δm_{apr} = 0.33 **Δm_{mirror} = 0.32**

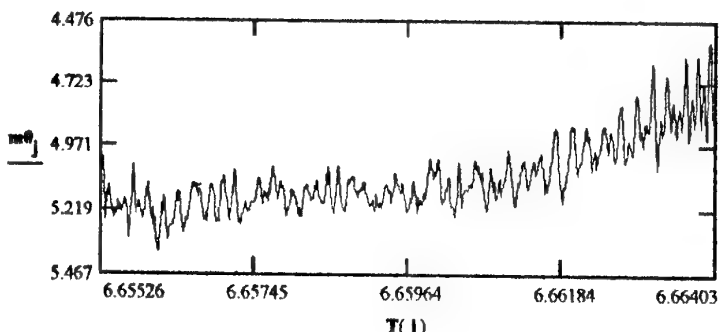
Δm_{mes} = 0.40

Vector at
t00=06h37m29s

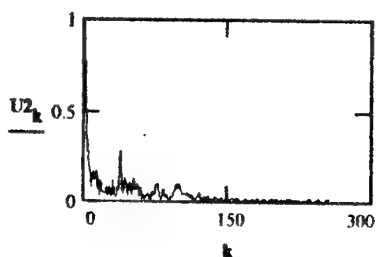
φ0 = 46.0 **φm = 44.9**
M00 = 17.32 **a = 7037.077**
e = 0.001005

m1 = 4.56 **In = 56.979**
m2 = 5.38 **OM = 126.402**
t0 = 6.65526 **w = 94.084**
tm = 6.66403 **u = 42.686**
dT = 31.6 s **n = 9**

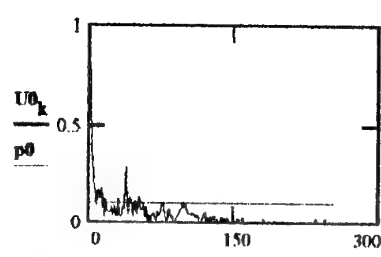
F = 25 Gc
np = 50 **p0 = 0.100**



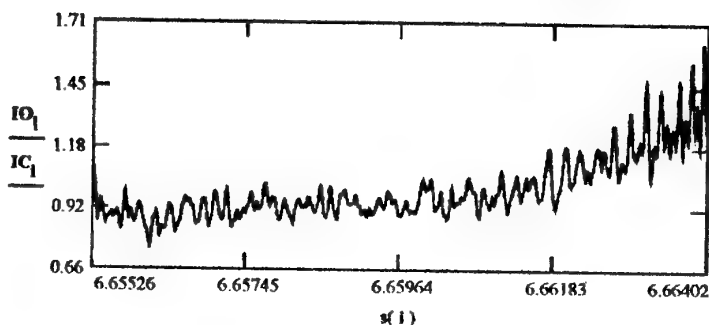
Initial curve of brightness (m; st.mag.)



FFT from intencity of the obj.(U2)



Restored and smoothed spectrum of the intencity of object(U0)



Initial (IO) and restored (IC) curves of brightness (Intensity at relative units)

U0m = 0.457
U01 = 0.168
U02 = 0.173
U03 = 0.125
U04 = 0.118
U05 = 0.120
U06 = 0.284
U07 = 0.132
U08 = 0.108

Tm = 10.53 s
T1 = 2.83 s
T2 = 2.24 s
T3 = 1.97 s
T4 = 1.76 s
T5 = 1.02 s
T6 = 0.80 s
T7 = 0.73 s
T8 = 0.66 s

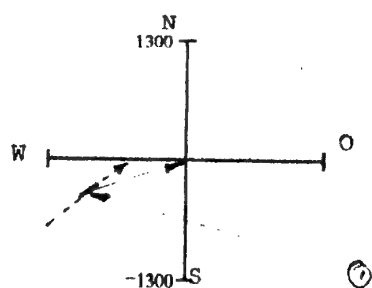


Fig. 4.25.1

Pic = 88106.109
FILE = 88106.100
Nkesr = 881060
Nkoint = 88106.002

Nkonor = 0.00000
(Lacross-2, USA)

Day = 4

Month = 12

Year = 1996

$\Delta m_{apr} = -0.31$

$\Delta m_{mirror} = -0.17$

$\Delta m_{mes} = 0.11$

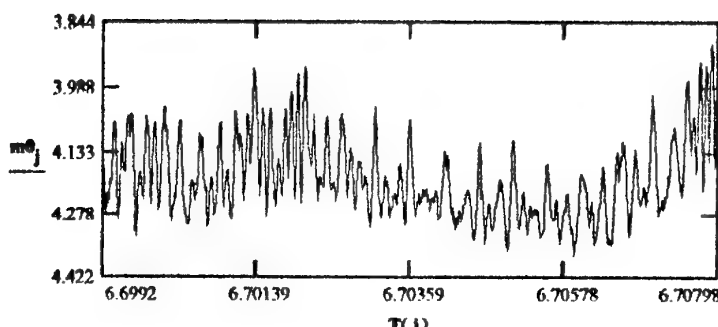
R0 = 735.9
Az0 = 339.1
h0 = 62.7

Rm = 794.9
Azm = 367.4
hm = 54.5

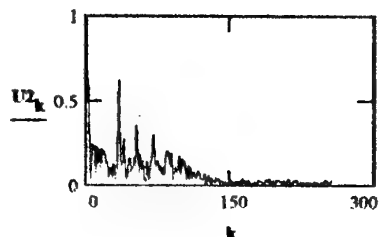
Vector at
t00=06h37m29s

$\phi_0 = 63.6$ $\phi_m = 74.1$
M00 = 17.32 a = 7037.077
e = 0.001005

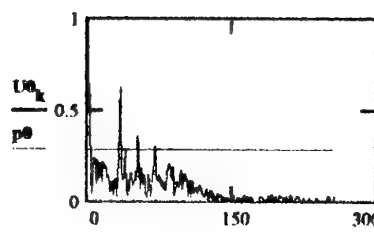
m1 = 3.89 In = 56.979
m2 = 4.37 OM = 126.402
t0 = 6.69920 w = 94.084
tm = 6.70798 u = 42.686
dT = 31.6 s n = 9
F = 25 Gc
np = 50 p0 = 0.286



Initial curve of brightness (m; st. mag.)

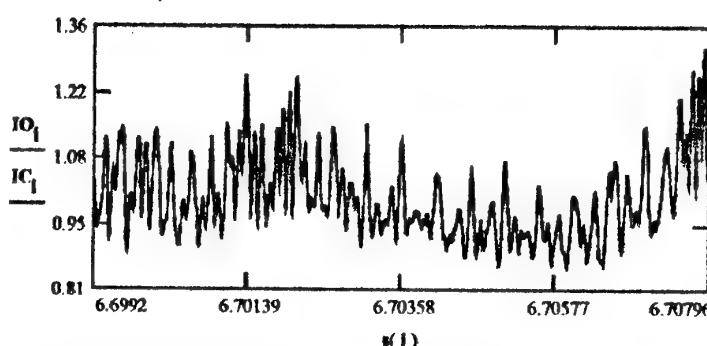


FFT from intensity of the obj.(U2)



Restored and smoothed spectrum of the Intensity of object(U0)

U0m = 1.000
U01 = 0.592
U02 = 0.628
U03 = 0.356
U04 = 0.301
U05 = 0.000
U06 = 0.000
U07 = 0.000
U08 = 0.000



Initial (IO) and restored (IC) curves of brightness (Intensity at relative units)

Tm = 0.90 S
T1 = 10.03 S
T2 = 0.9 S
T3 = 0.60 S
T4 = 0.45 S
T5 = 0.45 S
T6 = 0.45 S
T7 = 0.45 S
T8 = 0.45 S

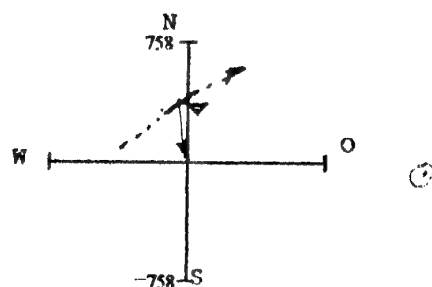


Fig. 4.25.2

4.2.2.3. Presentation and description of obtained light curves of the spacecraft 92023001.

Set and structure of figures

Fig. 5.1.0, 5.2.0, ..., 5.11.0 show general views of light curves obtained from 11 sessions of the spacecraft for a complete time interval of each session. In all figures of this paper (light curves) there was used the same form of information presentation and the same acronyms:

- Year, Month, Day of observation;
- Δm_{apr} - a priori calculated changes of light for the beginning and the end of observation interval dT taking into account change of distance and phase angle;
- Δm_{mirror} - a priori calculated changes of light for the beginning and the end of observation interval dT taking into account change of distance only;
- Δm_{mes} - measured changes of light for the beginning and the end of observation interval dT with averaging at 2 s interval (50 readings);
 t_0, t_m - time moments of the beginning and the end of presented interval dT (Moscow winter time);
- $(R_0, \text{Az}_0, h_0, \varphi_0)$ and $(R_m, \text{Az}_m, h_m, \varphi_m)$ - distance (km), azimuth (degrees), height (degrees), phase angle (degrees) for the beginning (t_0) and end (t_m) of the interval dT respectively;
- R_k, h_k - distance and height at the spacecraft culmination point (they are pointed out if the culmination moment is inside the presented interval dT);
- φ_{00} - minimal phase angle (degrees) for the interval dT ;
- t_{00} - moment of time for which the vector of the spacecraft orbital elements: a, e, I_n, OM, w, u for the specified date is given;
- m_1, m_2 - maximal and minimal measured light of the spacecraft (in V star magnitudes) for the presented interval dT ;
- F - discretization frequency of the presented information (in all figures for the 92023001 this frequency is a constant equal to the maximal sampling frequency of photometric information $F=25$ Hz);
- np - a factor defining the threshold p_{00} of Fourier-spectrum amplitude (U_{0k}) of the initial light curve (m_0): $p_{00}=\max(U_{0k})/np$;
- p_0 - threshold amplitude for Fourier-spectrum U_{0k} : it defines numeric values of amplitudes of spectral components exceeding p_0 ($U_{0j}, j=1, 2, \dots, 8$) and corresponding Fourier-periods T_j ;
- n - degree of used Fourier-expansion for the given interval dT ;
- M_{00} - value of the reference point determined from the preliminary calibration of photometric channel.

Right (upper) figure is an initial curve of the spacecraft light: dependence V of the spacecraft light (in star magnitudes) from time: $m_0=f(T)$.

With this, in fig. 5.1.0, ..., 5.8.0 values m_0 are obtained from the initial videosignal's integral in the measurement strobe minus average integral of background videosignal in the same strobe. The level of background signal in the measurement strobe is defined for three points of the spacecraft trajectory (initial part, culmination, final part).

Fig. 5.9.0, 5.10.0, 5.11.0 show results of evaluation of m_0 when background measurement is made simultaneously with signal measurement in forestalling point in a separate forestalling strobe going along the trajectory ahead of the measurement strobe. As a result, the signal ISF_j is registered in each TV frame in the measurement strobe, and IF_j - in the forestalling strobe, and light value m_0 is recovered from calibration curve where as an argument there is used a difference $I_0=I_0(t_j)=ISF(t_j)-IF(t_j-\tau)$ where τ - delay defined by the spacecraft motion along its trajectory at the moment t_j .

The effects related to the presence of the same stars in the measurement and forestalling strobe are very clearly seen in these last figures. So, stars are always selected during spacecraft photometry and there is no any misunderstanding because of them.

Left middle figure $U_{2k}=U_2(k)$ - magnitude of normalized Fourier spectrum of the integral $I_0(t)$, and right middle picture differs from U_{2k} with threshold cut off (p_0) of noise spectral components and by the function $\exp(-k^2/b^2)$. The lower figure shows the recovered light curve I_C from the spectrum U_{0k} as an intensity in relative units together with the main curve I_0 . To the right from this picture there are given values of periods of spectral components k_j corresponding to the maximums of the spectral amplitudes U_{0j} ($T_j \sim dT/k_j$).

Finally, in the right lower corner of the figure there is given a projection of the observed trajectory of the spacecraft on the horizontal plane of station coordinate system and projection of sunlight illumination direction (scale of distances along N-S (as well as W-O) axis is given in kilometers).

Pic = 92023000.000

FILE = 92023000.000

Nkonor = 0.00000

Day = 29

Month = 11

Year = 1996

Nkosr = 920230

(Ferret-D, USA)

Nkoint = 92023.001

Δm_apr = -0.91 **Δm_mirror** = 0.78

Δm_mes = 0.11

R0 = 1343.8

Rm = 1917.7

Vector at
t00=19h04m34s

Az0 = 306.1

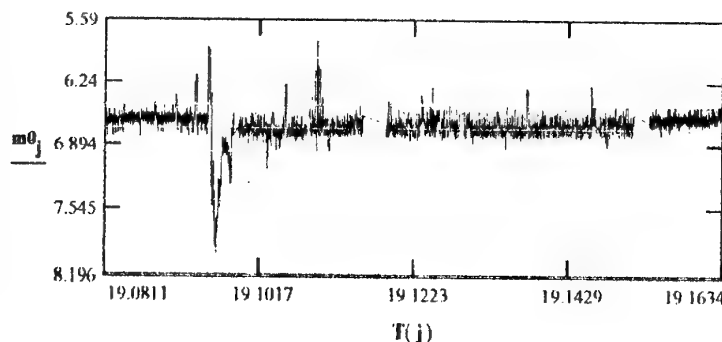
Azm = 214.6

φ0 = 109.8 **φm** = 114.7
M00 = 17.26 **α** = 7167.587
 e = 0.001178

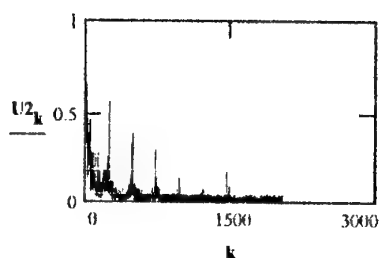
h0 = 31.8

hm = 16.9

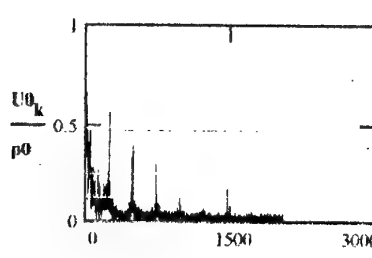
m1 = 5.81 **In** = 85.007
m2 = 7.98 **OM** = 165.939
t0 = 19.08109 **w** = 44.458
tm = 19.16344 **u** = 130.307
dT = 296.5s **n** = 12
F = 25 **Gc**
np = 50 **p0** = 0.476



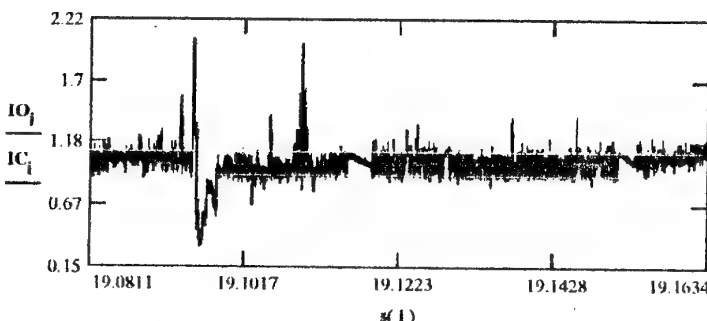
Initial curve of brightness (m; st. mag.)



FFT from intencity of the obj.(U2)



Restored and smoothed
spectrum of the intencity of
object(U0)



Initial (IO) and restored (IC) curves of brightness (Intensity at relative units)

Tm = 137.90 **s**
T1 = 137.9 **s**
T2 = 58.13 **s**
T3 = 42.35 **s**
T4 = 26.95 **s**
T5 = 21.18 **s**
T6 = 16.94 **s**
T7 = 1.21 **s**
T8 = 1.21 **s**

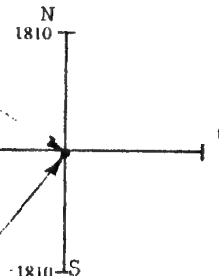
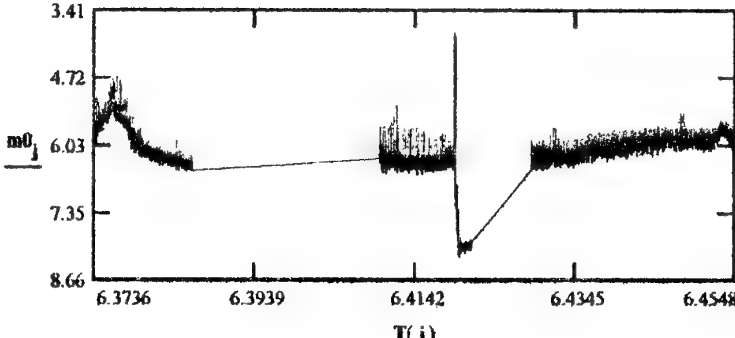
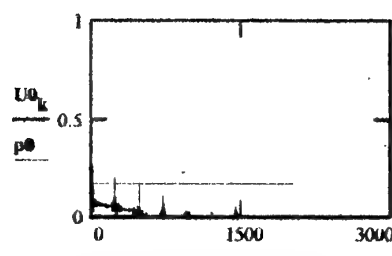
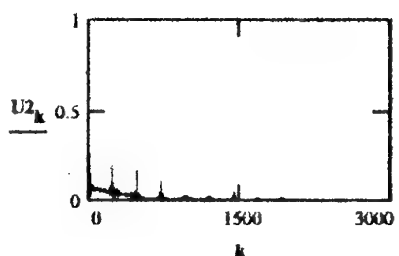


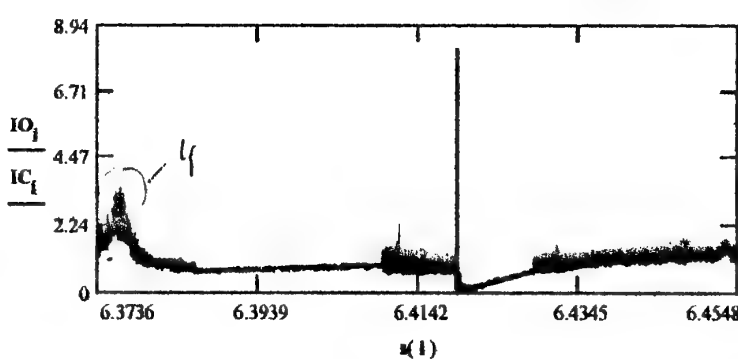
Fig. 5.1.3

Pic = 92023100
 FILE = 92023100 Nkonor = 0.00000 Day = 30 Month = 11 Year = 1996
 Nkosr = 920230 (Ferret-D, USA) $\Delta m_{\text{apr}} = 1.59$ $\Delta m_{\text{mirror}} = 0.93$ $\Delta m_{\text{mes}} = -0.14$
 Nkoint = 92023.001
 R0 = 1833.4 Rk = 1062.5 Rm = 1198.2
 Az0 = 153.1 $\phi_0 = 106.1$ Azm = 50.3
 h0 = 18.5 hk = 45.6 hm = 37.9


Initial curve of brightness (m; st.mag.)



$U_{01} = 1.000$
 $U_{02} = 0.494$
 $U_{03} = 0.385$
 $U_{04} = 0.261$
 $U_{05} = 0.210$
 $U_{06} = 0.207$
 $U_{07} = 0.196$
 $U_{08} = 0.170$
 $U_{09} = 0.000$



$T_m = 73.08$ s
 $T_1 = 70.44$ s
 $T_2 = 47.92$ s
 $T_3 = 36.54$ s
 $T_4 = 29.23$ s
 $T_5 = 24.36$ s
 $T_6 = 1.21$ s
 $T_7 = 0.61$ s
 $T_8 = 0.61$ s

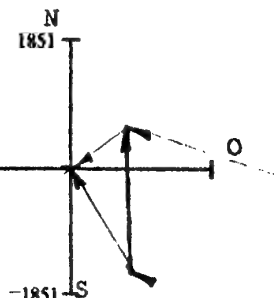


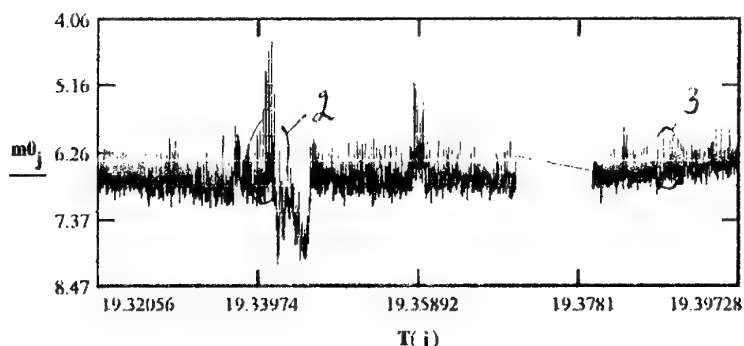
Fig. 5.2.0.

Pic = 92023200
FILE = 92023200
Nkonor = 0.00000
Nkosr = 920230
Nkoint = 92023.001

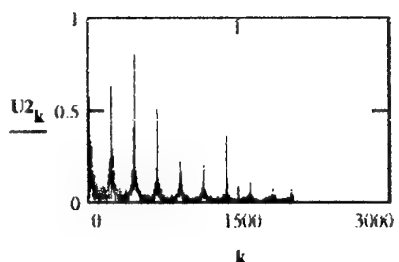
(Ferret-D, USA)

Day = 2 **Month** = 12 **Year** = 1996
 Δm_{apr} = -0.64 Δm_{mirror} = -0.31 Δm_{mes} = 0.29

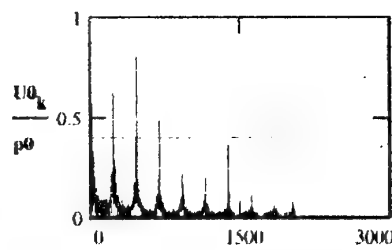
R0 = 1917.8 **Rk** = 1803.0 **Rm** = 2206.1
Az0 = 301.4 **φ00** = 123.0 **Azm** = 240.5
h0 = 17.0 **hk** = 19.2 **hm** = 12.1



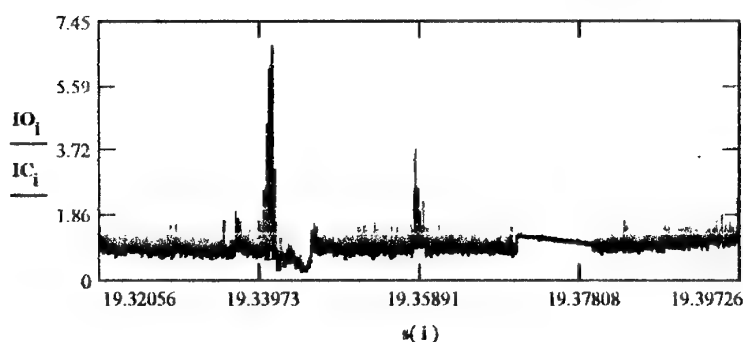
Initial curve of brightness (m; st.mag.)



FFT from intencity of the obj.(U2)



Restored and smoothed spectrum of the intencity of object(U0)



Initial (IO) and restored (IC) curves of brightness (Intensity at relative units)

Vector at
t00=19h19m14s
 $\varphi_0 = 123.0$ $\varphi_m = 131.6$
M00 = 17.45 $a = 7167.528$
 $e = 0.001153$
m1 = 4.42 **ln** = 85.008
m2 = 8.10 **OM** = 164.212
t0 = 19.32056 **w** = 44.224
tm = 19.39728 **u** = 130.107
dT = 276.2s **n** = 12
F = 25 **Gc**
np = 50 **p0** = 0.400

U0m = 1.000
U01 = 0.775
U02 = 0.707
U03 = 0.540
U04 = 0.633
U05 = 0.485
U06 = 0.803
U07 = 0.504
U08 = 0.000

Tm = 0.60 **s**
T1 = 66.55 **s**
T2 = 38.9 **s**
T3 = 21.25 **s**
T4 = 1.20 **s**
T5 = 1.19 **s**
T6 = 0.60 **s**
T7 = 0.40 **s**
T8 = 0.40 **s**

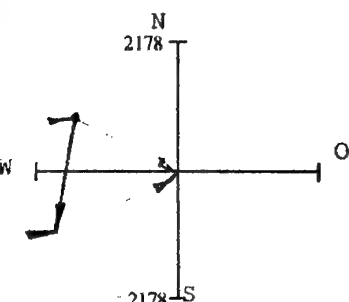


Fig 5.3.6

Pic = 92023300

FILE = 92023300

Nkosc = 920230

Nkoint = 92023.001

Nkonor = 0.00000

Day = 4

Month = 12

Year = 1996

(Ferret-D, USA)

Am_apr = 1.96

Am_mirror = 1.48

Am_mes = 0.30

R0 = 2119.8

Rk = 925.1

Rm = 1075.9

Vector at

Az0 = 166.1

phi0 = 95.9

Azm = 41

t00=06h07m27s

h0 = 13.4

hk = 57.5

hm = 44.9

phi0 = 115.1

phi_m = 95.9

M00 = 18.02

a = 7174.342

e = 0.001464

m1 = 3.83

ln = 85.009

m2 = 6.47

OM = 163.383

t0 = 6.12417

w = 96.620

tm = 6.22169

u = 27.281

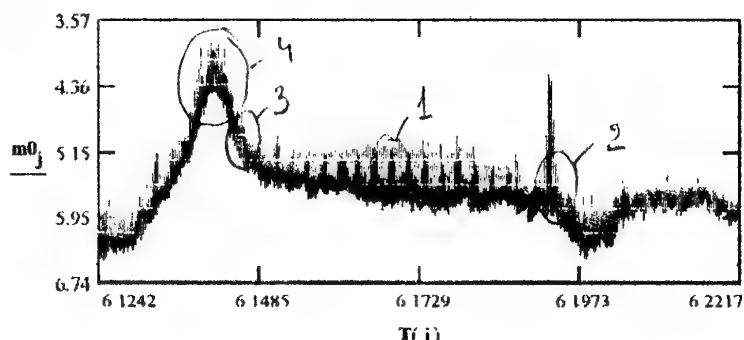
dT = 351.1 s

n = 12

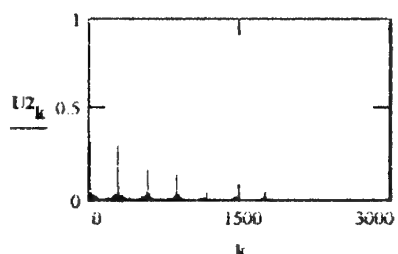
F = 25 Gc

np = 50

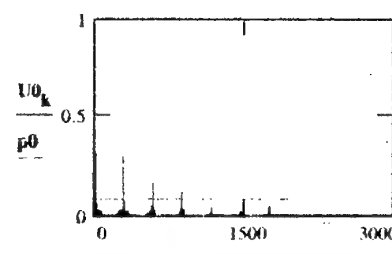
p0 = 0.083



Initial curve of brightness (m; st.mag.)



FFT from intencity of the obj.(U2)



Restored and smoothed spectrum of the intencity of object(U0)

U0m = 1.000

U01 = 0.792

U02 = 0.311

U03 = 0.160

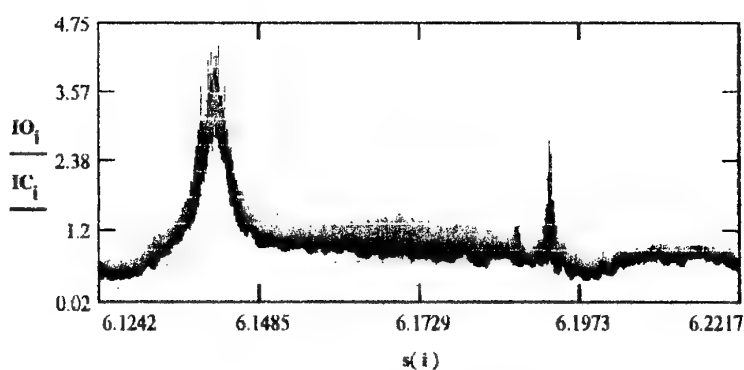
U04 = 0.115

U05 = 0.294

U06 = 0.168

U07 = 0.140

U08 = 0.000



Initial (IO) and restored (IC) curves of brightness (Intensity at relative units)

Tm = 117.03 s
T1 = 111.45 s
T2 = 43.34 s
T3 = 27.01 s
T4 = 23.41 s
T5 = 1.20 s
T6 = 0.60 s
T7 = 0.40 s
T8 = 0.40 s

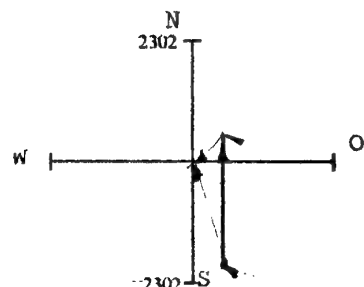


Fig. 5.4.0

Pic = 92023500
FILE = 92023500
Nkosc = 920230
Nkont = 92023.001

Nkonor = 0.00000
(Ferret-D, USA)

Day = 11 **Month** = 12 **Year** = 1996

Am_apr = 0.39 **Am_mirror** = 0.39 **Am_mes** = 0.00

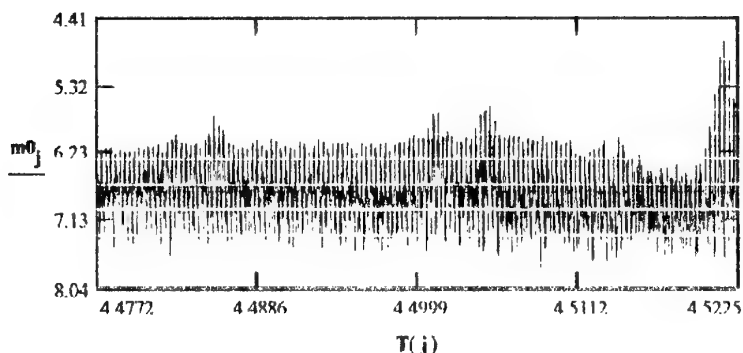
R0 = 2232.2
Az0 = 116.7
h0 = 11.8

Rm = 1868.6
Azm = 83.3
hm = 17.9

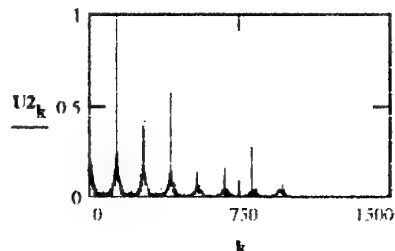
Vector at
t00=04h28m38s

phi0 = 128.8 **phi_m** = 128.7
M00 = 16.55 **a** = 7172.373
e = 0.001423

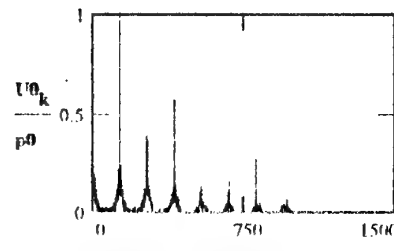
m1 = 4.72 **In** = 85.006
m2 = 7.74 **OM** = 159.403
t0 = 4.47722 **w** = 107.451
tm = 4.52254 **u** = 33.915
dT = 163.2s **n** = 11
F = 25 **Gc**
np = 50 **p0** = 0.250



Initial curve of brightness (m; st mag.)

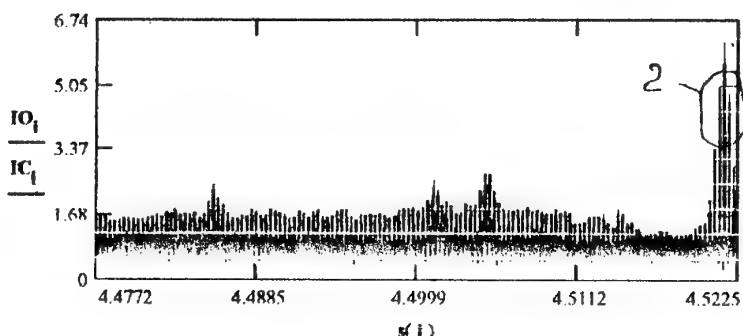


FFT from intencity of the obj. (U2)



Restored and smoothed spectrum of the intencity of object(U0)

U0m = 1.000
U01 = 0.350
U02 = 1.000
U03 = 0.322
U04 = 0.393
U05 = 0.579
U06 = 0.275
U07 = 0.000
U08 = 0.000



Initial (IO) and restored (IC) curves of brightness (Intensity at relative units)

Tm = 1.21 **s**
T1 = 75.89 **s**
T2 = 1.21 **s**
T3 = 1.19 **s**
T4 = 0.60 **s**
T5 = 0.40 **s**
T6 = 0.20 **s**
T7 = 0.20 **s**
T8 = 0.20 **s**

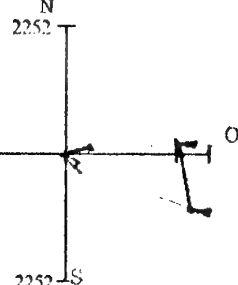


Fig. 5.6.0.

Pic = 92023510
FILE = 92023510
Nkosc = 920230
Nkoint = 92023.001

Nkonor = 0.00000
(Ferret-D, USA)

Day = 11 **Month** = 12 **Year** = 1996

Am_apr = 2.12 **Am_mirror** = 1.63 **Am_mes** = -1.48

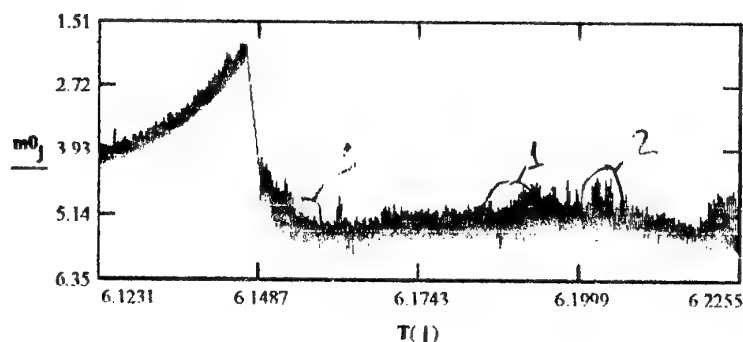
R0 = 2241.4 **Rk** = 924.9
Az0 = 199.4 **φ00** = 41.9
h0 = 11.6 **hk** = 57.6

Rm = 1060.6
Azm = 326
hm = 45.9

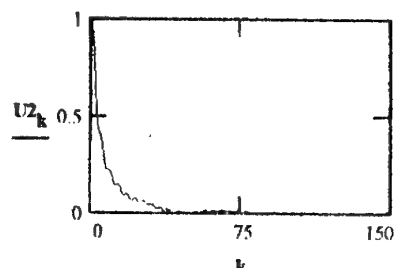
Vector at
t00=06h07m23s

φ0 = 84.6 **φm** = 44.7
M00 = 14.55 **a** = 7174.455
e = 0.001484

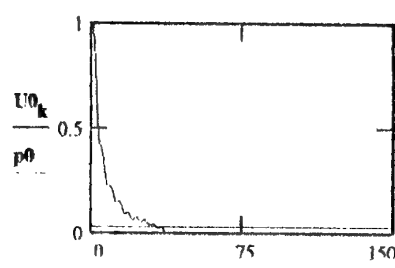
m1 = 1.91 **In** = 85.008
m2 = 5.94 **OM** = 159.363
t0 = 6.12306 **w** = 95.808
tm = 6.22546 **u** = 26.563
dT = 368.6s **n** = 12
F = 25 **Gc**
np = 50 **p0** = 0.033



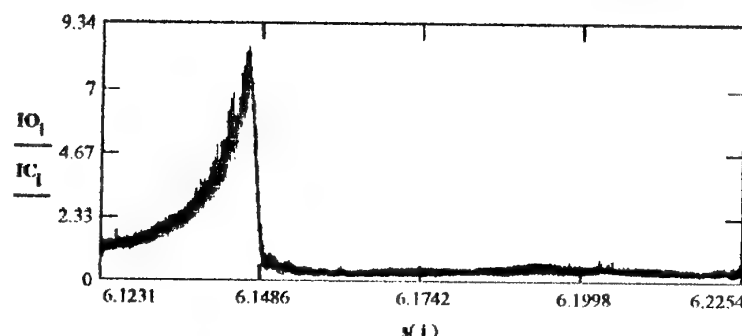
Initial curve of brightness (m; st.mag.)



FFT from intencity of the obj.(U2)

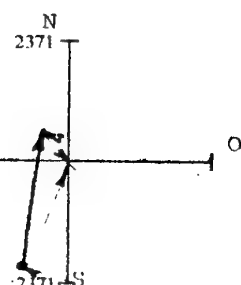


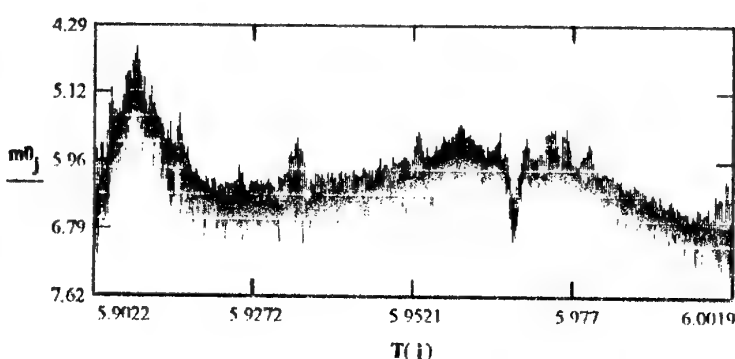
Restored and smoothed
spectrum of the intencity of
object(U0)



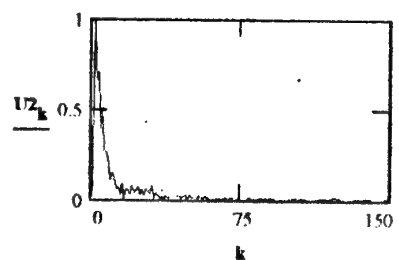
Initial (IO) and restored (IC) curves of brightness (Intensity at relative units)

Tm = 122.88 **s**
T1 = 41.65 **s**
T2 = 26.52 **s**
T3 = 20.48 **s**
T4 = 16.76 **s**
T5 = 13.65 **s**
T6 = 11.89 **s**
T7 = 1.21 **s**
T8 = 0.40 **s**

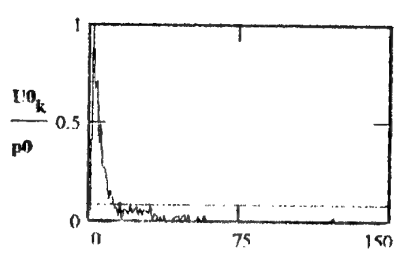


Pic = 92023620
 FILE = 92023620 Nkonor = 0.00000 Day = 15 Month = 12 Year = 1996
 Nkosr = 920230 (Ferret-D, USA) Am_apr = 1.27 Am_mirror = 0.96 Am_mes = -0.48
 Nkoint = 92023.001
 R0 = 2025.7 Rk = 1058.6 Rm = 1303.2 Vector at
 Az0 = 210.4 phi0 = 28.0 Azm = 327.9 t00=05h54m08s
 h0 = 14.9 hk = 45.9 hm = 33.3


Initial curve of brightness (m; st.mag.)

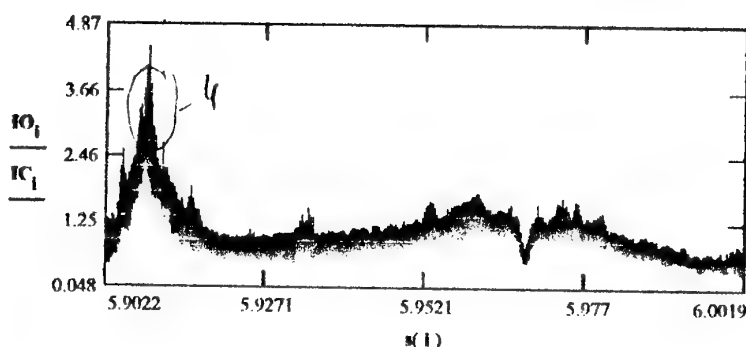


FFT from intencity of the obj. (U2)



Restored and smoothed spectrum of the intencity of object(U0)

U0m = 1.000
 U01 = 1.000
 U02 = 0.715
 U03 = 0.492
 U04 = 0.148
 U05 = 0.091
 U06 = 0.201
 U07 = 0.123
 U08 = 0.152



Initial (IO) and restored (IC) curves of brightness (Intensity at relative units)

Tm = 194.05 s
 T1 = 194.05 s
 T2 = 92.05 s
 T3 = 59.83 s
 T4 = 32.64 s
 T5 = 22.44 s
 T6 = 1.21 s
 T7 = 0.60 s
 T8 = 0.40 s

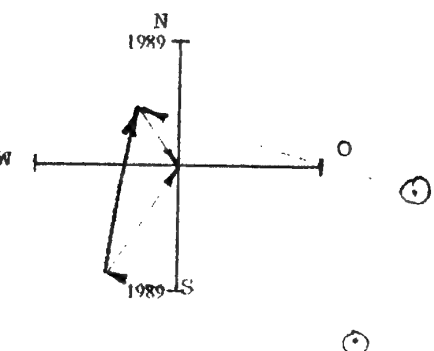
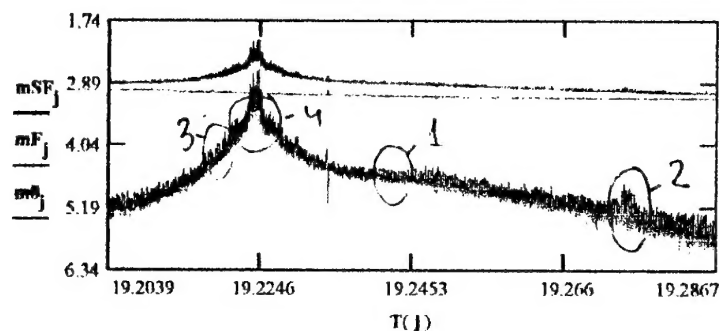


Fig. 5.9.0.

Pic = 92023710.000
FILE = 92023710.000 **Nkonor** = 0.00000 **Day** = 13 **Month** = 3 **Year** = 1997
Nkosr = 920230 (Ferret-D, USA)
Nkoint = 92023.001 **Am_apr** = 0.97 **Am_mirror** = 0.90 **Am_mes** = -0.38

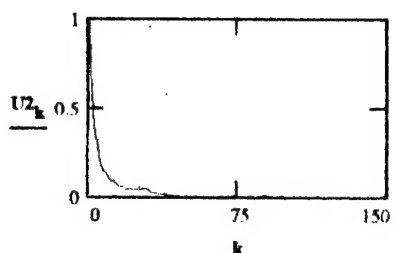
R0 = 2255.9 **Rk** = 1449.4 **Rm** = 1491.5 **M00** = 14.72
φ0 = 42.3 **φ00** = 16.0 **φm** = 31.6
Az0 = 139.6 **hk** = 28.1 **Azm** = 68
h0 = 11.4 **hm** = 26.9



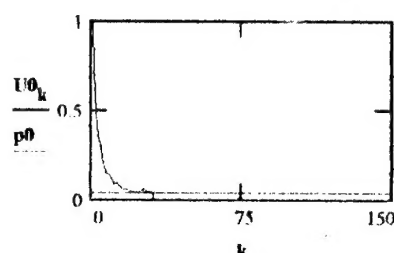
Initial curve of brightness (m_0 ; st.mag.), phone (m_F), signal+phone (m_{SF})

Vector at t00=19h12m00s:

α = 7167.724
t0n = 3.9 e = 0.001213
m1 = 2.63 In = 85.0055
m2 = 6.01 OM = 106.2830
t0 = 19.20389 w = 44.1547
tm = 19.28670 u = 131.3086
dT = 298.12 s n = 12
F = 25.0 Gc
np = 30.0 $p0$ = 0.04

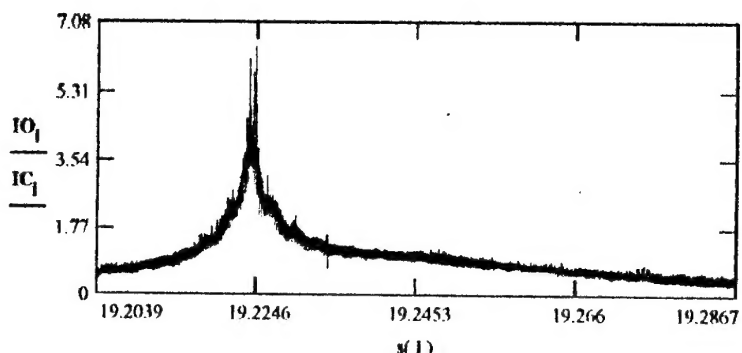


FFT from intencity of the obj.(U2)



Restored and smoothed spectrum of the intencity of object(U0)

U0m = 1.0
U01 = 0.1
U02 = 0.06
U03 = 0.05
U04 = 0.05
U05 = 0.04
U06 = 0.07
U07 = 0.06
U08 = 0.05



Initial (IO) and restored (IC) curves of brightness (Intensity at relative units)

Tm = 85.18 s
T1 = 23.85 s
T2 = 16.84 s
T3 = 14.20 s
T4 = 11.47 s
T5 = 9.94 s
T6 = 1.20 s
T7 = 0.60 s
T8 = 0.20 s

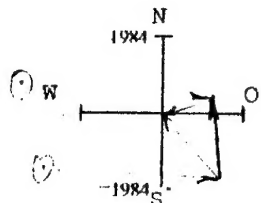


Fig 5.9.0.

Pic = 92023720

FILE = 92023720

Nkonor = 0.00000

Day = 13

Month = 3

Year = 1997

Nkossr = 920230

(Ferret-D, USA)

Nkoint = 92023.001

Am_apr = 0.75

Am_mirror = 1.24

Am_mes = -0.7

R0 = 2185.3

Rk = 1235.9

Rm = 1238.5

M00 = 16.72

phi0 = 94.6

phi00 = 94.6

phi_m = 114.5

Vector at t00=20h53m05s:

Az0 = 222.9

Azm = 307.1

h0 = 17.2

hk = 36.7

hm = 33.6

a = 7173.728

ten = 4.0 **e** = 0.00145

m1 = 3.81 **In** = 85.0092

m2 = 7.03 **OM** = 106.2197

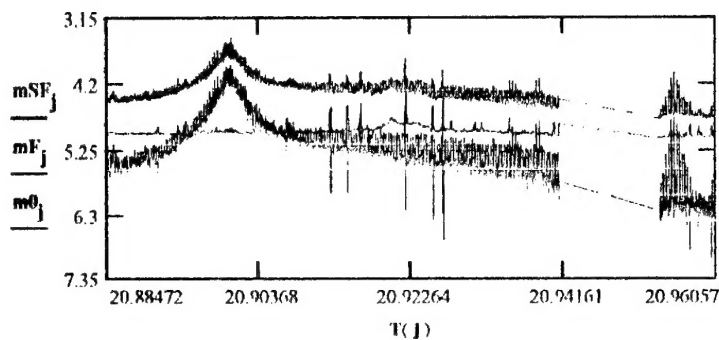
t0 = 20.88472 **w** = 97.3342

tm = 20.96057 **u** = 29.2378

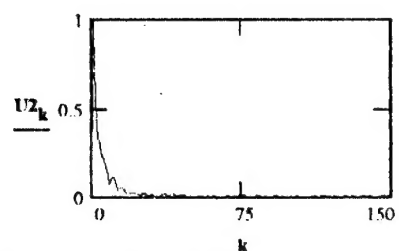
dT = 273.04 s **n** = 12

F = 25.0 Gc

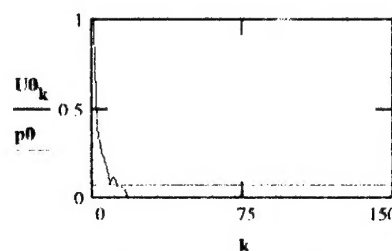
np = 30.0 **p0** = 0.07



Initial curve of brightness (m0; st. mag.), phone (mF),
signal+phone (mSF)



FFT from intencity of the obj.(U2)



Restored and smoothed
spectrum of the intencity of
object(U0)

U0m = 1.0

U01 = 0.12

U02 = 0.15

U03 = 0.09

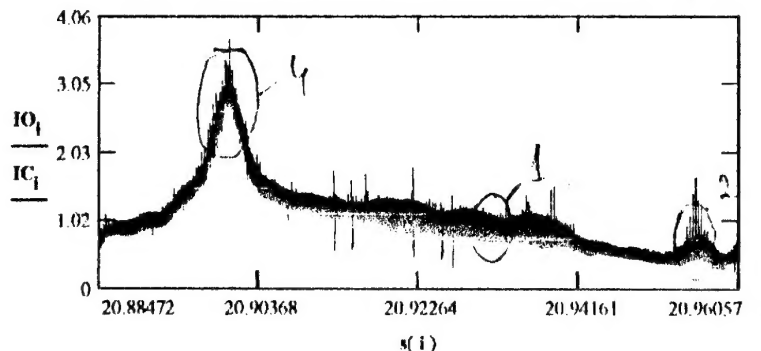
U04 = 0.08

U05 = 0

U06 = 0

U07 = 0

U08 = 0



Initial (IO) and restored (IC) curves of brightness (Intensity at relative units)

Tm = 91.01 s

T1 = 26 s

T2 = 1.20 s

T3 = 0.60 s

T4 = 0.40 s

T5 = 0.40 s

T6 = 0.40 s

T7 = 0.40 s

T8 = 0.40 s

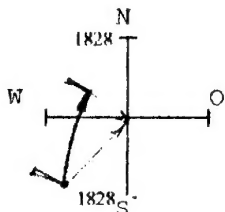
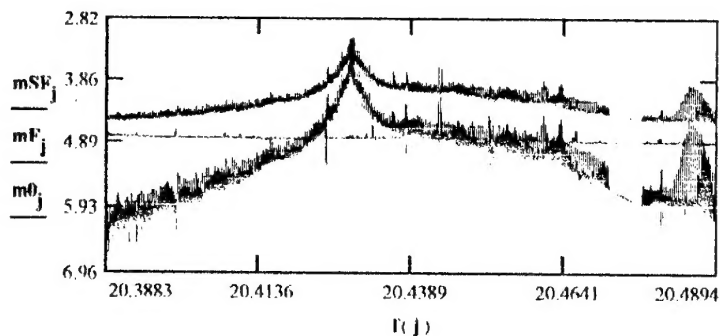


Fig 5.10.0

Pic = 92023730
 FILE = 92023730 Nkonor = 0.00000 Day = 14 Month = 3 Year = 1997
 Nkosr = 920230 (Ferret-D, USA)
 Nkoint = 92023.001 Am_apr = 1.54 Am_mirror = 1.89 Am_mes = 0.38

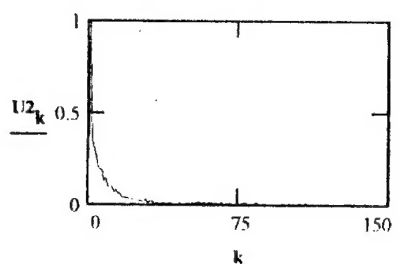
R0 = 2357.3 Rk = 924.3 Rm = 992.4 M00 = 16.42
 φ0 = 84.9 φ00 = 84.9 φm = 102
 Az0 = 198.7 Azm = 315.2
 h0 = 10 hk = 57.6 hm = 51



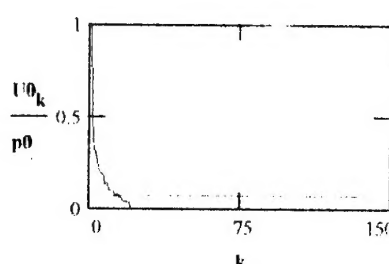
Initial curve of brightness (m0; st.mag.), phone (mF),
signal+phone (mSF)

Vector at t00=20h23m15s:

a = 7161.024
 ten = 5.3 e = 0.002651
 m1 = 3.41 In = 85.0041
 m2 = 6.64 OM = 105.6641
 t0 = 20.38833 w = 101.7622
 tm = 20.48941 u = 284.4757
 dT = 363.88 s n = 12
 F = 25.0 Gc
 np = 30.0 p0 = 0.07

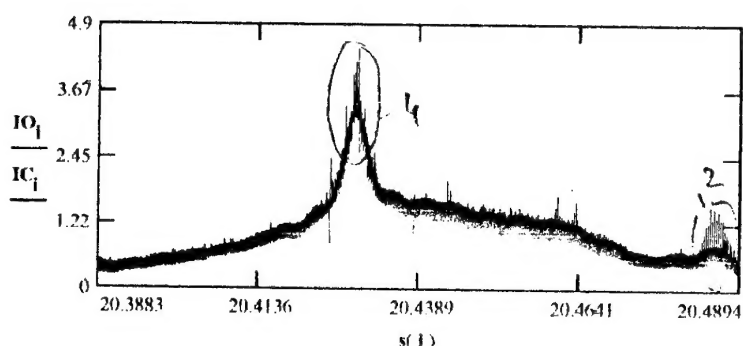


FFT from intencity of the obj.(U2)



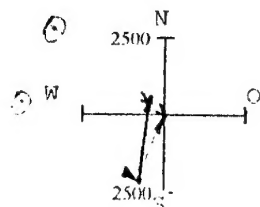
Restored and smoothed
spectrum of the intencity of
object(U0)

U0m = 1.0
 U01 = 0.15
 U02 = 0.1
 U03 = 0.08
 U04 = 0.11
 U05 = 0.08
 U06 = 0
 U07 = 0
 U08 = 0



Initial (IO) and restored (IC) curves of brightness (Intensity at relative units)

Tm = 121.26s
 T1 = 42.81 s
 T2 = 31.10 s
 T3 = 25.99 s
 T4 = 1.20 s
 T5 = 0.60 s
 T6 = 0.60 s
 T7 = 0.60 s
 T8 = 0.60 s



Conclusion

The present final report contains all necessary information on the tasks formulated in the Statement of Work. The presented report answers not only all questions of the Statement of Work, but also contains an additional information included in the report for completeness of picture on the problem of photometry of space objects. The last section includes a big amount of experimental material on the photometry of GSO and LOSO. With this, there are given data on 11 GSO and 2 LOSO (8 GSO and 2 LOSO - according to the SOW).

In the final report there are demonstrated our scientific and technical abilities in the field of satellite photometry, processing and interpretation of experimental data for determination of non-orbital motion of spacecraft, definition of its purpose and functional state, definition of its function in the given mode (whether it is operative or already belongs to a space "junk").

Theoretical analysis of experimental data with processing of photometric observations of LOSO and their topical images allows, at first approach, to solve the following problems:

Determination of the specific periodical components of the spacecraft motion relative to the center of mass.

Reliable information about presence and intensity of these components will allow to make a conclusion about type of spacecraft stabilization in orbit and about some specific geometry and physical parameters of spacecraft form and reflecting surface.

Determination of orientation of the main kinetic momentum of the spacecraft and local orientation of symmetry axes of some structural elements of the spacecraft.

Determination of geometric characteristics of main elements of the spacecraft structure, containing determined symmetry axes.

Recovery (first approach) of the generalized form of the spacecraft.

Definition of requirements (basing on analysis results) to the quality of optical observations of the spacecraft (coordinates, photometry, images, quantity and class of sessions, etc.) for solution of further problems of determination of form, characteristics of own motion, functional state and elements of functional purpose of the spacecraft, including requirements to synchronous or quasi-synchronous optical and radio observations of the spacecraft.

Solution of these problems based on the obtained experimental information assumes involvement of high-qualified scientists in frames of an additional contract.

We hope for the future fruitful cooperation with the Customer in the frame of a new contract in the field of spacecraft photometry and interpretation of obtained information in the near future.